EXPLORING URBAN AGRICULTURE AS A CLIMATE CHANGE MITIGATION STRATEGY AT THE NEIGHBORHOOD SCALE

A Dissertation
Presented to
The Academic Faculty

By

Dana M. Habeeb

In Partial Fulfillment
of the Requirements for the Degree
Doctor of Philosophy in the
School of City and Regional Planning

Georgia Institute of Technology

December 2017

EXPLORING URBAN AGRICULTURE AS A CLIMATE CHANGE MITIGATION STRATEGY AT THE NEIGHBORHOOD SCALE

Approved by:

Dr. Brian Stone, Jr. Advisor
School of City and Regional Planning
Georgia Institute of Technology

Dr. Michael Elliott
School of City and Regional Planning
Georgia Institute of Technology

Dr. Nisha Boshwey
School of City and Regional Planning
Georgia Institute of Technology

Dr. Perry Yang
School of City and Regional Planning
Georgia Institute of Technology

Dr. Armistead G. Russell
School of Civil and Environmental Engineering
Georgia Institute of Technology

Date Approved: August 15, 2017

The real wealth of a planet is in its landscape, how we take part in that basic source of civilization — agriculture.

Frank Herbert - Dune

To James, Marlo, and Madeline. You have given me more strength than you will ever know. You are my rock. You are my heart. You are my life.

ACKNOWLEDGEMENTS

I am deeply indebted to all of the teachers, students and administrators who gave their time and energy in helping me during my tenure at Georgia Tech. I am grateful for the guidance, support, and encouragement of my advisor, Dr. Brian Stone, Jr. for guiding me through the journey of birthing a dissertation and completing a PhD. Thank you Brian for all of the support, advice, and encouragement you have given over these many years. Your guidance through my entire Ph.D. has shaped me into the researcher I am today. Your insightful and critical intellect coupled with your southern etiquette has taught me how to navigate the academic world. I am proud to have been a member of the Urban Climate Lab from its creation and to contribute to our research efforts and aspirations. Thank you for helping me focus on my strengths, develop new skills and sharpen my critical thinking so that I can find new ways to try to make our world and our community a better place. Thank you for always making time for me and for your continued support and advice in every aspect of my career. I know, even though I am now leaving Georgia Tech, these past years will continue to shape me as a researcher and as a teacher.

I would like to thank my committee for their advice and support throughout. Ted, thank you for your help and guidance while tackling my research. Thank you for inviting me to join your team, to be part of the NSF SRN, and to be a community member in your lab. It has been invaluable to see how you work and communicate and to look at the research world through the civil engineering lens. You have created a family of academics and I am grateful to be a part of that.

Michael, thank you for all of your help over my long academic career. I have always appreciated and taken much advantage of your open door policy. No matter how busy, you have always made time for me. Your advice is never sugar coated but is sincere and honest. Your ability to critically analyze and vet research questions from so many points of views has challenged me while simultaneously giving more confidence about my work. Thank

for always asking the hard questions and always taking the time to chat about anything from Sci-Fi to parenting.

Nisha, thank you for agreeing to be on my committee and for all of your support navigating the overwhelming obstacle of finishing a dissertation. Thank you for helping me make timetables so I could understand how to turn a huge endeavor into bite size pieces. Thank you for your advice, encouragement, and support both inside and outside of the academy. You are a wonderful role model as a researcher, teacher, and mentor and a beautiful example of how to balance a loving family and a successful career.

Perry, thank you for your guidance and advice in tackling challenging urban design and morphology questions. Urban design will always be my core and your enthusiasm for the field is infectious. Thank you for taking the time to discuss fun and challenging urban design questions and for always addressing me as a colleague and an equal contributor to the dialogue. Thank you for your help on my dissertation, specifically for giving me access to use your Viewsphere software for calculating sky view factor. It was important to try to define local climate zones to the best of my ability and learning about and having the opportunity to use your software, I believe, made that endeavor stronger.

I would like to also thank Tony Giarrusso for all of your help conducting my research. Tony, thank you for always making available high-quality data, for always being there to answers spatial analysis questions, and for always being open to discussing life, the universe and everything. Thank you specifically for giving me assess to Atlanta's quickbird data to use in my dissertation. The dataset made my methodology stronger in area of the research field where high resolution data is hard to come by. Thank you to the College of Design's (formerly Architecture) IT department especially Jeff Langston and Perry Minyard. I could not have completed my analysis work and therefore my dissertation without this great team who was always willing to do IT gymnastics in order to meet my computational demands. For setting up special drives and a computer so that I could run unique software to always being so timely when any technical problem arose, I hope I always have

IT support like this even into the afterlife.

I will always remember the love and support given to me by my family and friends. Thank you! Thank you! Your constant encouragement and belief in me kept me on track and focused on my goal. Now I hope to have a little more time to spend with each of you to show you how much I appreciate your unconditional support in my life. I want to thank my husband for always being there to help, to think through ideas, to argue points of views, to remind me of my strength and my abilities, and to lift me up when I felt down. I want to thank my amazing daughters for always giving me perspective on what is important in life.

TABLE OF CONTENTS

LIST OF TABLES

LIST OF FIGURES

SUMMARY

Extreme heat events are responsible for more annual fatalities in the United States than any other form of extreme weather. Urban centers are particularly vulnerable to the threats of excessive heat as most cities are home to large populations of lower income individuals who often lack access to air conditioning or adequate healthcare facilities. Urban populations are also more likely to be exposed to extreme heat due to the urban heat island (UHI) phenomenon. As the global population continues to urbanize, the number of vulnerable individuals will continue to increase making urban heat island mitigation strategies all the more important. This research explores urban agriculture as an urban heat island mitigation strategy. Though previous work has examined the role of vegetation in mitigating the UHI effect, the potential of urban agriculture as a mitigation strategy has yet to be investigated. I focus my investigation in the city of Atlanta, GA, as Atlanta has one of the fastest growing urban heat islands, and has exhibited significant increasing trends in heat waves.

In this dissertation, I conduct a land cover analysis to investigate the climate effect of urban agriculture on local temperatures. I use satellite temperature data, land cover data, and urban form metrics to estimate how the percent change in urban agriculture impacts local temperatures. My research shows that urban agriculture decreases high nighttime temperatures during summer months, which is an important public health finding as nighttime temperatures are a better metric for capturing negative health effects from extreme heat than daytime temperatures. At the local level, an increase of 10-acres per km^2 in agricultural land cover can reduce nighttime temperatures by approximately 0.65°F accounting for approximately 10% of Atlanta's UHI effect. Agricultural lands outperformed forested land cover as a nighttime cooling mechanism across the Atlanta MSA. Though agricultural lands can act as a successful heat mitigation strategy by lowering nighttime temperatures, during heat waves the magnitude of the cooling effect is diminished. As such, I argue for an active management strategy to ensure that urban agriculture maintains its cooling potential

during extreme heat conditions.

To investigate whether the urban form of a neighborhood plays an important role in how well vegetative strategies perform in reducing temperatures, I create urban form typologies based on Atlanta's urban morphology. The urban form typologies are based on characteristics that have been used to define "local climate zones". Specifically, I investigate how urban form at the neighborhood scale impacts the relationship between urban agriculture and local climate and uncover an interaction effect between urban agriculture and urban form when a heat wave is present. Agricultural implementations in dense urban neighborhoods decrease temperatures more than in the residential areas. Additionally, I found that a minimum of seven acres of agricultural lands must be implemented per km^2 before cooling effects will occur. As such, I argue that urban agriculture should not only be placed in cities but that the morphology of the built environment should be taken into consideration when selecting locations for urban agriculture.

My research builds on work examining the potential of urban agriculture to effectively revitalize neighborhoods with vacant properties and reclaim brownfield sites in urban areas. When designing heat mitigation strategies, it is important for planners and policy makers to quantify the difference between vegetative approaches in order to understand the tradeoffs they are making climatically, environmentally, and socially. As such the results of my research can help guide planners when selecting between vegetative UHI mitigation strategies and may further support the burgeoning urban agriculture movement.

CHAPTER 1

INTRODUCTION

Today, extreme heat events are responsible for more annual fatalities in the United States than any other form of extreme weather [1, 2]. This is seen most directly when extreme temperatures result in a high number of heat-related illnesses, such as heat exhaustion, heat cramps, and heat stroke, which can lead to death. Temperature extremes are known to exacerbate health conditions already compromised by cardiovascular and respiratory illness, leading to an increase in heat-related mortality [3, 4].

On average, yearly estimates of heat-related deaths in the United States range from 170-690 per year [1, 2, 3]. This range is large because heat related deaths are often difficult to classify and therefore frequently go unnoticed especially during heat waves that fall below the threshold of public awareness. Differing state standards on heat-related mortality classification as well as the large number of symptoms that can result in heat-related mortality further complicates accurate diagnosis [5]. In the United States, the Midwest heat waves of 1995 and 1999 claimed more than 1,000 and 300 lives, respectively. More recently, heat waves of unprecedented intensity and duration in Europe have resulted in much greater loss of life, with more than 70,000 fatalities estimated from a 2003 European heat wave and more than 50,000 from a 2010 heat wave in Russia [6, 7, 8]. These recent heat waves rank amongst the most deadly weather-related disasters on record in the last century.

Cities are particularly vulnerable to heat waves because of the urban heat island effect and because of the high number of socially vulnerable residents in cities. In its most basic form, the urban heat island effect is seen when temperatures in cities are higher than temperatures in their surrounding rural areas. This amplification in local urban temperatures is due to the creation of the urban environment where natural landscapes are displaced for impervious surfaces such as roads, buildings and parking lots, and where the overall albe-

dos of the urban environment are lowered due to asphalt roads and black rooftops among many other construction materials [9].

The built up environments of urban areas create urban canyons that further trap radiant heat and excess waste heat is generated through the continuous use of machines like air conditioners and vehicles. Due to urban heat islands, cities are not only warmer than their rural counterparts but they are warming at a faster rate, a rate that is twice as fast as the planet as a whole [10]. Cities are outpacing global temperatures changes due to climate change. This increased rate in temperature change makes cities particularly susceptible to extreme heat events and heat waves. Heat wave characteristics, such as frequency, timing, duration and intensity, have been found to be increasing for large US cities [11]. The increasing amplification of temperatures due to the urban heat island effect and increases in the number of heat waves over time place city residents in a very vulnerable position. Urban centers are particularly vulnerable to the threats of excessive heat as most cities are home to large populations of lower income individuals who often lack access to air conditioning or adequate healthcare facilities. As the global population continues to urbanize, the number of vulnerable individuals will continue to increase making urban heat island mitigation strategies all the more important [12].

Mitigation of a city's urban heat island is an important focus for all major cities. Extreme heat is a serious public health concern and by lessening the effect of urban heat islands cities can create cooler climates. Cities can effectively mitigate the urban heat island effect through numerous interventions by targeting albedo and waste heat, and employing vegetative strategies. Cities can use albedo enhancements through cool roofing and paving strategies to increase the albedo of urban surfaces and in turn lower the amount of solar radiation that is absorbed in urban environments [13, 14]. In places with sufficient rainfall, vegetation strategies have been shown to be the most effective strategy for lowering urban temperatures, with as much as a 50% reduction in the urban heat island [15, 16].

Cities like Chicago have implemented aggressive green roof policies to combat the ur-

ban heat island effect, and Los Angeles has committed to planting 1 million trees throughout the city in the near future [17, 18, 19]. Urban heat island research has extensively investigated the role of vegetation in cooling urban environments because of its efficacy. In essence, vegetative approaches are an attempt to revert the urban landscape back to its natural land cover in order to capture natural cooling mechanism embedded in vegetation. Of all the vegetative strategies explored for cooling strategies, urban agriculture remains largely unexplored. Cities across the country are making a move toward reintroducing agriculture inside city limits [20]. Though there are many social benefits resulting from urban agriculture a connection between urban agriculture and urban heat islands has yet to be made.

In my dissertation research I explore how urban agriculture affects the local (neighborhood scale) climate investigating the potential for urban agriculture to cool the local climate by lowering temperatures in urban areas. I will compare urban agriculture to other vegetative strategies, examine urban agriculture typologies and the urban form of neighborhoods to understand how form and context drive cooling effects, and will explore how well urban agriculture maintains its cooling strength during extreme heat conditions. Finally I will investigate the strategy of converting vacant parcels to urban agriculture in an effort to assess the opportunities that many cities presently have to quickly implement change. To address these research questions, I situate my investigation in the city of Atlanta, GA.

1.1 Research Question and Objectives

My research bridges two built environment and health research areas: urban heat islands (UHI) and urban agriculture. I am specifically interested in investigating the potential for urban agriculture to act as an urban heat island mitigation strategy at the neighborhood scale. I have five research objectives:

1. to examine the potential for urban agriculture to cool the local climate by lowering temperatures in urban areas;

3

2. to compare the performance of urban agriculture to the UHI mitigation strategy of urban forestation;

3. to quantify the amount of land that needs to be converted to urban agriculture in order to receive a measurable local climate benefit;

4. to investigate how different patterns of urbanization mediate the influence of urban agriculture on local climate;

5. to investigate whether urban agriculture as a heat mitigation strategy is as effective during extreme heat conditions.

Before addressing these research objectives, I first perform a comprehensive literature review to motivate my work and identify relevant gaps in the research literature. I then discuss my research approach and begin by giving a brief overview of my research methods revisiting my research questions with a table that synthesizes my research questions, research objectives, hypotheses, and methods, and discuss the rationale for choosing Atlanta, GA as the study site. Next I discuss the two methodical approaches that I will use to answer my research questions. My research design utilizes satellite temperature,land cover data and urban form metrics in multivariant regression models to evaluate the climate benefit of urban agriculture. I discuss the data, methods, and results for each research question in detail in the following chapters. The dissertation ends with policy recommendations that can further support urban agriculture in U.S. cities.

CHAPTER 2

RELATED WORK

The literature review begins by discussing climate change and the role that land cover change plays in climate change at the regional and local level. Next I present a review of the literature investigating why cities are vulnerable to extreme heat by demonstrating the increasing temperature trends in cities. I then explore various UHI mitigation strategies illustrating the potential for urban agriculture to be included amongst these strategies, specifically analyzing the physiological difference between urban afforestation and urban agriculture. Because urban agriculture has myriad benefits beyond the climate benefit, I investigate the current state of urban agriculture, exploring how and why urban agriculture is being implemented across the country. I conclude the literature review with a discussion of why a local analysis of UHI mitigation strategies is an important contribution to the research field as well as for communities.

2.1 Climate Change

Land cover change (LCC) is one of the main planetary modifications caused by human actions, yet it is almost completely ignored by climate change institutions as an area of focus for strategies addressing climate change mitigation. Climate change policy institutions usually consider atmospheric concentrations of greenhouse gasses as the main driver of climate change and therefore set mitigation policies designed to curb greenhouse gas emissions. These strategies overlook the impact of land cover change on global warming as well as the role that land cover change plays in the global, regional and local climate system.

The Intergovernmental Panel on Climate Change's (IPCC) Fifth Assessment claims that the Earth is warming and that this "warming of the climate system is unequivocal"(IPCC
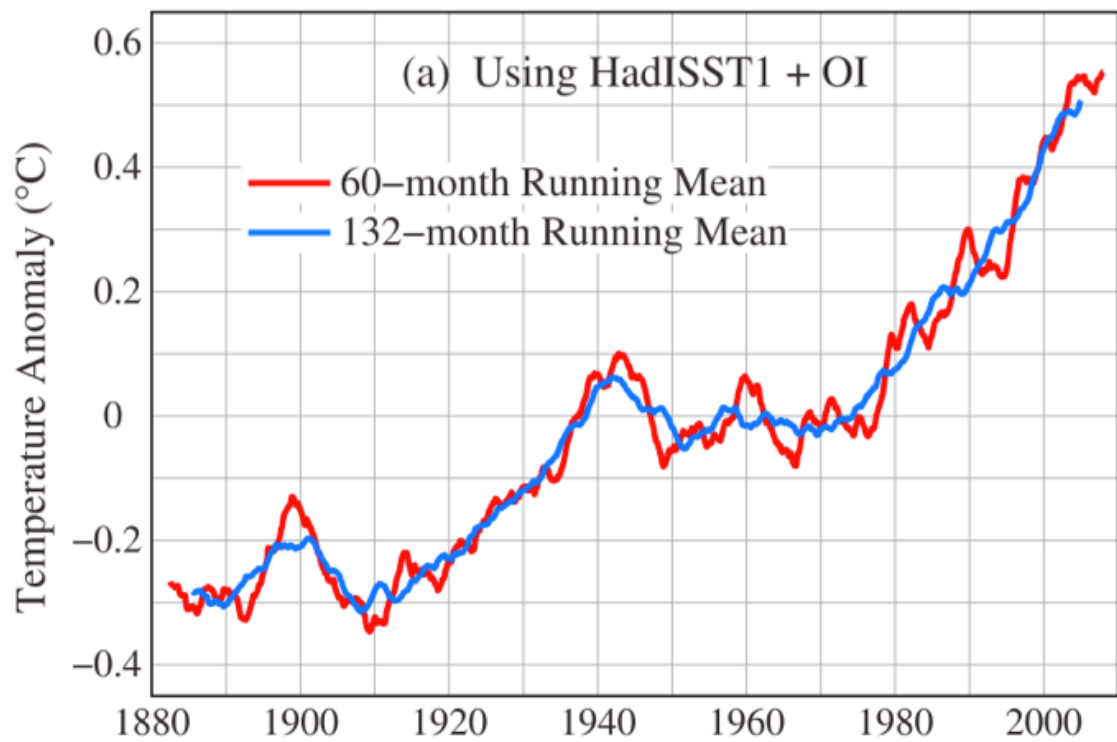
Figure 2.1: Global temperature anomalies illustrated with a 60 month and 132 month running average [21].

2014). Historical analyses have illustrated that since the 1970s, the global climate has increased by $0.2°C$ per decade (see Figure 2.1) [21]. The IPCC states that this warming trend is linked with anthropogenic forces and is due to the unprecedented levels of CO_2 in the atmosphere. Current climate change policy institutions, such as the IPCC and the US EPA, have set mitigation policies primarily focused on addressing atmospheric concentrations of greenhouse gas emissions. But are these mitigation policies going to be truly effective if they only target concentrations of greenhouse gases?

2.2 Greenhouse Gases

To understand the basic science behind greenhouse effect, it is important to first understand the three principal factors that influence the temperature of the Earth's surface:

1. The amount of incoming solar radiation entering Earth's atmosphere.

2. The albedo (reflectivity) of Earth's surface.

3. The presence of black bodies in the atmosphere [22].

Solar radiation is emitted from the sun as shortwave radiation. The frequency of radiation is directly related to the warmth of the emitted body- the higher the frequency, the higher the temperature. Therefore, the high temperature of the sun results in the emission of high frequency (shortwave) radiation. On the other hand, when solar radiation is absorbed by the Earth's surface it is reemitted as long wave radiation. The frequency decreases because the surface of the planet is much cooler than the temperature of the sun. For all intents and purposes we can consider the amount of incoming solar radiation to be fixed, though the level of incoming radiation changes marginally over time. Therefore the temperature of the planet is primarily affected by changes in its albedo and the amount of black bodies in the atmosphere.

The albedo of a surface refers to the amount of solar radiation that the surface material reflects instead of absorbing. Changes in land cover can have a dramatic affect on the

albedo of the Earth. For example, ice has a high albedo and therefore reflects more incoming solar radiation than other land cover classes. This reflected energy does not increase Earth's temperature because it leaves Earth's system. Black bodies are concentrations of greenhouse gases (GHGs) that reabsorb and emit long wave infrared radiation from the Earth's surface.

The major constituent gases present in the atmosphere do not absorb shortwave radiation. Instead the majority of solar radiation passes through the atmosphere. The radiation that is not reflected by Earth's surface is absorbed and warms the Earth. When the Earth absorbs incoming radiation that is not reflected back by albedo, it reemits this energy as long wave infrared radiation. The greenhouse gases in the atmosphere are not transparent to long wave radiation and therefore some if not all of the heat energy is absorbed and reemitted back to the ground level. This process is known as the greenhouse effect.

Water vapor is a very large contributor to the greenhouse gas effect. Water vapor in the atmosphere frequently condenses to form clouds. Clouds both reflect incoming solar radiation and absorb Earth's infrared radiation. The thickness of a cloudbank determines whether it cools or warms the environment. Clouds have a systematic feedback loop that can be positive or negative depending on the thickness of the cloud. Whether clouds act as a cooling mechanism depends on whether they cool or warm more, which is directly associated with the thickness of the cloud. The effects of clouds bring in a lot of uncertainty into climate models that are used for future temperature predictions.

Carbon dioxide is also a greenhouse gas and the presence of CO_2 in the atmosphere is tied to both natural and anthropogenic causes. One area of uncertainty in climate change science pertains to a lack of understanding of how much to attribute change to natural variability or to anthropogenic causes. From the use of proxy data, such as ice core samples, scientists have been able to determine that the amount of CO_2 in the atmosphere is at unprecedented levels which they link to the beginning of the industrial revolution and the burning of fossil fuels. Anthropocentric CO_2 emissions have drastically increased since the

(d)

Global anthropogenic CO$_2$ emissions
Quantitative information of CH$_4$ and N$_2$O emission time series from 1850 to 1970 is limited

Legend:
- Fossil fuels, cement and flaring
- Forestry and other land use

Y-axis: (GtCO$_2$/yr)
X-axis: Year
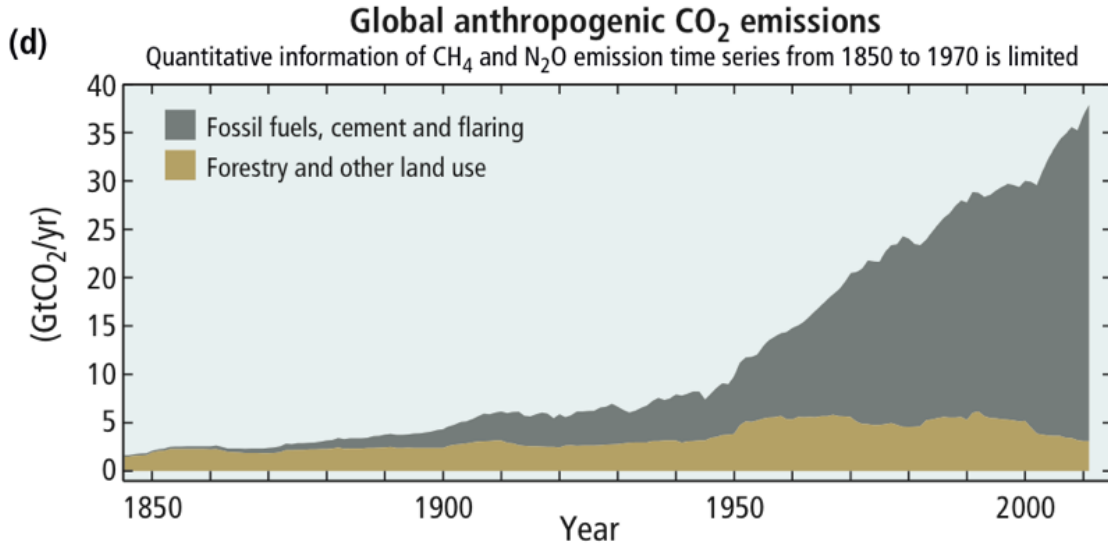
Figure 2.2: GlobalChanges in anthropogenic CO$_2$ emissions from 1850 -2010 [23].

pre-industrial era with 50% of anthropocentric CO$_2$ emissions occurring after 1970 (2.2) [23].“Pre-industrial levels concentrations of CO$_2$ were 280 parts per million. Today's levels are about 380 parts per million and many estimates suggest levels of 450 parts per million or higher by 2050” [24].

Carbon dioxide has a sophisticated and intricate life cycle within Earth's climate system that has a time span that ranges from diurnal cycles to cycles that take millions of years to complete. For example, the natural release of CO$_2$ through volcanoes is one of the main reasons why Earth's climate has never experienced a snow ball effect (plunged into an irretrievable ice age). However the volcanic release of CO$_2$ in the atmosphere is a process that takes thousands to millions of years to cycle through. By burning fossil fuels at our current rate, we are short-circuiting the planet's natural carbon cycle. This quick and intense change in the amount of CO$_2$ concentration may happen too rapidly for Earth's system to naturally respond. This uncertainty around how Earth's system will respond to the levels of CO$_2$ is one of the main driving forces behind the discussion of both the science of climate change [25], as well as how policies should be enacted in order to mitigate the problem of climate change.

2.3 Land Cover Change

Anthropogenic increases of greenhouse gases are not the only drivers of climate change, nor do they represent the complete spectrum of natural environmental alterations caused by human activity. Land cover change (LCC) resulting from urbanization and agricultural purposes is a very important driver of climate change. More than 30% of Earth's land surface has been modified by human activity [26]. Agricultural and pastureland make up more than 40% of the planetary surface representing one of the largest terrestrial biomes (see Figure 2.3). Since the 1970's irrigated agricultural lands have increased by more than 70% [27] but the IPCC has historically focused primarily on anthropogenic greenhouse gases and sets mitigation policies targeted at reducing their atmospheric concentrations. These strategies often overlook the impact of land cover change on global warming as well as the role that land cover change plays in the global, regional and local climate system.

A growing number of climate scientists argue that the discipline needs a new metric for climate change that will incorporate the effects of land cover change into these policy discussions [28, 29]. Because the regional effects of land use play a significant role in climate change, regional (as opposed to global) metrics are needed to best capture these effects. The current climate change metric, the global warming potential (GWP), does not address either the non-radiative forces of LCC or the importance of climate change at the regional and local scales. In understanding climate change, policy makers must understand the important role that land cover change has on the climate as well as understand that the scale at which we analyze the climate is also critical. Most of the policy debate and discussion of climate change focuses on the global level change and not the change happening at the regional and local levels. Pielke et al. argue that a new climate change metric is needed that takes into account regional changes as well as the forces from the hydrological and atmospheric cycle that will also heighten the awareness of the importance of land cover changes to our climate system. "Global averaged climate change may ... bear no well-defined rela-
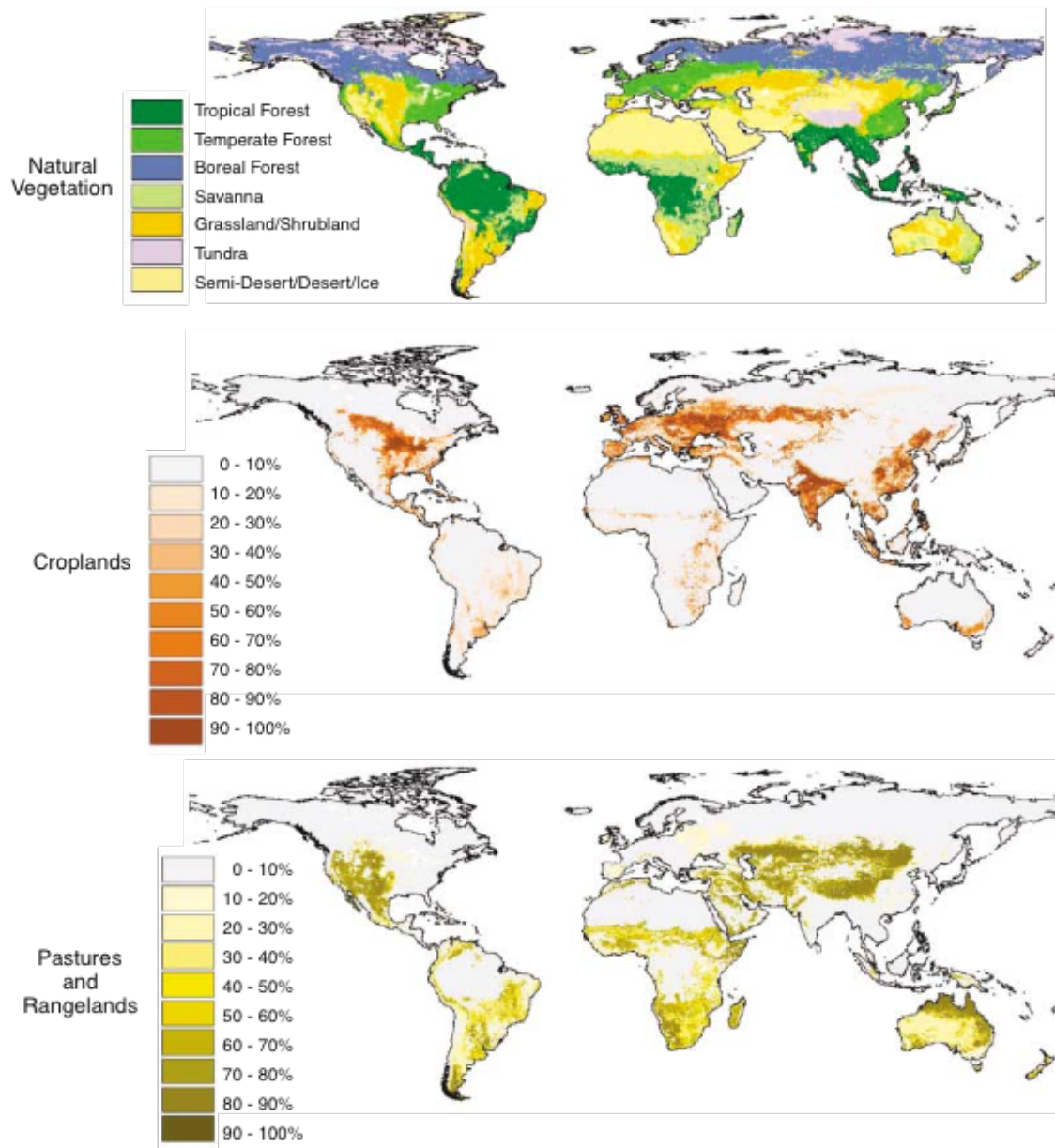
Figure 2.3: The top map illustrates the potential of natural vegetation without human influence and the bottom two maps illustrate the amount of croplands and pasturelands distributed across the globe in the 1990's [26].

tion to the real changes experienced in any region and these regional changes, which can be of any sign, are what impact people and will stimulate mitigation strategies to be applied" [29].

Regional and local climate change metrics address the climatic challenges that specific urban areas will face over the years to come and how climate changes will impact the places where people live. More people live in cities today than in rural areas and this percentage is expected to rise as high as 66% by 2050 [1] . The world's population is predicted to increase from its current level of 7.2 billion to 9.2 billion by 2050 [2]. The majority of this population increase will take place in developing countries. With a continuous migration to cities, we can expect the majority of these new world citizens to live in cities. As populations continue to increase, the demand on the food supply will also increase, resulting in a larger conversion of natural land cover to cropland and pastures. How we build, design and inherently change the local land cover will affect the regional and local climate. As such, it is imperative that we strive to understand the impacts that these changes have on the climate.

2.3.1 Regional Land Cover Change

The analysis of land cover change on temperature is a complicated and not always straightforward process. The combining of warming effects from land cover change is not a simple additive process to the global greenhouse effect. Land cover change creates nonlinear feedbacks, which are geographically dependent. Often the averaging of land cover change globally results in little to no effect on global temperatures. This offsetting problem makes land cover change as a climate forcing effect less straightforward than atmospheric greenhouse gases but not less important. The climate signal that results from coupling land cover change and the greenhouse gas effect will vary depending on if an analysis is being conducted at a regional scale or global scale. It also depends on the geographic location of the land cover change.

[1]The 2014 revision of the *World Urbanization Prospects* by UN DESA's Population Division
[2]World Population Prospects: The 2012 Revision by the United Nations.

The climate-forcing effect of anthropogenic land cover change primarily is a result of deforestation for the purpose of creating agricultural land and urban settlements. Areas that experience a decrease in forestation are prone to an increase in fluctuations of surface temperatures as well as a decrease in precipitation [30, 31]. Climate forcing effects from vegetational change result in land cover interactions with both atmospheric and oceanic systems.

Land cover change effects can be divided into two categories: biogeochemical and biogeophysical [32]. Biogeochemical processes are changes in the atmospheric chemical composition, such as carbon dioxide concentrations. For example deforestation affects the atmospheric carbon levels due to the decrease in the carbon cycle time for grasslands compared to the carbon cycle time for forests. Carbon emission due to land cover change, such as deforestation, accounted for more CO_2 emissions than the burning of fossil fuels until around 1960 [33]. Emissions of Atmospheric CO_2 between the years 1860-1980 are estimated to have be approximately 180 Gigatonne [33]. On the other hand, biogeophysical processes deal directly with effects from vegetation parameters.

Some vegetation parameters include surface albedo, surface roughness length, soil moisture and leaf area index. Surface albedo is a measure of the amount of reflectivity given off by a surface that is reflecting incoming solar radiation. Surface roughness length deals with the distribution of the surface with regard to height. Surface roughness length affects surface wind speeds as well as the wind gradients that create unstable environments for atmospheric mixing. Soil moisture represents the amount of available water at the surface that is available for evaporation. Leaf area index is a proxy for vegetation density and is described in more detail below. Changes in these parameters affect the climate in two main ways: first by changing the radiative forces of the land, which primarily results from the surface albedo change and second, by partitioning surface energy between sensible and latent heat through the altering of available water for evapotranspiration [30, 29, 34].

Leaf area index (LAI) is a descriptive measure of the planetary surface. LAI is "defined

as the ratio of leaf area to land surface area in a vertical column ... LAI is a representation of the density of vegetation at the surface" [30]. This ratio of leaf area to land surface can determine the amount of potential leaf canopy transpiration with greater LAI creating greater transpiration as well as the amount of stomatal conductance (how fast water transpires from the pores of a plant). LAI also affects the surface water balance by partitioning latent and sensible heat fluxes. The quantity of the LAI affects the role that soil moisture has in partitioning surface heat flux since dense vegetation cover decreases the impact of surface moisture on surface heat flux. LAI also describes how much sunlight hits both the soil and the individual leaves which directly affects the soil temperature and evaporation rate of soil moisture as well as affects a plants' stomatal conductance.

Many researchers have conducted historical land cover change simulations to investigate the climate-forcing effects from land cover change and to test the sensitivity of climate models [30, 34, 35]. Their goal was to illustrate that land cover is an integral climate factor, which is necessary for reproducing historic temperature trends. Their research illustrates the importance of anthropogenic land cover change as a climate-forcing factor.

Chase et al. examined the sensitivity of a climate model to changes in global leaf area index (LAI) in two scenarios over a ten year period. The researchers used the potential maximum LAI of a site for one scenario and the observed LAI from satellites as their second and control scenario in order to ascertain the sensitivity of the model to changes in LAI [30]. Zhao et al. conducted a similar study. Zhao et al. ran their model for a longer time period (17 years) and used a more conservative land cover pattern. In addition, they used an updated climate model that was coupled with a mixed layer ocean model instead of the model used by Chase et al. that used fixed sea surface temperatures [34]. Brovkin et al. conducted an analysis of historical human-induced LCC (specifically examining the result of deforestation to agriculture) over the last millennium. They examined how historical land cover change affects historical climate trends by specifically focusing on the biophysical effects [35].

All three studies arrived at similar conclusions and illustrated that the climate-forcing effects of land cover change are non-linear, depend on geographic location, and can be indirectly non-spatial. Changes in the regional climate that result from land cover change are dependent on the geographic condition. For example, deforestation in Boreal high latitude regions has a cooling effect, deforestation in the tropics has a warming effect and the climatic effects of temperate forests in the mid latitudes are mixed. As such, regional temperatures may increase or decrease depending on the latitude of the LCC and even areas that did not receive much LCC, specifically in the mid and high latitudes, could still be affected by spatially separate LCC.

The removal of boreal forests (high latitude LCC) has a large effect on the climate due to changes in radiative forces caused by surface albedo. The change in albedo from boreal deforestation provides a cooling of surface air temperatures that causes colder summer and winter temperatures [30, 35]. Bonan et al. [36] and Synder et al. [37] specifically examined the regional climate change due to deforestation at high latitudes. Bonan et al, [38] replaced the boreal forest with bare ground or tundra vegetation and found that the boreal forest both warms the winter and summer air temperatures. In the winter the boreal forest reduces the albedo of snow, (which is very high) and produces warmer winters. Therefore deforestation of the boreal forest would result in colder winters. The summers were also cooler because of a cooling lag effect from the winter. Because there was more snow and ice from a cooler winter as well as cooler ocean temperatures, the summer temperatures were lowered. Snyder et al. [37] analyzed the influence of six different vegetation biomes on the climate system. Their study compared the effects of removing all vegetation from a biome to the undisturbed biome. Snyder et al. findings are consistent with the findings from Bonan et al. [38] in that the removal of the boreal forest decreased temperatures due to enhanced albedo from snow-covered ground, with the snow persisting longer into spring.

At low latitudes, the transition of tropical forest to grasslands or agriculture result in changes of albedo and surface roughness as well as decreases in precipitation locally. In

snow free areas, the albedo change is not as important as the more dominate hydrological cycle. Deforestation affects the latent heat flux, which is due to the decrease in water transpiration from grasslands as compared to forest. This decrease in latent heat flux leads to higher surface air temperatures. Regional effects of deforestation from the conversion of forest to pastureland, agricultural or grass lands, were found to warm the region between 1.4°C - 2.5°C on an annual average [39, 40]. Coupling deforestation with a doubling of CO_2 resulted in warming as great as 3.5°C. The opposite is also true with regional afforestation over the tropics having a significant cooling over the region [41].

In addition to a decrease in local precipitation at the regional scale at the tropics, there also exists a decrease in precipitation that occurs at mid and high latitudes. This spatially decoupled effect is caused through teleconnections, related climate changes occurring over long distances, that illustrate the complexities of land cover change as a climate-forcing effect. The teleconnections result from changes in convective air circulation and changes in Hadley and Walker cells that are necessary for transporting water vapor and temperature towards the poles. Zhao and Chase arrived at opposite conclusion for the strength of the Hadley and Walker cells, but Zhao attributes this disagreement to their different land cover pattern assumptions. They both conclude that LCC impacts the atmosphere "by changing the position and strength of key elements of the general circulation" [34]. They also found that during the monsoon seasons in Asia there was a relationship between a decrease in LAI and a decrease in latent heat flux and precipitation as well as an increase in surface air temperatures [30].

From these studies we can see that effects of land cover change are geographically specific. In general tropical forests provide enhanced evaporative cooling and mitigate warming. Boreal forests on the other hand create a warming effect due to the low albedo of forest compared to snow. Forests in high latitudes mask high radiative reflection from snow by lowering the overall albedo. Though the regional effects of tropical and boreal forests are relatively straightforward, the effects of temperate forests are unclear. In essence "tropical

16

afforestation is likely to "slow down" global warming, whereas temperate afforestation has "little to no" climate benefit and boreal afforestation is "counterproductive" [42].

Due to the IPCCs myopic focus on atmospheric concentrations of greenhouse gasses, "carbon has become the currency used to assess the human intervention in the Earth's climate system" [29]. Because of this bias toward focusing on atmospheric greenhouse gases, studies have been conducted to compare the effects of carbon and land cover change on global temperatures, as well as, test the results of the IPCC scenarios when altered. Many researchers have conducted analyses that couple land cover change with greenhouse gases to illustrate that land cover change, though not straightforward, is an important climate forcing effect, and should be included in future global temperature analyses as it may alter predicted outcomes.

Chase et al. [43] conducted a study to compare a global climate simulation that used CO_2 and aerosols to a second global simulation that used land cover change data. Through the simulation of near surface temperatures the authors found that historical atmospheric greenhouse gases resulted in a temperature trend that was comparable to historical land cover change. The authors conclude that making the direct association of global warming to anthropogenic greenhouse gases a difficult and complicated task if land cover is not taken into consideration during analysis.

Feddema et al. [32] also address the problematic implications of linking temperature trends to greenhouse gases without the consideration of land cover change. In their research, the authors examine the outcome of adding land cover change to the IPCC's Special Report on Emissions Scenarios A2 and B1 in order to examine whether future land cover change will alter the outcomes predicted by the IPCC. They used a global model that combines anthropogenic greenhouse gases and land cover change and found that predicted regional climates at 2100 were significantly different than the original IPCC scenarios which only included GHGs. Their study shows that future land use decisions have the potential to alter IPCC climate change predictions since currently they are based solely on

atmospheric composition change" [28]. Though the simulations conducted by Feddema et al. [32] produce different regional climate outcomes as compared to the IPCC scenarios, the globally averaged temperature difference is less than 0.1°C. The authors argue that, "although land-cover effects are regional and tend to offset with respect to global average temperatures, they can significantly alter regional climate outcomes associated with global warming" [32].

Since land cover change creates nonlinear feedbacks, which are geographically dependent, the averaging of land cover change globally results in a zero effect on global temperatures. This offsetting problem makes land cover change as a climate forcing effect less straight forward as compared to atmospheric greenhouse gases but not less important. The "link between LCC in the tropics and higher latitude temperature changes" [34] illustrate the importance of including LCC when investigating global change.

2.3.2 Agricultural Land Cover Change

As populations continue to increase, the demand on the food supply will also increase, resulting in a large conversion of natural land cover to cropland and pastures. Over the past 300 years, land has aggressively been converted for agricultural purposes, resulting in approximately a six-fold increase of land cover change accounting for up to 5 billion hectares of land converted for use as both agricultural and pastureland [44]. The land patterns changed not only as a function of time but also as a function of geography, with the most recent massive land cover change for agricultural purposes occurring in the tropics, as opposed to Europe, the US, or Russia, which had previously been the most impacted areas [44].

Regional deforestation in the tropics converting forest to agriculture can alter not just the regional but also the global climate due to the long-range effects of teleconnections, as discussed previously. Feddema et al. [32] found that warming over the Amazon due to the conversion of forest to agriculture resulted in a temperature increase of more than 2°C.

Costa and Foley [39], illustrate this effect could increase as much as $3.5°C$ if one takes CO_2 emissions into account.

In the United States, Kalnay and Cai, [45], using an observation-minus-reanalysis (OMR) methodology, found that more than 50% of regional warming is due to land cover change, primarily from agriculture and urbanization as opposed to increases due to the greenhouse gases. Fall et al. [46] conducted a U.S. historical land cover change analysis and found that when agricultural lands were converted to any other land cover type, there was a warming effect. "The shift to agriculture results in a cooling for all conversion types and presents the largest magnitudes of cooling" [46]. This temperature trend even includes land cover conversion of forested land, which showed warming effects except when converted to agriculture. Agricultural land cover changes in temperate regions are driving regional climate change, and when land is converted to agriculture a cooling of near surface air temperatures results [46, 47, 48].

For the United States and specifically the Southeast, the non-radiative forcing effect of evapotranspiration has a stronger effect on regional climate than the radiative force of albedo. Increases in evapotranspiration from increased leaf area index cool surface temperatures at a higher magnitude than the albedo warming effect resulting in a net cooling [49, 50]. The albedo of agricultural land ranges between 0.17 to 0.23 and changes seasonally getting larger during the winter months. Evergreens on the other hand have an albedo of around 0.12 all year round. Therefore the increase of albedo from converting forested land to agriculture does not account for the full reason why agricultural lands are cooling regional temperatures throughout the US. The stomatal resistance of agriculture is approximately 40s/m as compared to 125 s/m for evergreens. A lower stomatal resistance allows for the release of more water than a higher stomatal resistance value. This increases water available for evapotranspiration and begins to explain the cooling effect [51].

Irrigation of croplands is another very important factor leading to cooler regional temperatures. Irrigation increases the soil moisture for plants and therefore increases the
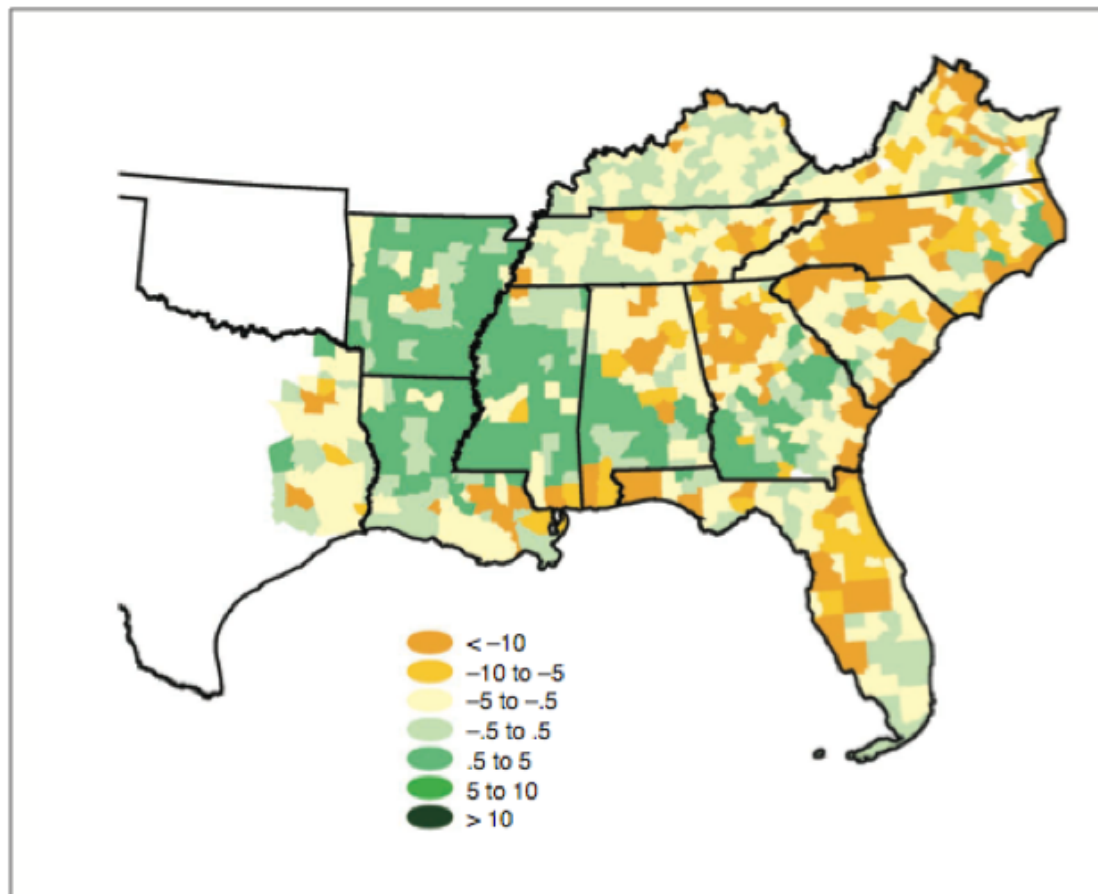
Figure 2.4: Forecast percentage change in forest cover, 1992–2020 [52].

amount of water available for evaporation. Researchers have studied the effects of irrigated crops on regional temperatures across the US and found cooling effects to produce a 1.6°C-5.0°C decrease in temperatures. [47, 48]. Lobell and Bonfills [47] examined the impact of temperature due to irrigation across California. They examined both daily minimum and maximum temperatures during summer months and found changes in maximum temperatures to be as low as 5.0°C due to irrigated cropland. The irrigation of croplands can help agricultural lands out perform forested land cover in lowering regional summer temperatures.

Over the recent decades, the southeastern US has experienced gradual land cover change resulting in a reforestation of previous agricultural lands (see Figure 2.4) [52]. Approximately 10 million acres of agricultural lands will be converted to forest between the years 1992-2020 [52]. This change in land cover, from agriculture to forest, represents the dominant land cover conversion in this region [51, 52]. Juang et al. [49] examined this reforestation process over the Southeastern United States. They analyzed the climate difference between a grass covered abandoned agricultural field, a planted pine tree field and a hardwood field. In their analysis they separated the radiative and non-radiative effects and found that the increased evapotranspiration in forested land tends to cool more than the decreased albedo warms. Evapotranspiration when analyzed alone can cool the surface by 2.9°C. They found that the conversion from the abandoned agricultural field to pine or hardwoods led to a cooling effect. Though grassland can be exchangeable for crops and pastures because of their similar properties, which affect the heat balance as well as the hydrological and carbon cycle [35], this result indicates that they are not a perfect substitute. The abandoned field in the study has a smaller LAI and surface roughness compared to agriculture and the field does not have increased soil moisture due to irrigation.

As opposed to Juang et al. [49], Bonan [36] and Trail et al. [51] found that land cover change resulting in agriculture tends to cool surface temperatures in the Southeastern US. Bonan [36] conducted a land simulation model over the US comparing modern vegetation

cover with natural vegetation cover. In his modern vegetation scenario he estimated current land cover and created a "maximum agriculture" scenario where he replaced the majority of forests, both coniferous and deciduous, with croplands. He found that maximum agriculture has the greatest cooling effect, cooling the Southeast more than 1°C. This cooling can be attributed to increases in albedo and the latent heat flux.

Trail et al. [51] examined temperature changes in the year 2050 in the Southeast for three different scenarios: a current land cover scenario, a reforested land cover scenario, and an increased agricultural scenario. They found that agricultural lands tend to have a cooling effect on surface temperatures for the majority of the Southeastern region, specifically in the spring and summer. This cooling effect is maximized during the summer months and when land is converted from deciduous trees to agriculture. The cooling can be attributed to an increase in albedo and decrease in stomatal resistance, especially since surface temperatures were found to be most sensitive to the stomatal resistance parameter. These studies illustrate that "land use practices that resulted in extensive deforestation in the Eastern United States, replacing forests with crop, have resulted in a significant climate change that is comparable to other well known anthropogenic climate forcings" [36].

2.3.3   Local Land Cover Change & the Urban Heat Island Effect

The influence of land use on climate is most pronounced at the scale of urbanized regions due to the urban heat island effect. As previously discussed, in its most generalized form, the UHI effect can be defined as the temperature differential between adjacent urban and rural areas. Urban heat island formation occurs due to changes in natural land cover associated with urbanization combined with the release of waste heat from urban activities, such as the operation of vehicles and air conditioning systems. Urban land cover changes include the reduction of vegetative covers and local soil moisture, as well as the resurfacing of natural land covers with the impervious materials of roads, buildings, and parking lots. These land surface changes tend to enhance the absorption and storage of solar radiation

and reduce evaporative cooling. The urban morphology of cities, such as in dense, downtown areas, can also enhance the UHI effect by serving to further trap and absorb reflected and emitted radiation resulting in elevated temperatures [53, 9].

Land cover changes in cities alter the parameters of the surface influencing the urban heat island effect. Some of the prominent surface characteristics affecting the urban heat island are albedo; the partitioning of the turbulent convective heat fluxes of latent and sensible heat; and the heat storage of the materials in the urban environment. As mentioned above, the albedo of a surface refers to the amount of solar radiation that the surface material reflects instead of absorbing. For example, fresh snow has a very high albedo (around 0.9) and therefore reflects the majority of incoming solar radiation. When surface materials change during urbanization, their albedo also changes. For an urban environment the average albedo is around 0.15, which is lower than a rural environment except for forest (which has a quite low albedo) and dark soils [9]. Since urban areas have on average a lower albedo than their surrounding areas this means that they absorb more solar radiation, which in turn warms the surface.

The partitioning of turbulent heat fluxes is one of the most important surface characteristics affecting the UHI (See Figure 2.5). Sensible and latent heat fluxes are both examples of convective heat transfer, which transports heat vertically through the atmosphere. The sensible heat flux occurs when the boundary layer is unstable (hot air below cold air). This instability occurs because the sun warms the Earth's surface during the day making the Earth's surface warmer than the air above it. Because hot air is less dense than cold air, the near surface air rises in turbulent eddies exchanging heat with the atmosphere as it mixes with the air.

The latent heat flux is directly related to moisture level (soil, plant, body of water) of the surface and occurs when water is evaporated, thus changing phases from a liquid to a gas. This phase change requires energy input, which is taken from the environment and cools the area. This is known as evaporative cooling and is the same phenomenon that

incoming and
reflected solar

greenhouse effect

greenhouse + heat island effect
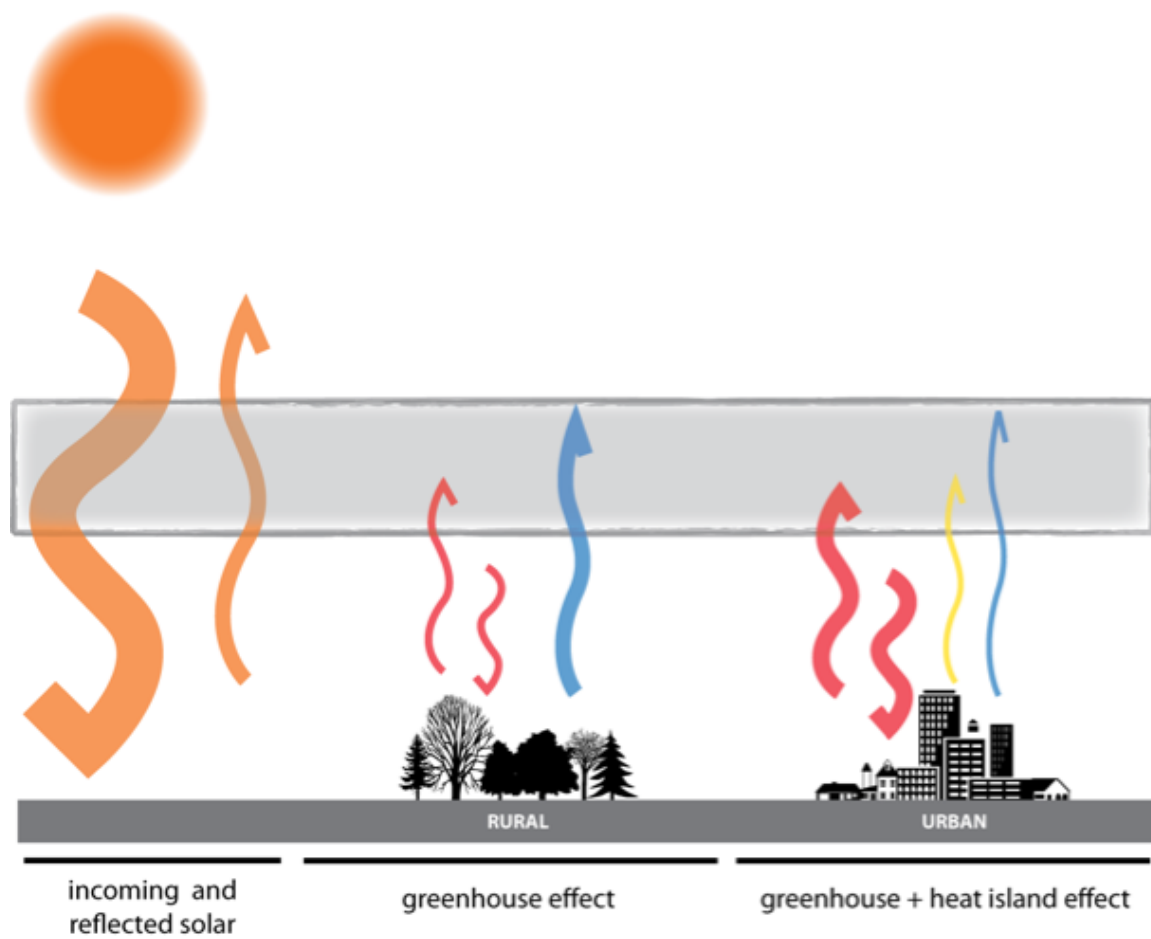
Figure 2.5: This image illustrates how the partitioning of the turbulent heat flux changes in an urban condition versus a rural condition. The rural area has a much larger partitioning of latent heat whereas sensible heat is the primary driver in the urban condition (www.urbanclimate.gatech.edu).

cools the body when one sweats. The sweat is evaporated off the skin, which takes needed heat from the body's surface in order for sweat to change phases from a liquid to a gas, thus cooling the body. Latent means that the heat is released later in the process. A water particle rises in the atmosphere until it reaches a height where the surrounding air is cooler than the water particle. When this occurs, the water particle expands doing work on the environment, and condenses, which releases the heat (which was taken from the surface) into the atmosphere.

The Bowen ratio is the ratio of sensible heat to latent heat (Qh/Qle), and this ratio influences the surrounding climate by affecting the way stored surface energy is released into the environment. When the sensible heat is greater than latent heat, then the sensible heat flux is the primary transport of surface energy and represents a warmer climate. When latent heat is greater than sensible heat then the climate will be cooler and wetter. Tropical forests have a Bowen's ratio of 0.1-0.3 whereas deserts have a Bowen's ratio of 10 [9]. Therefore, as land use changes in an urban environment, converting natural vegetation to impervious surfaces (streets, parking lots, buildings), these surfaces become sealed off to moisture. The moisture level decreases in the soil and vegetation, and even in bodies of water, as many cities have chosen to bury their streams underneath the surface. "Probably the most important change is the lower evapotranspiration in the city leading to a preferential channeling of energy into sensible form (Qh and ΔQS) and therefore a warming of that environment. The sensible heat appears to be put mainly into greater storage in the morning and released to the atmosphere in the late afternoon and evening" [9].

The conversion of vegetation in urban land uses not only decreases moisture level for evaporation but also decreases the process of transpiration from vegetation. Transpiration is an inevitable byproduct of photosynthesis that occurs when a plants stomata opens to take in or release CO_2. This process simultaneously evaporates moisture from within the plant. Transpiration is an effective way of evaporating the moisture deep in the soil. Soil moisture is taken into the plant through the root system and evaporated through the stomata

in the leaves. Therefore the presence of vegetative land cover, such as lawns, parks, street trees, green roofs, etc. lowers the near air surface temperatures through evapotranspiration (evaporation + transpiration).

The change in land cover also brings about a change in the heat storage of an urban environment. As discussed earlier, when the Bowen's ratio increases then the sensible heat is stored in the daytime in the impervious surface of the urban environment. The geometry of the urban environment (buildings) also increases heat storage capacity by increasing the surface area. This increase in surface area allows for more absorption of solar and long wave radiation, which increases the energy at the surface. Since most building and street materials have a low heat capacity, less energy is needed to raise the temperature of these urban materials. Low heat capacity makes a material more susceptible to heat changes. Therefore, in the evening when the sun sets, the energy stored in these materials is exchanged with the air, further raising the near surface air temperatures. This process contributes to urban heat islands having higher minimum temperatures than their surrounding rural areas.

Sky view factor is another characteristic that can contribute to urban heat islands and increase the minimum temperatures. Sky view factor is a measure of the percentage of canopy cover that obstructs the view of the sky. It is a percentage of the sky that can be viewed from the ground, and can be used as measure of urban canyons as well as forests. An open field has a sky view factor of ~ 1, whereas a floor in a street canyon can have a sky view factor of ~ 0.4 [9]. The lower the factor, the more obstructed the sky. The obstruction of the sky inhibits the ability of ground surfaces to release long wave radiation to the atmosphere. Urban forests that have a reduced sky view factor within their canopies can produce excess nighttime temperatures due to their sky view factor [54].

UHI measures

There has been extensive research identifying and measuring urban heat islands since the 1960s. The UHI intensity varies from city to city and the range can vary from 4°F to as large as 22°F due to city design, size, and morphology [9]. In the US specifically, large cities have been found not only to exhibit a prominent urban heat island effect with higher temperatures than their proximate rural areas but also to be warming over recent decades at a significantly higher rate, resulting in a rising number of excessively hot days in urban areas [55, 56]. Analyzing weather station data form the Global Historical Climatology Network, Stone [55] examined temperature anomalies for paired rural and urban weather stations. Using meteorological observations from 50 of the most populous US cities along with population data coupled with light intensity satellite images to identify paired urban/rural stations, Stone examined the influence of land use on climate at the local scale from 1957 to 2006 and measured the rate of change in urban heat island intensity in each decade. The results illustrated the impact of land use on climate change in two respects: first, urban weather stations were always between 1.2°C and 1.8°C warmer than rural stations and, second, the mean rate of warming was higher in urban areas than in rural areas.

In a more recent study looking at a similar set of large US cities, Stone et al. [10] found over the years of 1961-2010 that cities were warming on average approximately twice as fast as rural areas, and in essence the planet as a whole. This amplified rate of warming in cities holds direct implications for heat-related health effects and health effects associated with heat-induced air pollution.

2.4 Climate Change and Health in Cities

Climate change is projected to significantly impact public health across the globe in numerous ways. A rapidly changing climate will bring severe weather patterns such as hurricanes, droughts, and heat waves. These extreme weather patterns will exacerbate global

health challenges such as malnutrition, infectious diseases, food born illnesses, and heat stress, to name a few. Presently extreme heat is responsible for more annual fatalities in the United States than any other form of extreme weather [1], and the exposure to these extreme heat conditions is only expected to intensify with climate change, especially in our urban environments. Rising temperatures directly result in a high number of occurrences of heat stress and heat stroke, and indirectly result in mortality due to cardiovascular and respiratory diseases. Additionally, air quality will also worsen in our cities with increasing urban temperatures [57]. Urban populations are particularly vulnerable to threats of excessive heat as they have increased health exposures compared to their counterparts in rural areas. The urban heat island effect makes these populations more susceptible to risks associated with extreme heat [58, 59]. In addition, urban areas are home to a large number of vulnerable communities who lack the necessary resources needed to adapt to these trying conditions.

On average, yearly estimates of heat-related deaths in the United States range from 170-690 per year [1, 2, 3]. This range is large because heat-related deaths are difficult to classify and therefore often go unnoticed especially during heat waves that fall below the threshold of public awareness. Differing state standards on heat-related mortality classification and the wide variety and number of symptoms that can result in heat-related mortality further complicate accurate diagnosis [3, 60]. Extreme heat can result in numerous heat-related illnesses such as heat camps, fatigue, heat stress, heat stroke and even death. Heat-related illnesses occur during extreme heat conditions because of the body's inability to adequately cool itself through sweating resulting in high body temperatures that can be damaging to a person's health. Extreme heat further complicates existing chronic diseases such as those associated with cardiovascular or respiratory illnesses. Individuals at elevated risk to extreme heat include, infants, the elderly, individuals with mental illness or those with an existing comprised health conditions [1]. The climatic conditions underlying extreme heat are influenced by both global and local scale drivers. At the global scale, historical analyses

have illustrated that since the 1970s, the global climate has increased by 0.2°C per decade [21]. Recent work has found trends in minimum temperatures, apparent temperatures, and the duration of the frost-free season to be increasing in recent decades across the US [61, 62, 63, 64, 65, 66]. The frost-free season has an average increase of approximately two weeks across the US, with most dramatic changes occurring in the Western United States [61, 64].

Gaffen and Ross [65] found minimum apparent temperatures to be increasing by 25% or more for most areas of the US, between 1949 to 1995. They found that all US regions are experiencing significant positive trends in three and four-day heat waves and that there was a 20% increase in frequency of heat waves over the 47-year study period for the eastern and western US. Extreme heat events, defined as days in which apparent temperatures exceed the 85th percentile of the long-term temperature average for a particular location, have also been found to be increasing by two days per decade over the period from 1956 to 2005 in large US cities [67].

Habeeb et al. [11] found that heat waves are intensifying in large cities across the United States. In their study, they examined changes in four heat wave characteristics: frequency, duration, intensity, and timing, from 1961 to 2010, in 50 large US cities (See Figure 2.6). They found these heat wave trends to be significantly increasing across the board. The heat wave season is extending, by starting earlier and ending later, and heat waves are happening more frequently and lasting longer with higher temperatures. These heat wave trends begin to illustrate the extent to which urban populations are increasingly exposed to heat-related health hazards resulting from changing trends in extreme heat. These increases in heat wave characteristics can have negative public health consequences. It is especially important to raise awareness of these trends in increasingly vulnerable cities, especially cities which might not be considered "hot" cities like Portland or San Francisco. For example the researchers, found, in San Francisco, heat waves are starting 1.5 months earlier in 2000 than they did in 1960 [11].
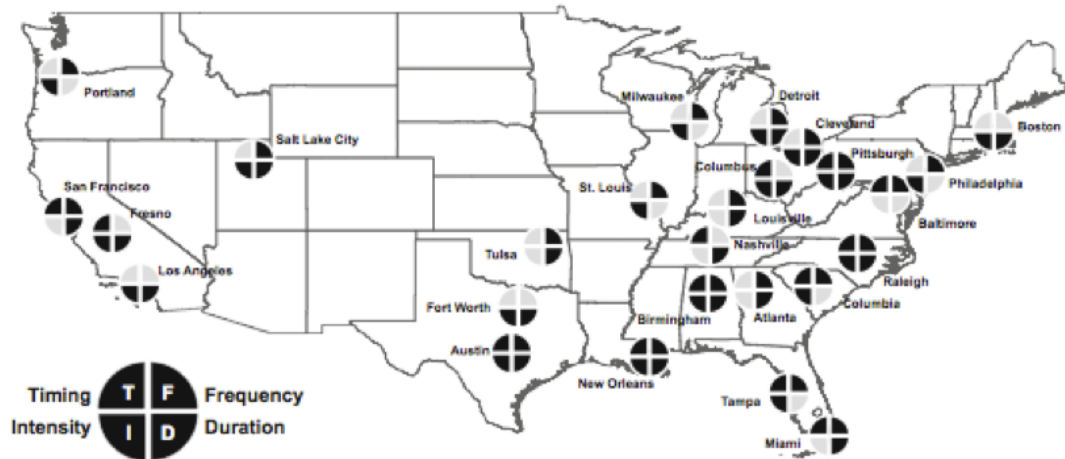
Figure 2.6: This map shows the cities that have at least two heat wave characteristics with significant trends above the national average. The sections of the pie represent heat wave characteristics (upper left, timing; upper right, frequency; lower left, intensity; lower right, duration) [11].

In the future, cities will become even more vulnerable to extreme heat events as a result of global climate change. Recent studies indicate that global climate change may be increasing the number and duration of heat waves in areas that are already experiencing extreme heat events [68]. Using global climate models to predict future weather patterns has shown that the southwest, southeast and midwestern regions of the United States are expected to have increases in heat waves with some cities experiencing a 25% increase in heat wave frequency [68, 69]. Studies examining the relationship between global climate change and mortality have shown that with a "Business as Usual" emissions scenarios the US can expect a doubling of heat related deaths by the end of the century, with some estimates as high as 2,200 heat related deaths occurring annually [70, 71].

At the local scale, the urban heat island effect serves to magnify the impacts of summer heat waves with cities often experiencing a rise in temperatures that is several degrees higher than the comparable rise of temperatures experienced in rural areas [6]. With elevated urban temperatures during heat waves comes greater heat- related fatality rate in cities. In examining a 1998 heat wave in Shanghai, Tan [59] found the heat mortality rate

30

to be about four times greater for urban areas compared to exurban areas. A similar outcome was observed in Europe in the aftermath of the 2003 heat wave, where post event assessments found the rate of heat fatality to be greater in cities than in the surrounding rural areas [58]. Heat index measurements during this event were found to be as much as 50% higher in the city center than in the surrounding rural areas – an outcome associated with the urban heat island effect [72].

Additional studies have illustrated climate change will increase the minimum temperatures in cities. In accounting for both global climate change and urban heat island effects, McCarthy et al. find the number of extremely hot nights to increase by as much as 50% in large global cities when compared to their rural areas by 2050 [73]. Their research showed through a simulation of eight large international cities that though climate change increased maximum temperature at a similar magnitude for urban and rural areas, the minimum temperature increased more rapidly in urban areas for all eight international cities than in rural areas.

With regard to urban air pollution, climate change is expected to play a significant role in the formation of secondary air pollutants, such as tropospheric ozone (O3) and fine particulate matter (PM2.5). In his survey paper, *Climate Change, Air Quality and Human Health*, Kinney [74] presents the findings from numerous studies examining the effect of climate change on air quality. These studies range from historical episodic analysis to complex algorithmic models used for climate and air quality predictions. From his research examining these studies there is a consistent conclusion that climate change, including rising temperatures, will increase concentrations of ozone, with recent studies suggesting metropolitan ozone levels may increase 5 to 10% by 2050 as a product of climate change alone [74]. As many large metropolitan regions fail to meet health-based air quality standards, even a small increase in ozone concentrations can translate into significant increases in the number of exceedances of air quality standards. Future levels of PM2.5 are also expected to impact human health as a result of climate change. Almost 20,000 additional

31

premature deaths are anticipated based on the effects of climate-induced air pollution by 2080, with fine particulates found to be responsible for more than 90% of the increase in mortality and ozone accounting for the remainder [75].

Not only does the presence of cities impact the regional climate but also studies suggest clear linkages between the structure of the built environment and health exposures such as extreme heat events and air pollution. The physical structure of urban environments has been associated with the frequency of ozone exceedances in large U.S. cities, and sprawling regions may be more vulnerable to the effects of climate change than regions characterized by compact development patterns. Stone et al. [67] have examined the association of frequency of EHEs and urban form at the level of the metropolitan region over a five-decade period. Using the sprawl index to measure urban form and calculating the mean annual rate of change in extreme events between 1956 and 2005, Stone et al. [67] found that the rate of increase in the annual number of extreme heat events in the most sprawling metropolitan regions is more than double the rate of increase observed in the most compact metropolitan regions. This association can be attributed to a higher rate of deforestation and urban heat island formation in rapidly decentralizing metropolitan areas [67].

The greater frequency of ozone in sprawling cities is believed to result from both increased emissions and enhanced temperatures associated with the urban heat island effect. In the research study *Urban Sprawl and Air Quality in Large US Cities* [57]. Stone examines the association between the extent of urban decentralization and the average number ozone exceedances of the 8-h national ambient air quality standard. The study found that the most sprawling cities experience 62% more high ozone days annually, on average, than the most compact cities. Controlling for ozone precursors, the analysis showed that the correlation between sprawl and increased air pollution continues to hold illustrating that increased urban temperatures due to the UHI to be a dominant driver in ozone exceedences.

2.5 Urban Heat Island Mitigation- Is urban agriculture a viable UHI mitigation strategy?

UHI mitigation strategies are important for cities since the urban heat island effect increases a city's vulnerability to heat-related mortality. There are many strategies for mitigating the urban heat island effect, such as albedo and vegetation enhancements as well as strategies to reduce anthropogenic heat waste. When implemented city-wide, cool roofing and paving strategies have also been shown to significantly lower air temperatures [13, 14]. For regions with sufficient annual precipitation, tree planting and other vegetative strategies – such as the installation of green roofs – have been found to be the single most effective approach to moderating the urban heat island effect [76]. These strategies have been shown to reduce the urban heat island effect in some modeling studies by more than 50% [15, 16]. Though previous studies have examined the role of vegetation in mitigating the UHI effect, none of them have investigated the potential of urban agriculture as a mitigation strategy.

2.5.1 Urban Forests vs. Urban Agriculture

When investigating urban agriculture as a UHI mitigation strategy it is important to understand the limitations that this vegetative strategy may have especially when compared to other strategies like urban forestation. Large-scale vegetation strategies have been shown to be the most effective means of mitigating the UHI effect with afforestation having the greatest impact [76]. A forest's large canopy and leaf area index generate more evapotranspiration than any other vegetation and therefore are more effective at cooling local areas. As previously discussed, the process of evaporative cooling is extremely beneficial when it comes to cooling cities. In addition to evaporative cooling, the shading from tree canopies effectively cools areas by blocking out solar radiation. Hart and Sailor [77] from their investigation of Portland's heat islands concluded that canopy cover was "the most important urban characteristic separating warmer from cooler regions" (pg.405). Due to

their high evapotranspiration and shading, forested areas can create an oasis effect in dry warm cities. By creating a moist and cool climate, advective turbulence horizontally transports cool moist air from the cool forested area to warmer areas nearby. A forested area can be as much as 6°C cooler than the surrounding built environment [54]. Forested areas are also more effective at intercepting precipitation, which can help to alleviate rainwater runoff. Deciduous forests can intercept between 10-25% of the total annual precipitation and coniferous forests can intercept between 15-40% [9]. Agricultural crops also exhibit these same characteristics: evapotranspiration, shading, precipitation interception and oasis effects, but to a smaller degree as compared to forests.

Urban agricultural crops do have some climatic advantages over forested areas. First, crops have a higher albedo than forested areas. The albedo of vegetation is to some extinct a function of the plant's height. As the plant's height increase then its albedo decreases. For most crops with vegetation less than 1 meter, they have an albedo between 0.18-0.25. Since trees are well above this height, their albedo is much lower. On average the albedo for trees is around .09, but this value spans a range between 0.05-0.2 depending on the type of tree [9]. Since crops have a higher albedo, then they are more effective at reflecting short wave solar radiation. Also, agricultural crops have a much larger sky view factor and therefore do not inhibit the emissions of long wave radiation to the atmosphere. This effect is especially pronounced during the evening. Due to the difference in sky view factors, forested parks have a different timing in their maximum "park cool island" (PCI) effect (which is synonymous to the oasis effect) as compared to gardens or open grass parks. A forested park is coolest relative to its surroundings during the afternoon, therefore having an afternoon maximum PCI, whereas gardens or open grass parks have a nocturnal maximum PCI [54]. This diurnal difference in cooling may make urban agriculture more effective at decreasing minimum temperatures than urban afforestation. High minimum temperatures (high nighttime temperatures) have been shown to be most closely associated with adverse health outcomes during extreme heat events [78, 79, 80]. If urban agriculture is more

successful at cooling nighttime temperatures than reforestation, then urban agriculture may have a higher potential to reduce the public health risks associated with heat waves.

The irrigation of agricultural crops coupled with its lower stomatal resistance may offset the difference in evaporative cooling from the larger LAI from forested land. Irrigated lawns have been shown to have large effects on cooling of near surface air temperatures. A suburban area with irrigated lawns was shown to have 80% greater evaporation rates than rural rates [53, 81]. Fall et al. [46] conducted a U.S. land cover change analysis coupled with an observation-minus-reanalysis (OMR) methodology and found that when agricultural lands were converted to any other land cover type, there was a warming effect and vice versa. The primary environmental/climate benefit of using urban agriculture as a UHI mitigation technique is that irrigated agriculture has the potential to decrease UHI through increased evaporative cooling. Though irrigation enhances evaporative cooling for crops, this comes with a disadvantage, as water in many urban cities is becoming a precious commodity.

2.5.2 Benefits of Urban Agriculture Beyond Climate

In addition to potentially being a viable urban heat island mitigation strategy, there are many other advantages to increasing the amount of land engaged in urban agriculture. Forestation brings with it many advantages, such as increase habitation, reduction in stormwater runoff, as well as provide recreation sites. However, from the perspective of planning policies, there are many advantages for increasing the portion of land engaged in urban agriculture such as environmental, social and economic advantages. From an environmental standpoint, urban agriculture - from urban farms, to community and back yard garden - is developing as a valid alternative to industrial agriculture. Industrial agriculture is a huge source of environmental degradation from air pollution, to surface and groundwater contamination due to use of heavy pesticides and fertilizers. Additionally, these agricultural practices produce extensive soil erosion, which destroys the landscape making agricultural

sites eventually unsuitable for farming while also further polluting the waterways. Bio-diversity is lost due to monoculture production, use of pesticides, deforestation, and the use of Genetically Modified Organisms (GMOs) [82, 83].

In addition to these environmental problems, transportation costs with respect to energy use and greenhouse gas production have become significant environmental challenges that arise from industrial agriculture. It is estimated that food travels 25% further today than it did in 1980, traveling as much as 1,500 to 2,500 miles from point of production to point of consumption with "more food ... shipped from markets outside the U.S. than at anytime in history" [84, 85]. Fruits and produce can spend from seven to fourteen days in shipment with approximately 50% of all food spoiling due to this extended shipment time. Additionally, greenhouse gas emissions from industrial agriculture now represent 6% of the total emissions in the United States [86].

Urban agriculture is attempting to reverse these current trends from the industrial food system by providing valuable ecological services to an urban area. Urban gardens reduce the negative environmental externalities associated with transportation by locating within urban areas and close to customers. It is estimated that food waste, including food packaging makes up over a third of the waste that ends up in municipal landfills [87]. Much of this waste could be diverted from landfills by limiting the need for excessive packaging due to limited transportation distances and the ability to compost food waste for urban agricultural production. In addition, urban agriculture enhances storm water management by increasing the amount of pervious surface in the city, and preserving open space, which helps to mitigate the effects of noise and air pollution [88].

Urban agriculture also provides social advantages by building community and reconnecting people with food production as well as with the environment. Currently there is a lack of visibility of the food system within cities. Urban agriculture can begin to change this through the involvement of local community gardens, local farmers market, and teaching programs. Urban agriculture can illustrate the importance of integrating the city with

the environment. It can also begin to create local and self-reliant food systems. This makes communities more resilient to potential threats in food production systems. It has been recommended that in order to prepare for emergencies, local communities should be able to supply up to one-third of the food required by their citizens. Currently this number is less than 5% [87].

Urban agriculture can also provide viable economic opportunities to cities. Currently small farms in the U.S. are able to be profitable, even organically certified ones [89]. Urban commercial gardens utilize raised beds, soil amendments, and season extenders such as row covers and hoop houses to produce yields that can be thirteen times more per acre than rural farms [90]. "Consumer demand for organic products is growing sharply, leading to significant price premiums and good financial opportunities for producers." [89].

Urban agriculture can utilize Community Supported Agriculture (CSA), which is a program that allows people to receive a delivery of food for a specified time interval. By pre-purchasing food through CSAs, this allows farmers to have an identified list of buyers as well as generate upfront operating costs needed for production. Urban agriculture is also creating additional contract links with high-end "farm-to-table" restaurants and even with educational cafeteria programs. "According to the USDA, the number of farmers' markets has increased almost 50% since 1994" [90] and there are over 1,000 CSAs throughout the United States. This rise in the number of market distribution sites and options illustrates the further growing demand in locally produced agriculture from urban farms.

Urban agriculture has been utilized to revitalize neighborhoods with vacant properties and has also become an effective brownfield reclamation strategy in urban areas [86, 91]. Converting vacant and brownfield lots to active urban agriculture addresses environmental justice and social equity issues by promoting environmental health and access to healthy foods in food desert communities. Urban agriculture provides social advantages by building community and social capital and reconnecting people with food production as well as with the environment. As such, when selecting between vegetative UHI mitigation strate-

gies it is important for planners and policy makers to be able to quantify the difference between vegetative approaches in order to understand the tradeoffs they are making climatically, environmentally and socially.

2.6 Local scale and land area

My research investigates the impact of urban agriculture as a heat mitigation strategy at the local scale. Many urban heat island mitigation studies are conducted using regional climate models that have coarse resolutions of around 4 km^2. Local scale modeling, with resolutions of less than 1km^2, can be a useful tool for policy makers as it provides them with the ability to assess policy interventions by modeling the impacts of potential changes on the built environment at the neighborhood level. Local scale models allow for the investigation of how neighborhood urban design characteristics, such as street design and building heights, can impact land cover interventions. Urban heat island mitigation strategies implemented on smaller scales have also been shown to reduce heat related health risks [92]. Conducting a land cover analysis at a the local scale not only provides policy makers with information needed to promote more sustainable policies but also it empowers neighborhood residents by giving them the understanding of how changes to their built environment can affect the health of themselves and their neighbors.

In my research, the neighborhood scale analysis quantifies the impact of various sizes of urban agriculture interventions. There are differing urban agriculture typologies, from small backyard gardens to large community gardens and urban farms. Part of my future research will be aimed at determining the minimum size of a land cover change area that is needed to make a beneficial impact to the local climate. Determining impact size enables planners to understand the parameters needed to successfully implement urban agriculture as a UHI mitigation strategy.

2.7 Literature Summary

Land cover change is one of the main planetary modifications caused by humans. Over one-third of the surface of the planet has been modified by human activity. Agriculture and pastureland represent the largest of these anthropogenic land cover changes accounting for more than 40% of the planet's terrestrial biomes [26]. LCC can significantly impact the climate by altering the atmospheric concentrations of greenhouse gases and change the hydrological cycle by influencing the partitioning of latent and sensible heat. Though LCC represents a significant climate forcing effect that has been shown to be integral in projecting climate trends both globally and regionally [36, 43, 32], climate change policy institutions primarily focus on atmospheric concentrations as the main driver of climate change and set mitigation policies designed to solely curb greenhouse gas emissions.

This viewpoint on our changing climate overlooks the impact of land cover change on global warming as well as the role that land cover change plays in the global, regional and local climate system. In understanding climate change, policy makers must understand the important role that land cover change has on the climate as well as understand that the scale at which we analyze the climate is also critical. Most debate and discussion happens around the average change in climate at the global level and not the change happening at the regional and local levels. As such, my research examines the effect of land cover change on the local climate. Specifically I am examining the role that urban agriculture can play in lowering local temperatures. Climate scientists have well documented the effects of agricultural land conversions on both the regional and global climate [36, 39, 46, 32, 49, 45, 47, 48, 51] but the climatic effects of agriculture at the local level is a relatively unexplored research area.

At the regional scale, the effects of land cover change are geographically dependent. For example, deforestation in high latitudes can have the opposite effect on temperatures than deforestation in the low latitude tropics [42]. As such, it is important to understand

the context in which the application of land cover change is occurring. My research study site, Atlanta, GA, is located in mid latitudes. Researchers have shown that conversion of land cover to agriculture in mid-latitudes generally cools local climates specifically in the Southeastern United States [36, 46, 51]. Agricultural land in this region decreases local temperatures when converted from any other land cover including forested land [46]. The increase in albedo, decrease in stomatal resistance, and relatively similar leaf area index of agricultural land cover compared to forested areas coupled with the hydrological benefits of irrigation provide a set of parameters enabling these observed regional cooling effects [36, 47, 48, 51]. As such, I hypothesize that urban agriculture will lower local temperatures in the Atlanta area.

At the local level, land cover change is most pronounced in the urban heat island effect [9]. The UHI effect increases temperatures in urban areas specifically raising nighttime temperatures. These temperature increases make urban residents more vulnerable to extreme heat events [78, 79, 80]. High minimum temperatures have been shown to be most closely associated with adverse health outcomes during extreme heat events [78, 79, 80]. This increase in heat exposures can create serious negative public health effects, as extreme heat is responsible for more annual deaths in the United States than all other natural disasters combined [1, 3]. The urban heat island effect makes urban populations more susceptible to risks associated with extreme heat [58, 59] by magnifying the impacts of summer heat waves in cities resulting in greater heat related fatalities in urban areas [58, 72, 6, 59]. As such, I am proposing to analyze the effects of urban agricultural interventions during heat waves. Specifically, I am investigating whether urban agriculture maintains its cooling effect during extreme heat conditions.

As heat waves are increasing across large US cities [11], mitigating the urban heat island effect should be considered a public health priority. In places with sufficient rainfall, vegetation strategies have been shown to be the most effective strategy for lowering urban temperatures, with as much as a 50% reduction in the urban heat island effect [15,

16]. These vegetation strategies include forestation of urban areas as one of the main approaches. As discussed previously, agricultural lands have different biogeophysical parameters than forests. One parameter specifically tied to urban conditions is sky view factor. The large sky view factor associated with agriculture can affect the timing of the maximum "park cool island" (PCI). Gardens or open grass parks have a nocturnal maximum PCI [54] compared to the daytime maximum PCI for forested areas. This diurnal difference in cooling may make urban agriculture more effective at decreasing minimum temperatures than urban afforestation. As such, my research aims to not only investigate how urban agriculture acts as a heat mitigation strategy, but to compare urban agriculture to the vegetative mitigation strategy of urban forestation.

In addition to potentially cooling the climate, urban agriculture provides social advantages such as building community and social capital as well as reconnecting people with food production and with the environment. As such, when selecting between vegetative UHI mitigation strategies it is important for planners and policy makers to be able to quantify the difference between vegetative approaches in order to understand the tradeoffs they are making climatically, environmentally and socially.

CHAPTER 3

CONCEPTUAL FRAMEWORK AND METHODOLOGICAL APPROACH

My research bridges two built environment and health research areas: urban heat islands and urban agriculture. I am specifically interested in investigating the potential for urban agriculture to act as an urban heat island mitigation strategy at the neighborhood scale. Though previous work has examined the role of vegetation in mitigating the UHI effect, the potential for urban agriculture to act as a mitigation strategy is an unexplored research area. Exploring the connection between urban agriculture and urban heat islands is the main focus and contribution of my dissertation. Specifically, the aim of the dissertation is to demonstrate the potential for urban agriculture to cool the local climate by lowering temperatures in urban areas.

3.1 Conceptual Framework

My research draws from the disciplines of agriculture, climate change, and public health. These research domains create the three foci of my conceptual diagram (See Figure 3.1). At a high level, connections between these three domains are well established in the literature. Research has clearly illustrated how both agricultural lands and climate change impact each other as well as how climate change and agriculture directly impact public health. In the literature review above, I have discussed in detail how agricultural land cover change can affect temperature and precipitation at both the regional and global level [32, 36, 39, 45, 46, 47, 48, 49, 51]. Climate change on the other hand is expected to have profound impacts on agricultural production by decreasing productivity due to the prevalence of pests and diseases and by creating extreme conditions such as droughts and extreme heat [93]. Linkages between the domain of public health and agriculture and climate change are also well established. Climate change will bring severe weather patterns that will exacerbate

global health challenges such as malnutrition, infectious diseases, food born illnesses, and heat stress, to name a few [94]. Additionally, industrial agriculture is a huge source of environmental degradation from air pollution, to surface and groundwater contamination due to use of heavy pesticides and fertilizers [82, 83].

When examining these domains through the lens of the local urban environment, the relationships between these domains become more nuanced and less established. Not only do the relationships change but the domains themselves become more specific. For example, at the urban scale, agriculture becomes urban agriculture and climate change is referred to as the urban heat island effect. The conceptual diagram (Figure 3.1) illustrates these subdomains when the urban condition is intersected. Though there is strong evidence of the relationship between agriculture and climate change, the connection between UHI and urban agriculture has yet to be made. In my work, I attempt to establish a new connection between urban agriculture and the urban heat island effect. This new connection is illustrated in the conceptual diagram with a dotted red line.

At the urban environment level, public health takes on many different forms. Environmental hazards are just one possible subdiscipline. There is strong evidence in the research community that the UHI increases environmental hazards such as extreme heat events which in turn has serious public health effects due to increases in heat related mortality and increased air pollution [57, 67, 16]. Not only can the UHI exacerbate extreme heat conditions, but mitigation strategies have been shown to save lives by cooling local environments sufficiently to avoid heat related deaths [95]. This relationship is represented in the conceptual diagram by a solid blue line. Urban agriculture has many ties and associations with public health, from food desserts to mental health [96, 97], but currently no relationship exists in the literature exploring how urban agriculture could potentially save lives endangered by extreme heat. Though my dissertation will not explicitly measure this possible outcome, I hope to be able to indirectly link urban agriculture with the environmental hazards of extreme heat through the intervening variable of UHIs. This relationship
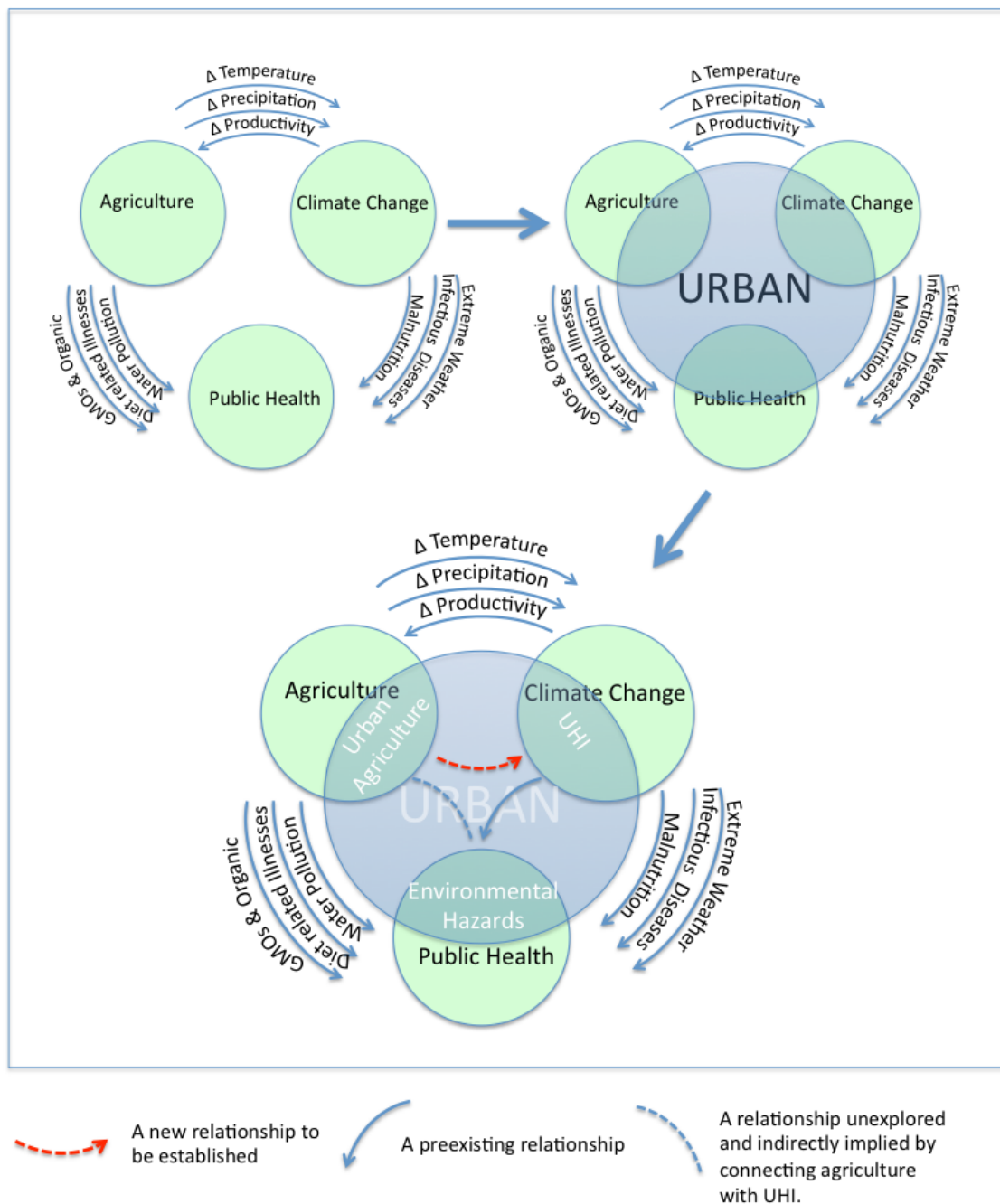
Figure 3.1: Conceptual Diagram - Connecting agriculture, climate change and public health in the urban sphere.
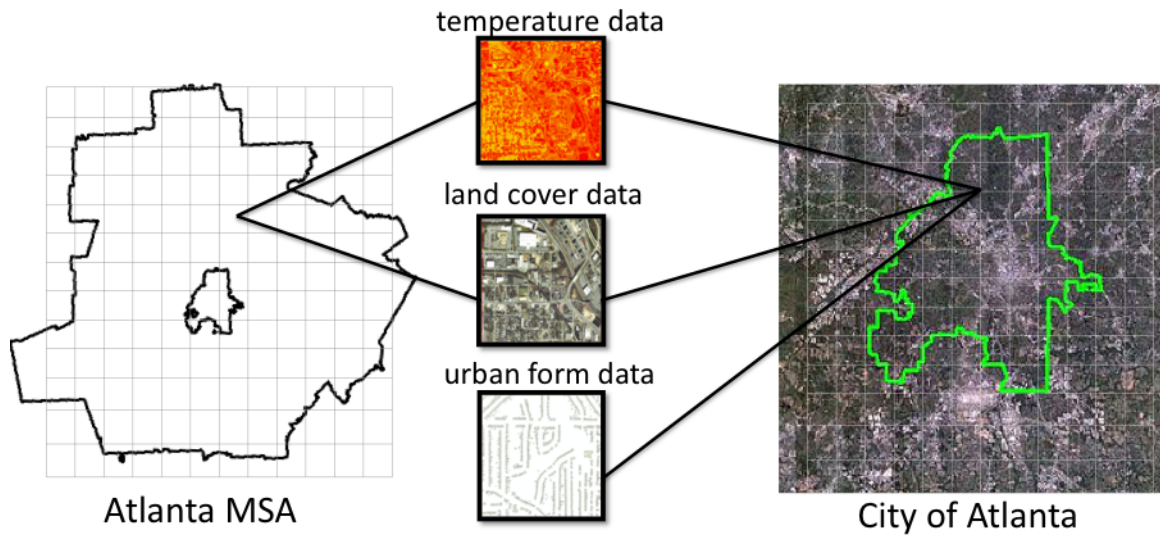
Figure 3.2: My analysis will take place at the both the MSA and city level scale incorporating temperature, land cover and urban form data.

is represented in the conceptual diagram by a dotted blue line.

3.2 Taking a two phase approach to investigating the impact of urban agriculture on local climate

My research proposes that urban agriculture can act as a successful UHI mitigation strategy by cooling the local climate. In order to investigate the effect of urban agriculture on local temperatures, I employ a two-phase methodological approach by examining the effect at two different scales: the MSA level and the city level. Through regression and GLM analysis, I use satellite temperature data and land cover data to estimate how the percent change in urban agriculture impacts local temperatures.

Specifically, I investigate how the average temperature for different land cover classes varies across the MSA and the city of Atlanta. The city level analysis will differ from the MSA level analysis by including an investigation of the effect of urban form. In the city level analysis, I use higher resolution land cover data to control for urban form conditions. This analysis will question whether the impact of agriculture on local temperature changes

Research Questions	Research Objectives	Hypothesis	Scale	Data
Q1. How does urban agriculture affect the local (neighborhood scale) climate?	To demonstrate the potential for urban agriculture to cool the local climate by lowering temperatures in urban areas.	An increase in urban agriculture will decrease temperature thus cooling the local climate.	MSA	**Temperature**: MODIS Nighttime 8-day Average; **Land cover**: National Land Cover Database 2011; USGS Digital Elevation Model; **Heatwave**: derived from National Climate Data Center
Q2. How does urban agriculture compare to urban forestation when used as a UHI mitigation strategy at the local scale?	To compare the performance of urban agriculture to the UHI mitigation strategy of urban forestation.	Urban forestation will have a larger effect on the local climate than urban agriculture.		
Q3. How does the effect of urban agriculture as a UHI mitigation strategy change during a heat wave event?	To investigate whether urban agriculture as a heat mitigation strategy is as effective during extreme heat conditions.	Urban agriculture (if not irrigated) will have less of a cooling effect during a heat wave.		
Q4. How does urban form change the relationship between urban agriculture and local climate?	To investigate how urban form at the neighborhood scale impacts the relationship between urban agriculture and local climate.	Urban agriculture will have a greater effect in more compact neighborhoods.	CITY	**Temperature**: MODIS Nighttime 8-day Average; **Land cover**: Quickbird Multi-spectral Imagery; Irrigated Agriculture derived from NDVI data; USGS Digital Elevation Model; **Urban Form**: Building Footprint; Building height derived from LiDAR, Sky view factor derived from Viewsphere
Q5. How much land area must be changed to urban agriculture to receive a local climate benefit?	To quantify the amount of land that needs to be converted to urban agriculture in order to receive a local climate benefit	There will be an indirect correlation between % area change and temperature. The larger the area the greater the likelihood of effecting change.		

Figure 3.3: The table list each of my research questions, objectives and hypotheses and also indicates the data that will be used to conduct the analysis.

depending on the urban form for where it is implemented.

For both scales, I place a uniform 1 km grid over the area. Each grid cell contains temperature and land cover data. At the city level, each grid cell will also include urban form variables. Analyzing at the city scale allows me to use more detailed parcel level urban form variables that are not available at the MSA level, such as building footprints and building heights. The MSA analysis provides a larger sample size and more opportunities for large scale agricultural land uses. Figure 3.2 illustrates that the MSA scale analysis will look at temperature and land cover whereas the city level scale will include urban data. Figure 3.3 lists my research questions, objectives and hypotheses, as well as the data I use to answer these questions.

3.3 City Selection: Atlanta, GA

I conduct my analysis in Atlanta, GA, at both the city and MSA scale. Atlanta was selected because it has the following traits: it is one of the fifty largest US cities, it has one of the fastest growing urban heat islands, and is has exhibited significant trends in heat wave characteristics such as frequency, timing, duration and intensity [10, 11, 55]. Figure 3.4
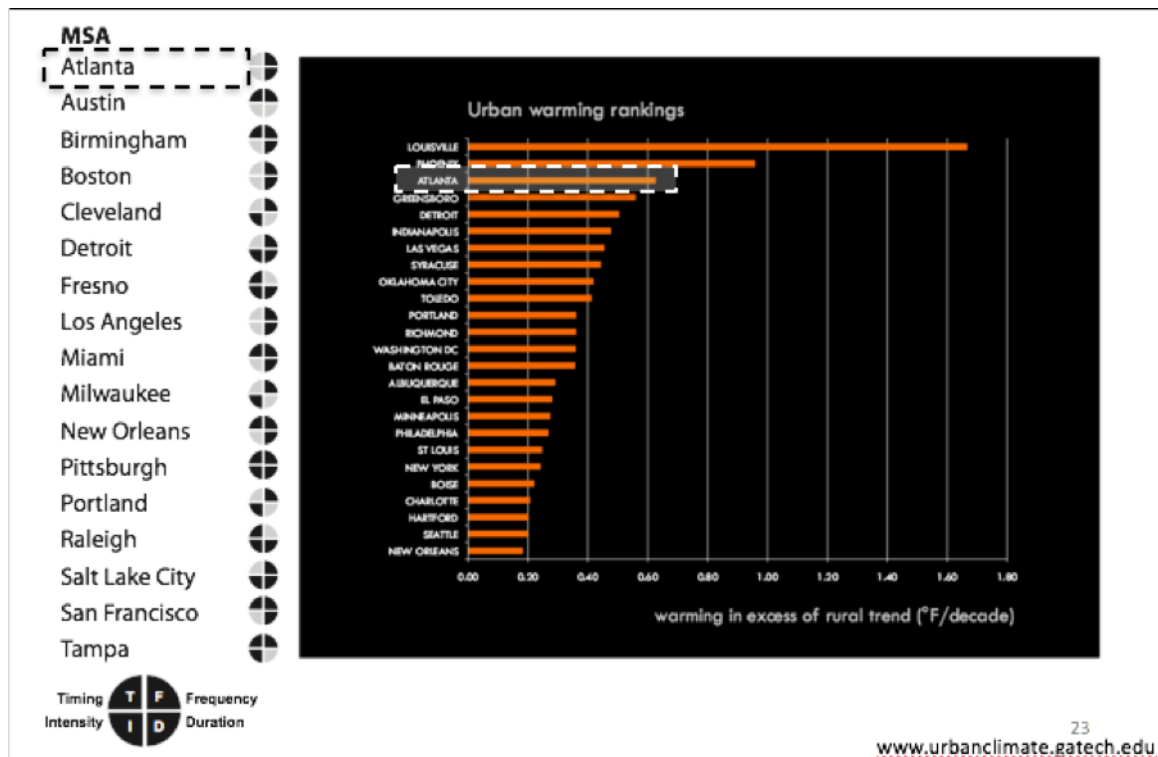
Figure 3.4: Image on the left: This image lists the US cities that have at least two increasing heat wave trends above the national average. The shaded quadrants show which heat wave trends are increasing in each city. Atlanta's heat waves are increasing both in frequency and duration compared to other large US cities. Image on the Right: Atlanta has one of the fastest growing urban heat islands in the US.

illustrates how Atlanta's growing UHI and heat wave characteristics rank as one of the highest in the United States. Additionally, Atlanta has a burgeoning urban agriculture movement, which will help inform the policy portion of this research.

CHAPTER 4

PHASE 1: MSA LEVEL ANALYSIS

RQ1: *How does urban agriculture affect the local climate?*

RQ2: *How does urban agriculture compare to urban forestation as a UHI mitigation strategy at the local scale?*

In Phase 1, I answer my first two research questions by investigating the impact of urban agriculture on local nighttime temperatures and comparing the efficacy of urban agriculture to urban forestation as a heat mitigation strategy. I investigate these first two research questions at the scale of the Atlanta MSA. As previously discussed, the use of urban agricultural lands in cities as a UHI mitigation strategy has yet to be explored. As urban agriculture becomes more popular in US cities, it is important to understand the climate potential for this type of green infrastructure. Not only is it important to understand the effect urban agriculture may have on local temperatures, it is also important to compare this climatic effect to other vegetative UHI mitigation strategies. For research question 2, I compare urban agriculture to forested land cover as urban forestation has been shown to be one of the most effective UHI mitigation strategies in cities with sufficient rainfall [15]. Comparing urban agriculture to one of the most effective UHI strategy will help to contextualize the potential of urban agriculture to successfully mitigate UHIs and can inform the UHI research community about the impact of this form of green infrastructure.

4.1 Methods

For my MSA Analysis, I conduct a multivariate Ordinary Least Squares (OLS) regression model. I place a 1 km grid across the Atlanta MSA. Each cell of the 1km x 1km grid represents an observation in the regression model with all variables aggregated to the cor-
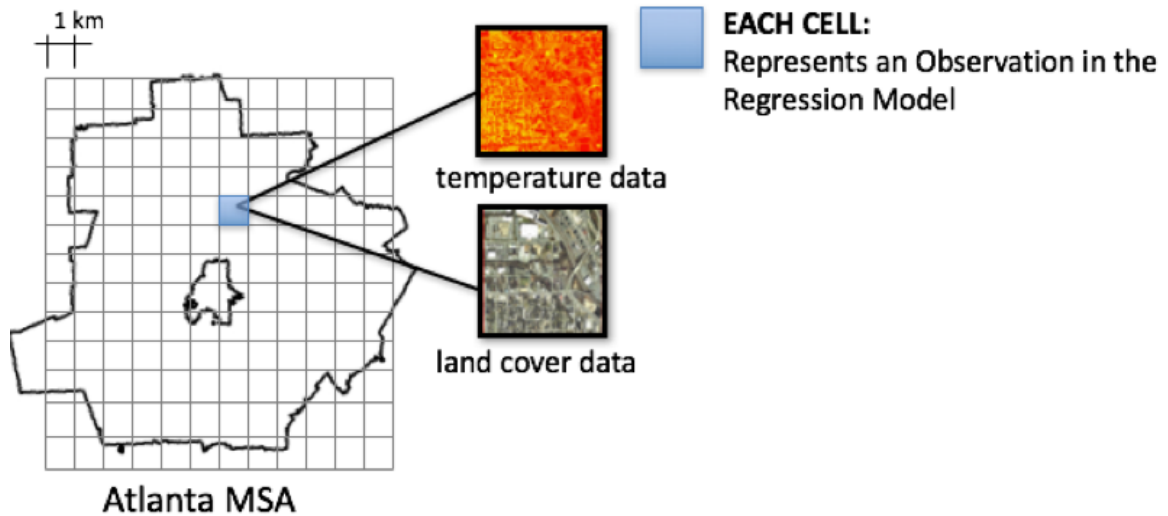
Figure 4.1: A 1 km grid is place over the Atlanta MSA. Each grid cell represents an observation in the regression model. Land cover data and temperature will be aggregated to each 1 km grid cell.

responding grid cell (See Figure 4.1). As presented in Table 4.1, the dependent variable is surface temperature and the independent variables are several classes of land covers, including the area of agricultural land and forest land. The control variables include the elevation of each of the grid cells, as well as other land cover variables, such as developed, barren, shrub, and water. Additional control variables are included by selecting the analysis day during a hot summer day that is not a heat wave and with relative cloud free conditions, which promotes maximum urban heat island effect.

4.1.1 Temperature Data

In my analysis, I use MODIS (Moderate Resolution Imaging Spectroradiometer) satellite data to generate night time surface temperature data. The MODIS sensor sits aboard two sister satellites: Terra and Aqua. The Terra and Aqua satellites orbit the planet in opposite paths ensuring that the entire planet is observed every 1-2 days. MODIS has a 36 band spectral resolution of 0.4 to 14.4 μm, a 12-bit radiometric resolution, and a daily temporal resolution for the southeast United States. The spatial resolution varies depending on the

Table 4.1: Variables for OLS Regression Model.

Variable Type	Variable Description	Data Source
Dependent	Surface Temperature	MODIS Satellite Data
Independent	Area of urban agriculture	NLCD 2011
	Area of forested land	NLCD 2011
Control	Grid cell avgerage elevation	USGS 30 meter DEM
	Land cover variables:	NLCD 2011
	Impervious, Barren, Water, Developed	
	Seasonal & Diurnal	Timing and day selection

wavelength with a range of 250m to 1 km. Surface temperature data is collected with a 1km spatial resolution. MODIS data is generated exactly the same aboard each satellite except for collection times. Aqua samples at approximately 1:30pm and 1:30am and Terra samples at approximately 10:30am and 10:30pm local time.

There are several data products generated from MODIS observations. Surface temperature data products are distributed by NASA's Land Processes Distributed Active Archive Center (DAAC). The land surface temperature products come preprocessed with digital numbers converted to radiance and to Kelvin using product specific algorithms and lookup tables. The temperature products include a 1km and a 5km daily surface temperature product, a 1km and 5-km 8-day product, and a 5-km monthly product.

For this analysis, I have selected the Aqua 8-day average surface temperature data. The timing of Aqua is much more suitable at capturing daily maximum and minimum temperatures as compared to the timing of Terra. Also the 8-day average product is created in order to minimize cloud contamination, as it is a composite of all acquisitions that are cloud free. MODIS 8-day product averages daily temperatures across all cloud free observations during the 8-day period. Minimal cloud cover is not only an important condition for maximum urban heat island effects but is also important to accurately estimate surface temperatures remotely.

The short name for the Aqua 8-day average surface temperature data product is MYD11A2

version 6. Version 6 is MODIS' newest update. Version 5 underestimated surface temperatures over bare soil, mainly in desert conditions by upwards of 2-3 K. The biggest change for version 6 is to fix this underestimation. This update may be important for urban areas as bare soils resulted from development practices can increase urban temperatures.

MODIS land surface temperature products are produced with the Sinusuidal projection and is divided and distributed as a non-overlapping tiled grid over the globe. Each grid tile is approximately 10 degrees squared at the equator. The tiles are organized by vertical tile number and by horizontal tile number. The Atlanta MSA is spread across two grid tiles: Tile 10h-5v and Tile 11h-5v (See Figure 4.2). The MODIS Data was retrieved from the LPDAAC website: `https://lpdaac.usgs.gov` and LPDAAC's "MODIS projection Tool (MPT)" was use to process the data for ArcGIS. I used the MRT tool to convert the native HDF files into geotiffs, to mosaic the two tiles of h11v5 and h10v5, to clip the scene approximately to the MSA boundary, and to re-project from sinusoidal to geographic with a NAD83 datum.

Resolution

MODIS temperature data has a 1km spatial resolution. It is possible to get higher resolution temperature data from other satellites. For example, Landsat downscales their temperature data to a 30-meter spatial resolution; however, Landsat data is only acquired during the daytime, which prevents measurement of high minimum temperatures at night. The highest resolution temperature data during the nighttime is MODIS. It is important to note that I am choosing to not optimize the resolution of the temperature data in order to investigate night time temperatures. This is a limitation of the analysis but necessary in order to look at agricultural cooling potential in the evenings. Night time temperatures are important for three reasons. Minimum temperatures have been shown to be more strongly associated with negative health effects due to extreme heat [78], temperatures in cities are amplified at night because of the urban heat island effects and these nighttime temperature will in-

51
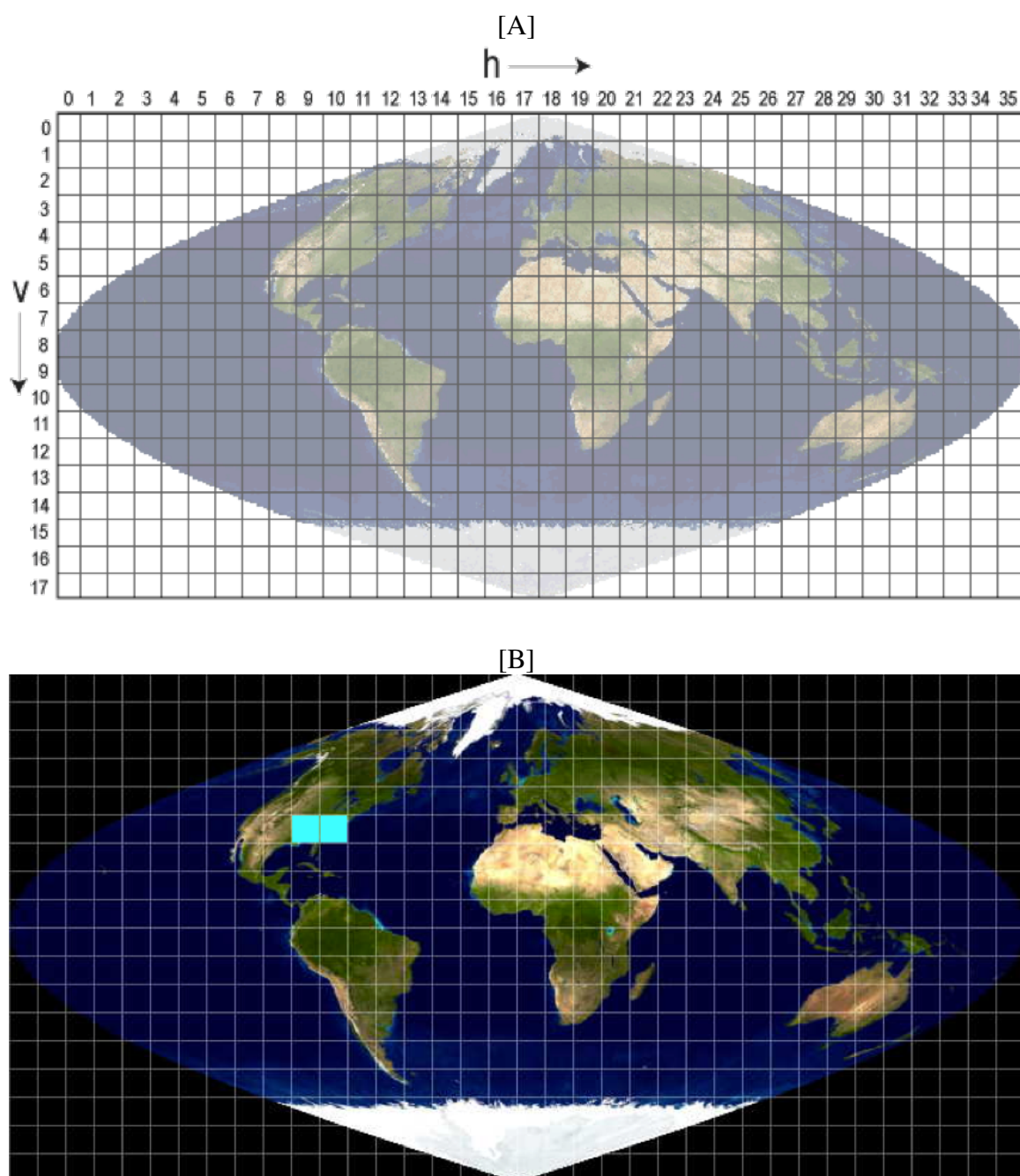
Figure 4.2: (A) depicts the MODIS global grid with its horizontal and vertical key and (B) illustrates the two tiles encompassing the Atlanta MSA.

crease faster due to climate change than day time temperatures [73], and agricultural land is hypothesized to have an advantage of cooling nighttime temperatures due to its low sky view factor (See Figure 4.3).

4.1.2   Date Selection

The date for the temperature data was selected based on heat wave days and cloud cover. The MODIS scene was selected so that there were no heat wave days included in the 8-day average and no missing data due to cloud contamination was present in the dataset. A heat wave, defined by Habeeb et al [11], consists of at least two consecutive extreme heat events (EHEs) and an EHE is defined as any day in which the minimum apparent temperature exceeds the 85th percentile for the long-term average for a particular location [65]. Minimum apparent temperatures and the local threshold for Atlanta were gathered from the National Climate Data Center (NCDC) heat stress index database to determine whether a day is classified as a heat wave day or a non-heat wave day [11].

I identified all 8-day ranges that did not have a heat wave day in its time period. There were four 8-day MODIS scenes that fit this criterion for the summer months of 2011. The first three weeks of the month of May fit this criterion, as well as the second week of June. Checking the quality control for each scene showed that May 17th - May 24th was missing 1.3% of the data due to cloud contamination and the three remaining scenes had no missing data. To ensure that the scene represented a relatively cloud free time period; I also checked the cloud cover for the 8 days for each scene.

Each MODIS scene comes with a "Clear Sky Nights" file that list the number of clear nights for the 8-day scene per pixel. Figure 4.4 illustrates the number of cloud free days per pixel for each of the four scenes. Scene May 9th only had 25% of the MSA free of clouds for the majority of the time period (5 or more days), as compared to Scene May 1st and Scene June 10th which had 61% and 59% of MSA respectively. Scene May 1st and Scene June 10th are relatively comparable with regard to cloud cover, but when examining the average
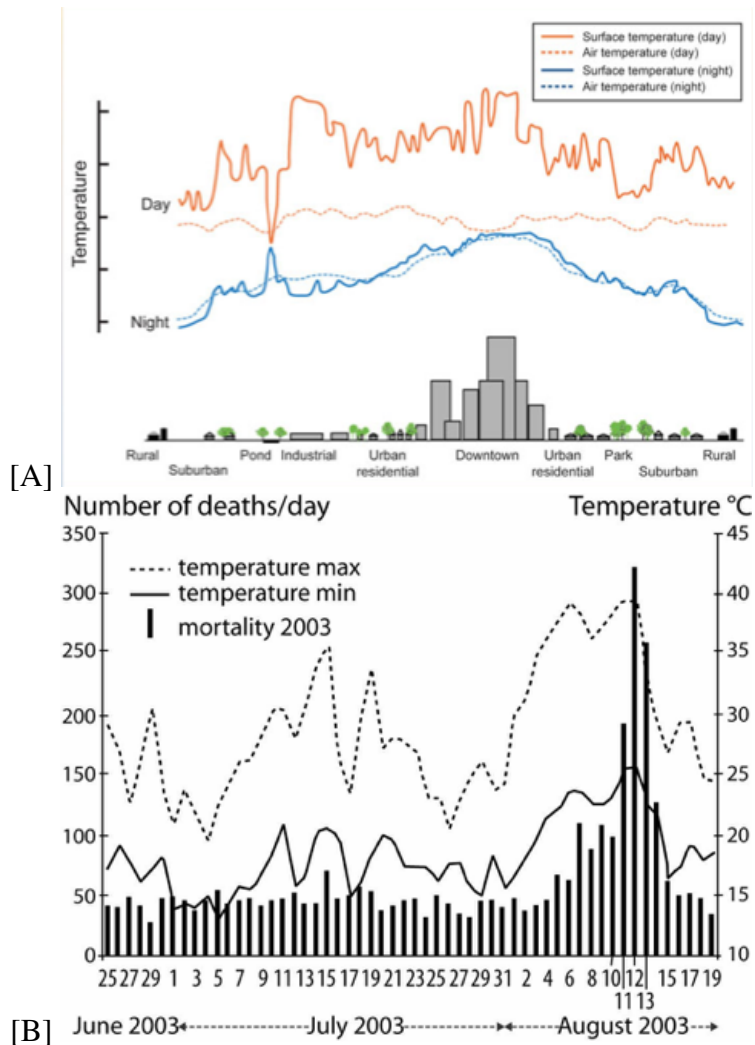
Figure 4.3: (A) Illustrates the increased temperatures at night due to the UHI (credit EPA) (B) (Benedicte Dousset) [92] Depicts the number of deaths per day during the 2003 European heat wave. The spike of deaths occurred when not only daytime temperatures were at the highest but also when nighttime temperatures where at the highest point.

05.01. – 05.08

Range: 2-6
Average: 4.78
Min Temp Avg: 53.13

>= 4 clear days
98.2%

>= 5 clear days
61%

05.09. – 05.16

Range: 1-6
Average: 3.87
Min Temp Avg:
65.63

>= 4 clear days
62.6%

>= 5 clear days
25.2%

Boundaries:
MSA

Atlanta

05.17 – 05.20

Range: 0-8
Average: 4.38
Min Temp Avg: 60.63

>= 4 clear days
65.2%

>= 5 clear days
47.6%

06.10 – 06.17

Range: 1-7
Average: 4.55
Min Temp Avg: 71.25

>= 4 clear days
77.4%

>= 5 clear days
59%

Cloud Free Days

- 0
- 1
- 2
- 3
- 4
- 5
- 6
- 7
- 8
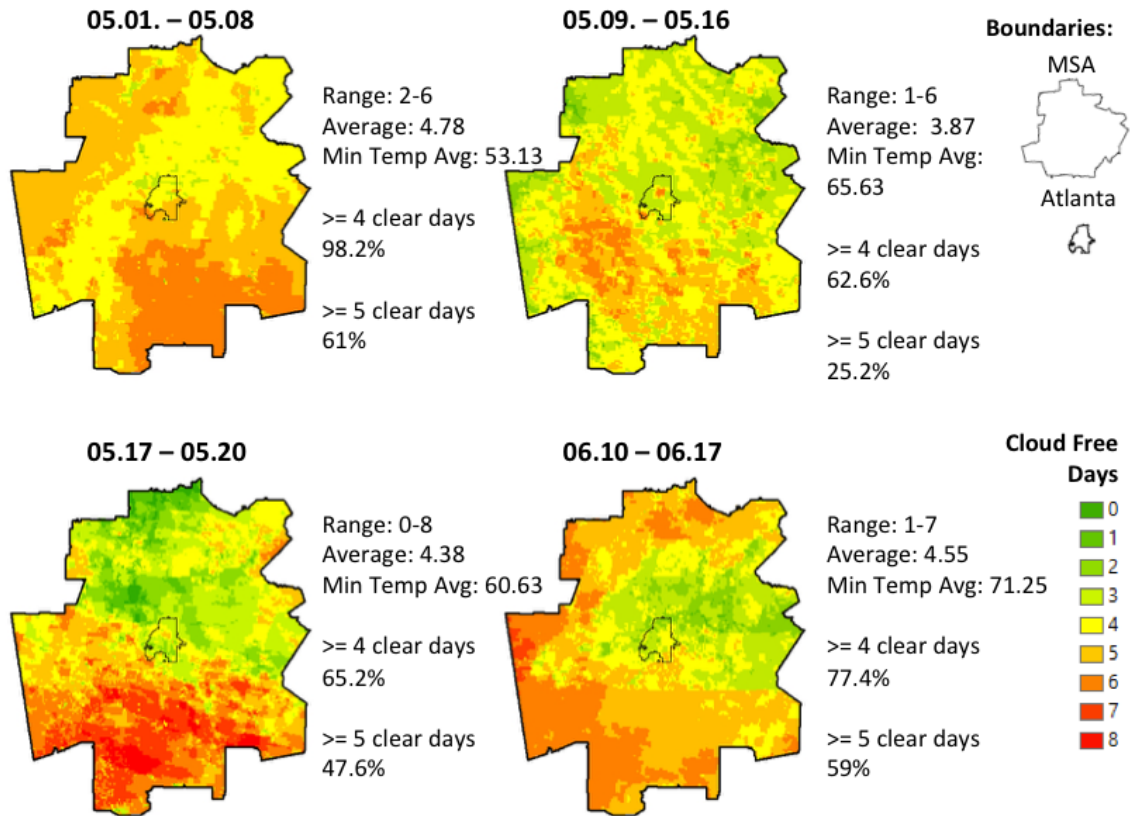
Figure 4.4: Illustrates the number of days of cloud free days per pixel for each scene.

minimum apparent temperature for each 8 days, June 10th had a higher temperature of 71.25°F as compared to 53.13°F for May 1st. The heat wave season for 2011 started June 1st with a 4-day heat wave. The June 10th MODIS Scene is the first 8-day scene of the heat wave season that does not have a heat wave day present during the time period. Picking a time period at the beginning of the heat wave season ensures that I am examining warm summer days but not excessively hot days as no EHE is included in the time period. MODIS scene 06.10-06.17 was chosen for the analysis.

4.1.3 Land Cover and Elevation Data

The land cover data used in the analysis is obtained from the USGS National Land Cover Database for 2011(NLCD). This land cover product is created by the Multi-Resolution Land Characteristics (MRLC) Consortium for the entire United States at a 30-meter spatial

resolution. NLCD uses Landsat satellite data and a decision tree classification process to consistently classify the entire United States into 16 land cover classes (see Figure 4.5 for a list of the classes). NLCD distinguishes between three different forest classes (deciduous, evergreen, and mixed), and includes a cultivated crop land cover class which will be used as the agriculture land cover in the analysis. The NLCD also classifies developed grid cells by urban development intensity (high, medium, low, open space) where the impervious surface for each category ranges from 80-100% for high to less than 20% for open space. The 2011 NLCD impervious and tree canopy datasets were also included. The impervious and tree canopy datasets indicate the percent of each 30-meter pixel that is either impervious or tree canopy. The impervious and tree canopy datasets were used to reclassify the developed pixels into impervious, tree canopy and other land cover. The raster datasets were reprojected in ArcGIS to NAD1983_StatePlane_Georgia_West_FIPS_1002_Feet (StatePlane) and clipped to the Atlanta MSA. Using spatial analysis tools in ArcGIS, the sum of the area for each land cover class was aggregated to the corresponding 1km grid cell for the regression model.

Elevation data was included into the model as a control variable. The USGS provides elevation and typography data for the entire United States at varying resolutions. The elevation data was downloaded from the USGS National Map which is part of their National Geospatial Program. One-third arc-second digital elevation model (DEM) from the USGS 3D elevation product was obtained for the MSA. A 1/3 arc-second DEM translates to an approximate 10-meter spatial resolution. Nine DEM tiles were needed to cover the Atlanta MSA. These elevation tiles were mosaicked, re-projected to state plane, and clipped to the MSA boundary in ArcGIS. The elevation was aggregated up to each 1 km grid cell by using the average elevation for each grid.

Once all of the data (temperature, land cover, elevation) was acquired, it was re-projected to state plane, clipped to the MSA, and aggregated to a 1-km grid that covers the Atlanta MSA and matches dimensions of the temperature data. Figure 4.6 illustrates the main

NLCD Land Cover Classification Legend
11 Open Water
12 Perennial Ice/ Snow
21 Developed, Open Space
22 Developed, Low Intensity
23 Developed, Medium Intensity
24 Developed, High Intensity
31 Barren Land (Rock/Sand/Clay)
41 Deciduous Forest
42 Evergreen Forest
43 Mixed Forest
51 Dwarf Scrub*
52 Shrub/Scrub
71 Grassland/Herbaceous
72 Sedge/Herbaceous*
73 Lichens*
74 Moss*
81 Pasture/Hay
82 Cultivated Crops
90 Woody Wetlands
95 Emergent Herbaceous Wetlands
* Alaska only

Figure 4.5: Lists the land cover classes in the 2011 NLCD.

datasets used in this analysis.

4.1.4   OLS Regression

The first two research questions were analyzed with ordinary least squares (OLS) regres-
sion. SPSS was used to run the OLS regression and to check for the assumptions of OLS.
In order to meet the assumptions needed to conduct an OLS regressions, outliers were
removed from the analysis based on both the Mahalanoga's critical value for outliers (a
critical value of 28 for 10 degrees of freedom) and standardized residuals (standardized
residuals > 3). The outliers represent 6% of the observations in the analysis. Removing
the outliers made the data conform with the assumptions of linearity and with normality.
Multicollinearity problems also existed between certain variables. Tree canopy and imper-
vious area were highly correlated (greater than 0.8), therefore both variables could not be
included in the model. To address the problem of multicollinearity I used a classification of
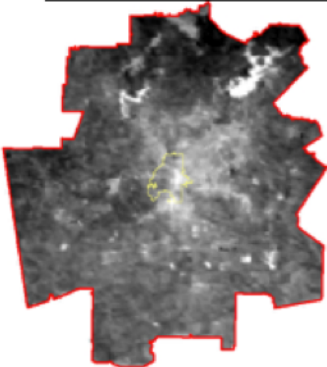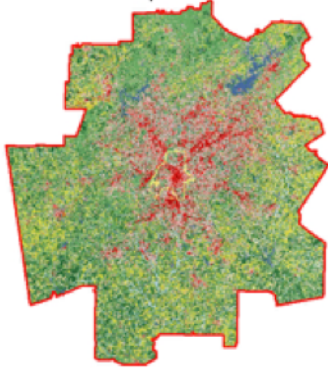
Figure 4.6: Lists all of the datasets included in the model and identifies the dependent and independent variables.

high- low intensity development instead of the impervious land cover dataset. Impervious land cover provides a better estimation of the impervious land present in each grid cell, but the problem of multicollinearity between impervious and tree canopy makes it statistically problematic to include it in the regression analysis.

High multicollinearity still existed between some variables. Tree canopy and Pasture-land were highly correlated with a correlation greater than 0.9. Since pastureland had the least land cover observations in the MSA, and since I was not directly investigating this type of land cover, I opted to remove Pasture from the analysis. The urban development class of high and medium developed were highly correlated with a correlation of 0.774. Developed medium also had the highest VIF correlations statistic of 5.408. Since these are control variables, one may argue it is not necessary to adjust them, but doing so creates more stability in the prediction model. To control for this correlation, I combined both Urban High Developed and Urban Medium Developed into one class named High-Med Developed. The removal of the impervious and pasture land covers as well as the creation of the High-Med Developed class resulted in no multicollinearity problems in the analysis.

The variables in the regression model include temperature, land cover and elevation data. The dependent variable is nighttime temperature collected at approximately 1:30 am and averaged over 8 days (of cloud free conditions) between the days of June 10th — June 17th. No local extreme heat events occurred during this time period ensuring that the days represent summer nights that are not excessively hot. There are nine land cover types in the model. Two of the land cover classes are the independent variables that are being investigated and the other seven are control variables. The two independent variables include cultivated crops which represents urban agriculture, and tree canopy land cover which includes all tree canopy in the Atlanta MSA: deciduous, evergreen and a mixture of the both deciduous and evergreen. The remaining land covers acting as control variables include: open water, developed- open space, developed-low, developed high/med, barren, shrubs, and grasslands.

4.2 Results

Averaging all observations across the MSA, the results from the analysis showed that a positive increase in agricultural lands resulted in a statistically significant (p<0.001) decrease in temperatures at a 1 km scale. Cultivated crops (agriculture) had a beta coefficient of -0.008°C, which means that a 1 unit increase in cultivated crops decreases temperatures by 0.008°C. The land cover was aggregated to the 1km grid cell as a total pixel count and therefore the unit of analysis is the resolution of the NLCD image which is 30m x 30m or 900m^2. As such, a 10-acre increase in agricultural lands would result in a 0.36°C decrease in temperature. A 0.36°C reduction in temperatures equates to a 0.648°F (0.36°C x 1.8) reduction in temperatures.

$$
\begin{aligned}
10acres &= 40468.6m^2 \\
40468m^2/900m^2 &= 45 \\
0.008x45 &= 0.36°C
\end{aligned}
\tag{4.1}
$$

On average, a 10-acre increase in agricultural lands resulted in a 0.648°F (0.36°C) reduction in nighttime temperatures at the local neighborhood scale. It is promising to find that agricultural lands as a heat mitigation strategy can statistically decrease nighttime temperatures for neighborhoods. When analyzing forested land, an increase in tree canopy resulted in small but statistically significant slightly increased (p< 0.05) in the nighttime temperatures. On average, a 10-acre increase in tree canopy land cover resulted in a 0.007°F (0.004°C) increase in temperatures. Comparing urban agriculture to tree canopy, urban agricultural lands outperform forested land cover as a nighttime cooling strategy across the Atlanta MSA.

The model had an R^2 of 0.496 indicating that approximately 50% of the variance in nighttime temperature (the dependent variable) is explained by the model. All other vari-

Table 4.2: OLS regression table. MODIS nighttime temperature is the dependent variable

| Model | Unstandardized Coefficients | | Standardized Coefficients | | |
	B	Std. Error	Beta	t	Sig.
Constant	20.755	0.035		586.501	0.000
Elevation	-0.008	0.000	-0.455	-84.783	0.000
Water	0.003	0.000	0.122	24.005	0.000
Dev Open	0.001	0.000	0.157	18.320	0.000
Dev Low	0.002	0.000	0.284	28.248	0.000
Barren Land	-0.002	0.000	-0.022	-4.263	0.000
Shrub	0.000	0.000	0.009	1.742	0.081
Herbaceuous	-0.001	0.000	-0.070	-11.901	0.000
Agriculture	-0.008	0.001	-0.057	-11.369	0.000
Tree Canopy	8.235E-5	0.000	0.021	2.763	0.006
DevHighMed	0.003	0.000	0.265	38.958	0.000

ables were statistically significant with at least a $p < 0.05$ except for shrub. Grassland and barren land both decreased night time temperatures, whereas all other land cover variables increased nighttime temperatures with High-Med Developed increasing the temperatures the most (see Table 4.2).

To contextualize this result, I compare the temperature reduction due to urban agriculture to Atlanta's nighttime UHI. I calculate Atlanta's nighttime UHI by subtracting the average urban temperature from the average rural temperature. I use the same temperature data from the analysis, which was taken during the second week of June in 2011. To compute the average rural temperature, I locate grid cells at the edge of the MSA that have a predominantly forested land area. I set the forested threshold to 90% so that I could identify grid cells surrounding the MSA that were predominately trees. I locate 8 grid cells outside of the city of Atlanta that were at least 90% forested. These 8 grid cells had an average temperature of 18.39°C. I chose 8 rural pixels so that each represented one of the 8 cardinal directions surrounding the MSA (see Figure 4.7). To compute the average urban temperature, I first identified all grid cells with centroids located inside Atlanta's city limits. Three
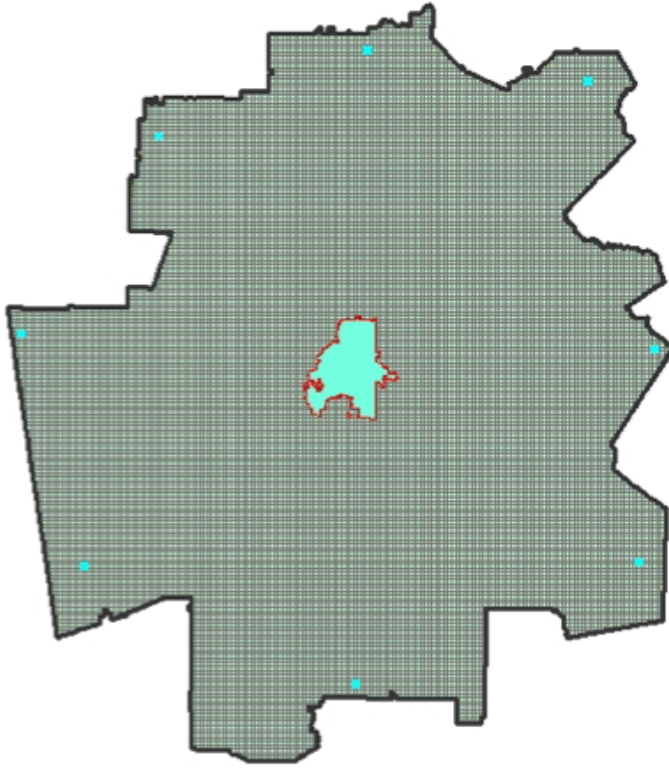
Figure 4.7: Pixel location for Atlanta's UHI calculation.

hundred thirty-four grid cells met this criterion and had an average temperature of 20.87°C. I then selected grid cells that were 100% developed and with at least 60% of the developed classification as either high or medium development. Forty grid cells met these criteria and had an average temperature of 22.07°C. Atlanta's nighttime UHI is estimated to be 3.68°C (6.62°F).

$$AtlantaNighttimeUHI = Avg.UrbanTemperature - Avg.RuralTemperature$$

$$22.07°C - 18.39°C = 3.68°C$$

$$3.68°Cx1.8 = 6.62°F$$

(4.2)

This number is similar to other UHI estimates. For example, Bounoua et al. (2015) esti-

mate the Atlanta surface urban heat island to be approximately 2°C. They define the surface UHI as surface temperature differential between the average temperature from NLCD urban pixels and the average of the most vegetated pixels outside of the urban classes. The maximum temperature differential between impervious surface area and vegetated area in Atlanta was 3.1°C occurring at 9am. At 3pm, the average time for summer months was a 1.6°C difference. Bounoua et al. is similar to this analysis as they are using surface temperatures as their UHI estimates and also using the NLCD to define urban and impervious land cover [98]. Their estimates are different from this study as this study only examines one period in time, whereas their estimates are derived from a climate model simulating temperatures from land cover and vegetative phenology which is average over summer months.

From the results, we can see that an increase in agricultural land can offset the growing urban heat island effect in Atlanta. This study showed that an increase in 10 acres of agricultural lands can decrease nighttime temperatures on average by 0.36°C. The magnitude of this temperature reduction is approximately 10% of the estimated Atlanta surface UHI. Assuming that the estimated UHI is uniform across the city, an agricultural intervention of 10 acres per 1km grid can offset approximately 10% of the UHI effect at a local level.

How much land does 10 acres represent in a 1km grid and how could 10 acres of agriculture be implanted in the city of Atlanta? Ten acres of agricultural lands represents 4% of a 1km grid cell. To contextualize what 10 acres of agricultural lands look like, I will use Gaia Gardens as a model which is located 4 miles from downtown Atlanta. Gaia gardens is a successful urban farm located in the city of Atlanta. The Gaia Gardens farm is part of a larger development known as the East Lake Commons which includes 67 townhomes and other community buildings (See Figure 4.8A). The East Lake Commons was developed in 2001 with a conservation subdivision approach. The housing is located close together in order to preserve open space attached to the development that would be used as agriculture. Gaia Gardens is approximately 5 acres of agricultural lands and the total development of

the East Lake Commons is around 10 acres. Therefore two developments of this style accounts for 8% of the grid (See Figure 4.8B) in essence, leaving plenty of space for modern urban development to occur in these grid cells.

4.3 Discussion

From the analysis, we can see that urban agricultural lands can provide a cooling benefit to local climates during summer nights. Examining the effect at the local level while holding all land covers constant, an increase in agricultural lands by 10 acres can reduce nighttime temperatures on average by approximately $0.65°F$. This temperature decrease represents an offset of approximately 10% of Atlanta's elevated temperatures from its citywide average UHI. The amount of agricultural lands needed for this temperature decrease represents approximately 4% of the observation area (a 1 square kilometer grid cell). This small land cover percentage alludes to the potential feasibility of agricultural implementation at local neighborhood scales.

Urban agricultural lands provide myriad benefits to communities from increasing food access and community development to decreasing negative environmental impacts from traditional industrial agricultural. Providing a climate benefit to local communities, specifically in decreasing urban temperatures has yet to be added to the urban agricultural arsenal. By investigating this climate benefit and illustrating the climate potential for agricultural lands in urban environment, stakeholders can better understand the benefits agricultural lands can provide to their communities. When deciding whether to support policies to increase agricultural uses in a community, stakeholders need to understand all the ways that agricultural lands can benefit their local environment which includes the benefit of decreasing nighttime temperatures.

The analysis also looks at the temperature impact from forested land cover and compares this to agriculture. Urban agricultural lands outperformed tree canopy in lowering nighttime temperatures with tree canopy having little impact on nighttime temperatures.
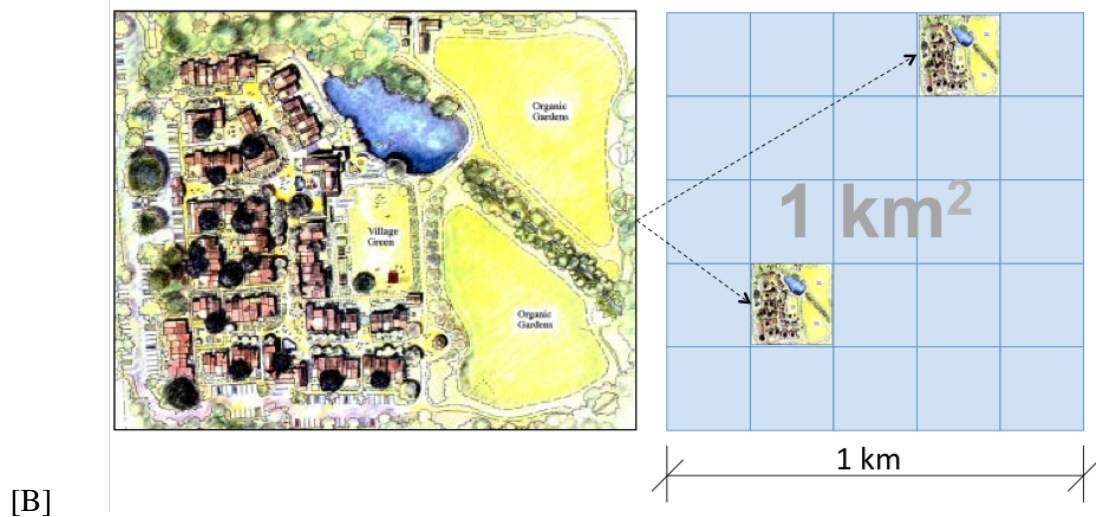
Figure 4.8: (A) An image of the East Lake Commons. In the foreground is Gaia Gardens. Source: `http://www.eastlakecommons.org/`. (B) On the left - The plan of East Lake Commons and Gaia Gardens. On the right- A representation of a 1 square kilometer grid cell with the area allocated for two developments similar to the East Lake Commons.

As previously discussed, urban forestation has been shown to be one of the most effective UHI mitigation strategies in cities with sufficient rainfall [15]. Comparing urban agriculture to the most effective vegetative UHI mitigation strategy, helps to contextualize its impact on nighttime temperatures. There are many reasons why forested land would outperform agricultural land with regard to cooling temperatures in urban environments, primarily in the daytime. One of the primary reasons is the large canopy exhibited by forested land, which provide larger shading as compared to agricultural lands. Shading from established tree canopy can reduce temperatures by at least two and half times as much as from evapotranspiration [99, 100].

On the other hand, agricultural lands have other parameters aiding to outperform forested lands. Climate scientists have well documented the effects of agricultural land cover change on temperatures at both the global and regional scale. At the regional scale, looking specifically at the United States, Fall et al. have shown that agricultural land cover change have resulted in "a cooling for all conversion types and presents the largest magnitude of cooling" [46] as compared to all other regional land cover changes. At a regional scale, agricultural land cover change (land cover that changes from any land cover to agriculture) cools the regional near surface air temperatures. One of the main reasons we see this cooling effect is because these croplands are often irrigated.

Another interesting difference between the parameters between agricultural and forested land is their sky view factor. Agricultural land has a much larger sky view factor than forested land. The sky view factor represents the percentage of sky that is visible due to the land cover. Having a larger sky view factor contributes to a more efficient cooling process by not inhibiting the transmission of longwave radiation into the atmosphere. A recent research study led by Middel et al., has shown that "before sunrise and after sunset, surface temperatures were higher under the tree canopy than in the open [101]." This is because the tree canopy traps long wave radiation from escaping into the atmosphere. This trapping of longwave radiation during the evening is why we also see elevated temperatures at night

66

in urban areas. During the day, impervious surfaces absorb incoming solar radiation, storing it throughout the day. In the evening, when the sun goes down the impervious surfaces slowly reradiate the stored radiation. In areas with low sky view factors such as in dense urban areas and forested areas, the longwave radiation gets reabsorbed by surfaces instead of escaping back into the atmosphere resulting in elevated temperatures. This trapping effect is why the sky view factor of vegetated lands can effect their cooling potential.

In an earlier study, Taha et al. illustrated how a park cool island effect can occur with different vegetation at varying times of the day [54]. A park cool island effect is when a consolidated land cover of similar type is much cooler than its surrounding environment. Taha et al. showed that both forested land and open parks would exhibit the same park cool island effect, but their maximum park cool island effect would happened at different times of the day (change over the course of the day) [54]. Forested areas would exhibit a maximum park cool island effect in the mid afternoon whereas open grass areas would have a maximum park cool island in the evenings.

Middel et al.[101], Fall et al. [46],and Taha et al. [54] illustrate some of the theory and reasons behind why agricultural land is beneficial in reducing minimum temperatures at the local scale and why agricultural lands are lowering temperatures at a higher rate than forested lands in the evening. High nighttime temperatures have been shown to have strong associations with negative health effects during heat waves. By examining the effect of land cover on nighttime temperatures, I am showing that agricultural lands may play a very important role in urban environments in maintaining cooler temperatures in the evening. These cooler temperatures may play an important role in the health of the community where these agricultural interventions are implemented specifically in decreasing exposure to high heat.

This analysis uncovered some methodical challenges with urban agricultural research: specifically agricultural sample size and multicollinearity between urban land covers classes. Agricultural lands were not very abundant throughout the Atlanta MSA. For example, the

NLCD does not identify any agricultural land within the Atlanta city limits. However, by 2011, Atlanta had several large urban agricultural farms such as Gaia Gardens. These farms are large enough that they should be identifiable with 30-meter resolution land cover data. Though it was not surprising to see a lack of vegetation within the city of Atlanta, it was surprising to see so little agriculture throughout the entire MSA.

The lack of agricultural lands in urban environments illustrates a methodical challenge one encounters in conducting empirically driven quantitative urban agriculture research. To address this challenge, I argue for the development of an irrigated agriculture proxy in order to study agricultural cooling potentials in urban environments. In the past, climate researchers have used other land covers to represent agriculture, such as grass, in climate studies. If we can identify all land cover in urban environments that have similar radiometric properties as urban agriculture and therefore behave similarly with regard to how they interact with incoming solar radiation, then we can start gaining a better idea of the cooling potential of agriculture in our cities and the effectiveness of agriculture as UHI mitigation strategy.

In my statistical analysis, I uncovered a problem with multicollinearity between varying land cover classes. For example, tree canopy and impervious land cover were so highly correlated that I could only include one of the variables in the regression model. When analyzing urban conditions, impervious and forested land covers are important land cover variables to include in a regression model as both land covers significantly influence the temperatures in an urban environment. To address multicollinearity one can either exclude a correlated variable or, if they wish to still control for both variables, one must somehow combine the correlated variables such as in an index or typology. To address the mulit-collinearity problem, I excluded the impervious land cover and instead I used the NLCD predefined urban classes. These classes are roughly defined and do not adequately describe the urban conditions in cities across the country. In order to address the challenge of highly correlated land cover variables, I suggest an urban classification scheme be developed in

order to control for urban conditions. In order to robustly analyze vegetation cooling potential in urban environments, I am arguing that a urban form typology needs to be created and tailored for the city under investigation. An urban form typology would address the problem of highly correlated independent variables. Both of these methodically challenges, limited agricultural lands and highly correlated land cover variables, will be addressed in Chapter 6.

CHAPTER 5

THE EFFECT OF HEAT WAVES ON URBAN AGRICULTURE COOLING

RQ3: *How does the effect of urban agriculture as a UHI mitigation strategy change during a heat wave event?*

In the United States, more people die per year from extreme heat than from all other natural disasters combined. On average between 600 - 1300 people are estimated to die annually from heat related complications [102, 2, 1]. More than 700 people lost their lives during the heat waves in Chicago in 1995 and 1999 [103, 104]. The more recent heat waves in Europe in 2003 and Russia in 2010 rank among the deadliest weather related event of this century, where tens of thousands of individuals died during these events[6, 7, 8]. The 2003 European heat wave encompassed the majority of central Europe spanning as far north as Great Britain and as far south as Italy. Claiming more than 70,000 lives, this event illustrates what can happen to a society who is unprepared to deal with such a catastrophe [8]. In France more than 12,000 people died during August of 2003[105]. The mortality count was so high and unexpected that morgues were over capacity and refrigerated trucks were needed to keep corpses[106]. Not only was the mortality extreme, but the built infrastructure took a toll further complicating matters and making communities all the more vulnerable. Roads and rail lines buckled blocking transportation networks[107]. Additionally there were over 25,000 forest fires from the extreme heat and drought across Europe that year[105]. These heat waves and others illustrate that extreme heat is a serious public health concern.

Cities are more vulnerable to extreme heat events and to heat waves because of the urban heat island effect. The elevated temperatures in cities during heat waves due to the UHI result in higher rates of mortality when controlling for population density[58, 59]. Not only are temperatures in large US cities consistently higher than their rural environs but the

UHI is increasing urban temperatures across the US at a faster pace than global temperatures due to climate change[10]. UHI increases both daytime and nighttime temperatures with research showing the largest temperature differences between urban and rural areas occurring in the evening[108, 56]. Minimum temperatures have been shown to be a better association with heat mortality than other temperature metrics[80, 78]. For example, when comparing the 2003 and 2006 European heat wave the consistently high minimum temperatures in 2003 were one of the main climate differences between these two heat waves[109].

In addition to the UHI effect, cities are vulnerable to extreme heat because they house a high concentration of vulnerable populations who often do not have access to air conditioning and who frequently live in less ventilated buildings [110]. Cities have a higher probability for power outages due to the increased electricity demand during heat waves. As air conditioning is the main response to combating heat mortality during heat waves, increased energy demand from air conditioning use can overwhelm electricity grids creating blackouts [111, 112] and these blackouts can further increase the risk of mortality [113].

NASA and NOAA have recently both announced that the year 2016 was the hottest year on record from start to finish [114] and cities are poised to become even more vulnerable to extreme heat events as a result of global climate change. Recent studies indicate that global climate change may be increasing the number and duration of heat waves in areas that are already experiencing extreme heat events. Studies examining the relationship between global climate change and mortality have found "business as usual" emissions scenarios to result in a doubling of heat-related deaths by the end of the century in the USA, with some estimates as high as 2,200 heat-related deaths occurring annually by 2100 [70]. McCarthy et al. project that the number of extremely hot nights will increase by as much as 50% by 2050 in large cities globally[73]. These cities are projected to have a much greater increase in hot nights than their surrounding rural areas, illustrating the susceptibility of urban populations to extreme heat due to the urban heat island effect.

Currently heat waves patterns are changing across large cities in the US [11]. Looking at climate data over fifty years, Habeeb et al. show that heat waves are increasing in frequency, duration, intensity and starting earlier and lasting longer into the heat wave season [11]. Heat waves were not isolated to a specific region in the US but instead were increasing in large US cities across all regions in the Untied States. This lack of regional effect, illustrates that no mater where large cities are located, they need to be prepared for more extreme heat waves. When examining Atlanta, GA, the study showed that Atlanta ranked amongst the most vulnerable cities with heat wave trends significantly above the national average for two heat wave characteristics. Coupled with the fact that Atlanta has one of the fastest growing UHIs and is one of the fastest growing MSAs in the past 5 years, these trends are making Atlanta an area of concern for heat mitigation.

As discussed previously, vegetative strategies in regions with sufficient rainfall have been shown to be very effective heat mitigation strategies for combating the UHI effect. Though vegetation has been upheld as an effective strategy, extreme heat conditions may reduce the cooling potential of vegetation. In Chapter 4, I showed that urban agriculture can reduce nighttime temperatures and outperform forested land cover in reducing nighttime temperatures at the MSA level. My next research question examines how urban agriculture performs during a heat wave.

RQ3: *How does the effect of urban agriculture as a UHI mitigation strategy change during a heat wave event?*

Vegetation functions change during extreme heat. Extreme heat puts stress on vegetation causing phenological functions to change during these extreme weather conditions. For example, during the 2003 European heat wave, researchers showed that tree canopy in Europe acted as a source for carbon dioxide instead of being a sink [115] Primary production reduced by as much as 30% as did vegetation respiration, a phenological function that creates a sink for atmospheric CO_2. The decrease in primary production and respiration was correlated with a decrease in evapotranspiration and soil moisture [115]. In addition to

increasing atmospheric CO_2, urban vegetation can increase ground level ozone during extreme heat events. During hot days, trees release more volatile organic compounds (VOCs) which is a necessary component to tropospheric ozone formation and urban vegetation have been shown to triple their VOC contributions during heat waves [116].

In addition to high temperatures during the Europe heat wave there was also extremely low soil moisture throughout the entire summer. The low soil moisture caused a decrease in evapotranspiration, latent cooling and these conditioned increased surface temperatures especially during the month of August when the heat wave was at its worse. Water stress from low soil moisture occurs when the extractable soil water decreases below 0.4in. After this threshold is crossed, transpiration decreases due to an increase in stomatal resistance [117]. The stomatal resistance increase enables plants to conserve water by decreasing evapotranspiration. Since evapotranspiration plays a large role in the cooling potential of vegetation especially agriculture, there is a possibility that vegetative strategies do not provide the cooling potential needed to lower urban temperatures during extreme heat events which is when urban residents most need relief from the heat.

5.1 Methods

In order to investigate this research question, I compare the temperature decrease from agriculture during a heat wave to the temperature decrease from agriculture during a non heat wave period in the same year. A continuation of the Chapter 4 analysis, I place a 1km grid across the Atlanta MSA. Each cell of the 1km x 1km grid represents an observation in the model with all variables aggregated to the corresponding grid cell (See Figure 5.1). As presented in Table 5.1, the dependent variables are surface temperatures (heat wave vs. non-heat wave) and the independent variables are several classes of land covers. The dependent variable is nighttime temperature collected at approximately 1:30 am and averaged over 8 days (of cloud free conditions). There are nine land cover types in the model. Two of the land cover classes are the independent variables that are being investigated and the other
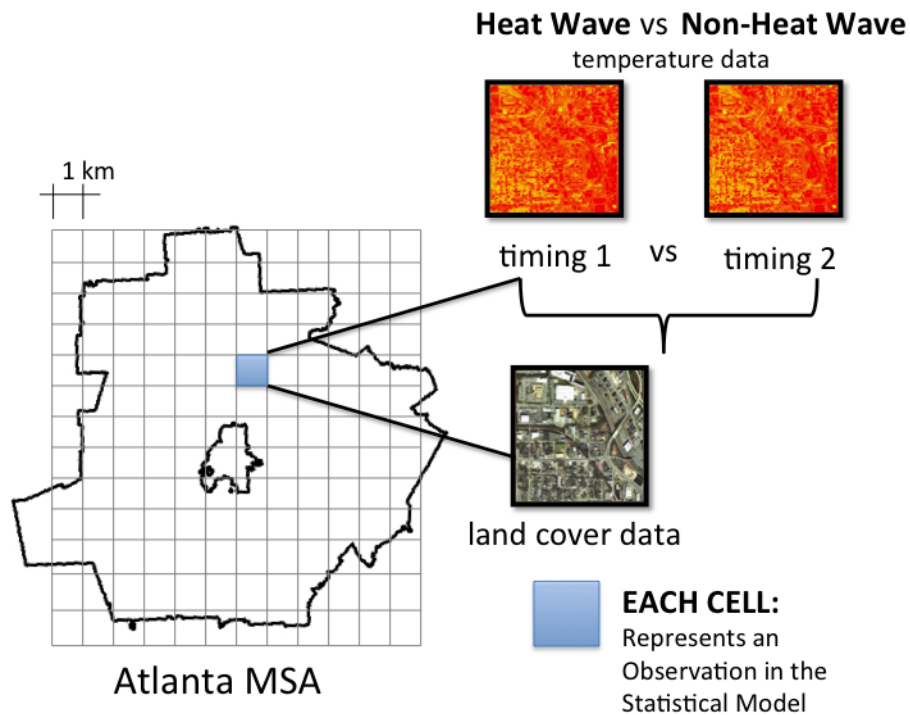
Figure 5.1: A 1 km grid is place over the Atlanta MSA. Each grid cell represents an observation in the model. Land cover data and temperature will be aggregated to each 1 km grid cell.

seven are control variables. The two independent variables include cultivated crops which represents urban agriculture, and tree canopy land cover which includes all tree canopy in the Atlanta MSA: deciduous, evergreen and a mixture of the both deciduous and evergreen. The remaining land covers acting as control variables include: open water, developed- open space, developed-low, developed high/med, barren, shrubs, and grasslands.

Research question 3 investigates whether the cooling potential of agricultural lands are maintained during an extreme heat wave or whether the cooling potential is diminished or even reverses its directional impact during extreme heat. To answer this research question, I use SPSS′s Advance Models, to test whether the coefficients from land cover are different during a heat wave versus a non heat wave. I conduct a repeated measures multiple regression using the general linear model (GLM) repeated measures procedure in SPSS. In the

Table 5.1: Variables for Heat Wave Analysis.

Variable Type	Variable Description	Data Source
Dependent	Surface Temperature	MODIS Satellite Data
Independent	Area of urban agriculture	NLCD 2011
	Area of forested land	NLCD 2011
Control	Grid cell avgerage elevation	USGS 30 meter DEM
	Land cover variables:	NLCD 2011
	Impervious, Barren, Water, Developed	
	Seasonal & Diurnal	Timing and day selection

multivariate repeated measures design, the same measurement is made more than once on each case or observation. For my design, I am measuring temperature for each 1km x 1km grid cell at two different time periods: June 10th, a non-heat wave period, and July 20th, a heat wave period. Using the GLM repeated measures allows me to test the null hypotheses involving the within-subject factors and the covariates. I test the null hypotheses that there is no difference between the effect of agriculture on temperature during a heat wave and non-heat wave period by investigating the covariate and within subject interactions and can test the null hypothesis involving the within-subjects factors to see if there is a temperature difference between a heat wave and non heat wave period.

In the GLM Repeated Measures procedure I created a "timing" factor with two levels to define the within-subject repeated measure factor and defined a single measure of Night Temperatures. The first level was defined as June 10th and the second level defined as July 20th. I ran a full factorial model to control for all covariate main effects and to obtain the within subject and covariate interactions. I use a Type III method for calculating the sum of squares in the model (as it is the most commonly used sum of squares method and the most encompassing for different model designs (SPSS Manual 17.0).) GLM repeated Measures produces estimates of parameters, which are the coefficients for each covariate. Commonly used a priori contrasts are available to perform hypothesis testing on between-subjects factors. I use the "difference" contrast to test the within subject and covariate

interactions. The difference contrast compares the covariate coefficient from of each level to the coefficient of the previous level.

5.1.1 Heat Waves

To begin this analysis, I identify all heat wave and non heat wave days for the year 2011. At present, there is no standard definition of heat waves [118, 119, 102]. Heat wave definitions vary depending on the length of consecutive days, the type of temperature metrics employed (minimum, average, maximum), the thresholds used to determine an extreme temperature, and whether humidity is taken into account.

For this analysis, a heat wave, defined by Habeeb et al. [11], consists of at least two consecutive extreme heat events (EHEs) and an EHE is defined as any day in which the minimum apparent temperature exceeds the 85th percentile for the long-term average (1961-1990) for a particular location [65]. Minimum temperatures refer to high nighttime temperatures and apparent temperature is a temperature metric that combines both temperature and humidity. Defining EHEs with a local heat index threshold, controls for regional differences in acclimatization and recognizes that human health responses to extreme heat vary across different climatic regions [120, 65, 78, 79].

Heat waves days for the summer of 2011 in Atlanta, GA were identified using data obtained from the National Climate Data Center (NCDC). Minimum apparent temperatures and the local long-term average threshold for Atlanta were gathered from the National Climate Data Center (NCDC) heat stress index database to determine whether a day is classified as a heat wave day or a non-heat wave day [11]. The NCDC extends a dataset originally developed by Gaffen and Ross [65] through which apparent temperature is measured for 187 US cities and compared to regional long-term distributions to identify anomalous heat events. The NCDC heat stress index database is based on temperature and humidity observations from first-order meteorological stations, which are primarily located at a city's airport.

76

Minimum apparent temperature is used to define heat waves, because high nighttime temperatures and humid nights have been shown to have a better association with negative health effects than other temperature metrics [78, 118]. While high daytime and nighttime temperature both stress physiological functions associated with cardiovascular and respiratory systems; it is the consistently high temperatures during the evenings that have a stronger association with an increase in physiological stress [78, 59]. The relentless heat exposure throughout the day and night does not provide time for the body to adequately recover leaving one more susceptible to an elevated risk of negative heat-related health effects. Also, it is important to include relative humidity because the body undergoes more stress during a humid hot day as compared to a non-humid hot day. The physical stress on the body is amplified during a day that is not only hot but also humid. Saturated air resulting from high humidity has less capacity to hold water and therefore slows the evaporation rate of perspiration, which is the body's cooling mechanism.

Atlanta heat waves and MODIS scene selection

For the summer of 2011, Atlanta had seven heat waves and forty heat wave days. The heat waves started at the beginning of June and lasted until the middle of August (see Figure 5.2). The average heat wave length was 5.7 days and the average minimum apparent temperature was 78.6°F. The longest heat wave and most intense (highest average minimum apparent temperature) heat wave was the fifth heat wave of the summer and started on July 19th and lasted 16 days.

To compare the temperature response from agricultural land during a heat wave and non heat wave event, I identify MODIS scenes that were during a heat wave and non heat wave period. As discussed in the previous chapter, I have selected the Aqua 8-day average surface temperature data for the analysis. The timing of Aqua and the minimization of cloud contamination from the 8-day product provide optimal conditions for maximum nighttime urban heat island effects and estimations of remotely sensed surface temperatures.
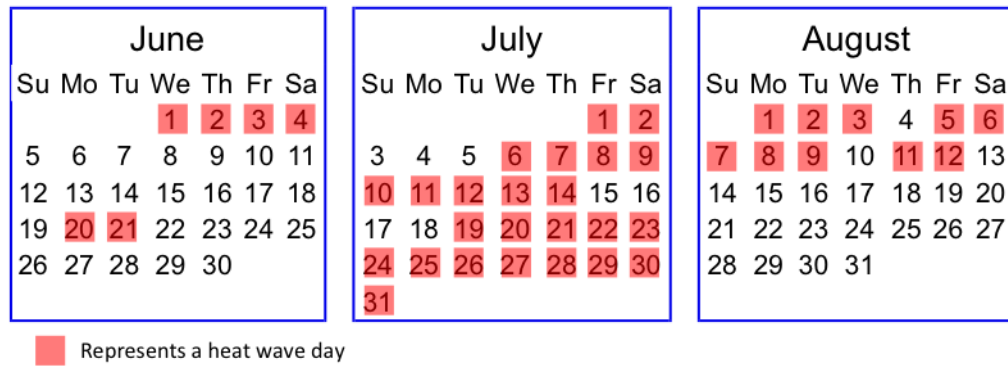
Figure 5.2: Summer 2011 heat wave calendar. The red box indicates a heat wave day.

The non-heat wave MODIS scene was selected so that there were no heat wave days included in the 8-day average and no missing data due to cloud contamination was present in the dataset. The June 10th -17th MODIS scene is the first 8-day scene of the heat wave season that fits this criteria. The scene does not have a heat wave day or an EHE present during the time period. Picking a time period at the beginning of the heat wave season ensures that I am examining warm summer days but not excessively hot days as no heat wave days or EHEs are included in the time period (See Chapter 4 for more discussion).

The heat wave MODIS scene was selected so that the entire 8-day average was during a heat wave and there was no missing data due to cloud contamination was present in the dataset. The July 20th-27th MODIS scene fits the criteria. The MODIS scene is the only scene with all 8 days during a heat wave and the dataset is taken during the hottest and longest heat wave for summer 2011. The scene is during the beginning of the 5th heat wave of the year and this heat wave represents the longest heat wave of the season with 16 consecutive EHEs with the highest average temperature. Selecting this scene ensures that I am capturing the response of agriculture during the hottest part of the summer and during the time when residents are at the highest risk for heat related mortality as research has shown that longer lasting and more intense heat waves increase the impact on heat-related mortality [121]. This is the only 8-day time period for 2011 where everyday is a heat wave day. In 2011, there are two other time periods where 7 of the 8 days are heat wave days

(July 28th scene – which is the end of the heat wave associated with the previous time period, and the August 5th scene).

5.2 Results

The average night time temperature for the June 10th and July 20th MODIS scenes are 19°C and 21°C respectively. The July 20th heat wave, the fifth heat wave of the season and the longest lasting and most intense heat wave, had night time temperatures that were on average 3°C above the average nighttime temperatures found in the June 10th scene. The multivariate tests for the repeated measure and each predictor was significant across all four multivariate statistics (Pillai's Trace, Wilks' Lamda, Hotelling's Trace and Roy's Largest Root)–See Figure5.3. This result indicates that regardless of which multivariate statistic is used, we can assume a statistical difference in the timing of the night time temperature measure. The temperature during the July 20th heat wave was statistically significantly different from the temperature at the beginning of the heat wave season affirming that selection of MODIS scenes. Though the measurement timing is statistically significant, the value of Wilk's Lambda indicate that only about (1-.985)*100= 1.5% of the variance of the dependent variable is accounted for by the timing of the measurements.

One of the advantages of using the repeated measure GLM model is that I can test whether land cover coefficients differ across different climatic events. The multivariate test and the test of within subject contrasts (Figure5.3 and Figure 5.4) show that no matter what multivariate statistic is used, there is a significant interaction between the timing of the night time temperature measure and the effect of agricultural land cover. The null hypothesis states that the agricultural land cover coefficient during a non heat wave period is equal to the agricultural land cover coefficient during a heat wave period. Utilizing the difference contrast in the full factorial model tests for the null hypothesis. The within subject contrast table indicates that there is statistically significant difference between the coefficients during a heat wave and non heat wave period indicating a rejection of the null

79

Repeated Measures Multivariate Tests							
Effect		Value	F	Hypothesis df	Error df	Sig.	Partial Eta^2
Timing	Pillai's Trace	0.015	311.8	1	20381	0.000	0.015
	Wilks' Lambda	0.985	311.8	1	20381	0.000	0.015
	Hotelling's	0.015	311.8	1	20381	0.000	0.015
	Roy's Largest	0.015	311.8	1	20381	0.000	0.015
Timing * Elevation	Pillai's Trace	0.061	1331.3	1	20381	0.000	0.061
	Wilks' Lambda	0.939	1331.3	1	20381	0.000	0.061
	Hotelling's	0.065	1331.3	1	20381	0.000	0.061
	Roy's Largest	0.065	1331.3	1	20381	0.000	0.061
Timing * Open Water	Pillai's Trace	0.003	61.7	1	20381	0.000	0.003
	Wilks' Lambda	0.997	61.7	1	20381	0.000	0.003
	Hotelling's	0.003	61.7	1	20381	0.000	0.003
	Roy's Largest	0.003	61.7	1	20381	0.000	0.003
Timing * Dev. Open	Pillai's Trace	0.006	130.0	1	20381	0.000	0.006
	Wilks' Lambda	0.994	130.0	1	20381	0.000	0.006
	Hotelling's	0.006	130.0	1	20381	0.000	0.006
	Roy's Largest	0.006	130.0	1	20381	0.000	0.006
Timing * Dev. Low	Pillai's Trace	0.001	15.3	1	20381	0.000	0.001
	Wilks' Lambda	0.999	15.3	1	20381	0.000	0.001
	Hotelling's	0.001	15.3	1	20381	0.000	0.001
	Roy's Largest	0.001	15.3	1	20381	0.000	0.001
Timing * Barren Land	Pillai's Trace	0.003	67.6	1	20381	0.000	0.003
	Wilks' Lambda	0.997	67.6	1	20381	0.000	0.003
	Hotelling's	0.003	67.6	1	20381	0.000	0.003
	Roy's Largest	0.003	67.6	1	20381	0.000	0.003
Timing * Shrub	Pillai's Trace	0.007	151.9	1	20381	0.000	0.007
	Wilks' Lambda	0.993	151.9	1	20381	0.000	0.007
	Hotelling's	0.007	151.9	1	20381	0.000	0.007
	Roy's Largest	0.007	151.9	1	20381	0.000	0.007
Timing * Herbaceous	Pillai's Trace	0.008	157.5	1	20381	0.000	0.008
	Wilks' Lambda	0.992	157.5	1	20381	0.000	0.008
	Hotelling's	0.008	157.5	1	20381	0.000	0.008
	Roy's Largest	0.008	157.5	1	20381	0.000	0.008
Timing * Agriculture	Pillai's Trace	0.002	41.6	1	20381	0.000	0.002
	Wilks' Lambda	0.998	41.6	1	20381	0.000	0.002
	Hotelling's	0.002	41.6	1	20381	0.000	0.002
	Roy's Largest	0.002	41.6	1	20381	0.000	0.002
Timing * Tree Canopy	Pillai's Trace	0.000	0.1	1	20381	0.747	0.000
	Wilks' Lambda	1.000	0.1	1	20381	0.747	0.000
	Hotelling's	0.000	0.1	1	20381	0.747	0.000
	Roy's Largest	0.000	0.1	1	20381	0.747	0.000
Timing *Dev High/Med	Pillai's Trace	0.003	64.4	1	20381	0.000	0.003
	Wilks' Lambda	0.997	64.4	1	20381	0.000	0.003
	Hotelling's	0.003	64.4	1	20381	0.000	0.003
	Roy's Largest	0.003	64.4	1	20381	0.000	0.003

Figure 5.3: Repeated Measures Multivariate Tests.

Tests of Within-Subjects Contrasts

Measure: Night Temperature

Source	Timing	Type III Sum of Squares	df	Mean Square	F	Sig.	Partial Eta Squared
Timing	Level 2 vs. Level 1	253.92	1	253.92	311.81	0.000	0.015
Timing * Elevation	Level 2 vs. Level 1	1084.13	1	1084.13	1331.29	0.000	0.061
Timing * Water	Level 2 vs. Level 1	50.28	1	50.28	61.74	0.000	0.003
Timing * Dev Open	Level 2 vs. Level 1	105.88	1	105.88	130.02	0.000	0.006
Timing * Dev Low	Level 2 vs. Level 1	12.49	1	12.49	15.34	0.000	0.001
Timing * Barren Land	Level 2 vs. Level 1	55.04	1	55.04	67.58	0.000	0.003
Timing * Shrub	Level 2 vs. Level 1	123.69	1	123.69	151.89	0.000	0.007
Timing * Herbaceuous	Level 2 vs. Level 1	128.29	1	128.29	157.53	0.000	0.008
Timing * Agriculture	Level 2 vs. Level 1	33.84	1	33.84	41.56	0.000	0.002
Timing * Tree Canopy	Level 2 vs. Level 1	0.08	1	0.08	0.10	0.747	0
Timing * DevHighMed	Level 2 vs. Level 1	52.44	1	52.44	64.40	0.000	0.003
Error(Timing)	Level 2 vs. Level 1	16597.10	20381	0.81			

Figure 5.4: Repeated Measures Within-Subject Contrast Tests.

hypothesis.

The GLM repeated measure model also outputs parameter estimates for each time period. Figure 5.5 indicates (as we saw in Chapter 4), that agricultural lands have a coefficient of -.008 during the non heat wave scene of June 10th. The coefficient indicate that a 1 unit increase in agricultural lands decreases local night temperatures by 0.008°C. Since the unit of analysis for land cover is 30m x 30 m then this effect translates to a 10 acre increase in agricultural lands decreasing temperatures on average by 0.65°F (see Equation 4.1). By examining the regression coefficient for each predictor during the two climatic events, we can assess not only if the coefficients of the covariates change depending on the extreme heat condition but we also can evaluate the direction and magnitude of the change. Figure 5.5 indicates that the coefficient for agricultural lands decrease from -.008 to -.002 (0.16°F) when measured during a heat wave. We also see that the interaction between forested land cover and the timing of the nighttime temperature measurement is not significant. There-

						95% Confidence Interval		Partial Eta
Dependent Variable	Parameter	B	Std. Error	t	Sig.	Lower Bound	Upper Bound	Squared
Non Heat Wave	Intercept	20.755	0.035	586.501	0.000	20.685	20.824	0.944
	Elevation	-0.008	9.34E-05	-84.783	0.000	-0.008	-0.008	0.261
	Open Water	0.003	0	24.005	0.000	0.002	0.003	0.027
	Dev. Open	0.001	6.41E-05	18.32	0.000	0.001	0.001	0.016
	Dev. Low	0.002	8.21E-05	28.248	0.000	0.002	0.002	0.038
	Barren Land	-0.002	0	-4.263	0.000	-0.003	-0.001	0.001
	Shrub	0.000	9.19E-05	1.742	0.081	-2.00E-05	0	0.000
	Herbaceuous	-0.001	9.55E-05	-11.901	0.000	-0.001	-0.001	0.007
	Agriculture	-0.008	0.001	-11.369	0.000	-0.009	-0.006	0.006
	Tree Canopy	8.24E-05	2.98E-05	2.763	0.006	2.39E-05	0	0.000
	DevHighMed	0.003	6.72E-05	38.958	0.000	0.002	0.003	0.069
Heat Wave	Intercept	21.523	0.04	531.939	0.000	21.444	21.602	0.933
	Elevation	-0.004	0.000	-34.901	0.000	-0.004	-0.004	0.056
	Open Water	0.002	0.000	12.542	0.000	0.001	0.002	0.008
	Dev. Open	0.002	7.33E-05	28.288	0.000	0.002	0.002	0.038
	Dev. Low	0.002	9.39E-05	20.493	0.000	0.002	0.002	0.020
	Barren Land	0.003	0.001	5.115	0.000	0.002	0.004	0.001
	Shrub	-0.001	0.000	-11.734	0.000	-0.001	-0.001	0.007
	Herbaceuous	0.000	0.000	3.093	0.002	0.000	0.001	0.000
	Agriculture	-0.002	0.001	-3.009	0.003	-0.004	-0.001	0.000
	Tree Canopy	7.05E-05	3.41E-05	2.07	0.038	3.76E-06	0.000	0.000
	DevHighMed	0.002	7.68E-05	25.44	0.000	0.002	0.002	0.031

Figure 5.5: Repeated Measures Parameter Estimates.

fore we can assume that the coefficient for forested land is equal during a heat wave or non heat wave event.

5.3 Discussion

By examining the regression coefficient for each predictor during the two climatic events (heat wave vs. non heat wave), the aim of this analysis is to determine whether the regression coefficients of the covariates change depending on the extreme heat condition. From the analysis we can see that there is statistically significant difference between the impact of agricultural lands on nighttime temperatures during a heat wave as compared to a non heat wave period. Agricultural lands decrease temperatures less during a heat wave as compared to a non heat wave period. This result indicates that though agricultural lands are under increased stress due to extreme heat, they still maintain their potential to cool local night time temperatures but this cooling potential is diminished. Though the effect from agriculture decreases in magnitude it does not change direction and becomes a heat source. This outcome is encouraging to find that though agricultural lands are not as effective during extreme heat conditions, retaining approximately 25% of its cooling potential, they still provide a cooling benefit to the local area, cooling temperatures when residents need it the most. On the other hand, tree canopy did not show a statistical significant difference in its impact on temperatures during a heat wave. Tree canopy maintains its impact on nighttime temperatures by having a slight warming effect. Tree canopy did not start providing cooling benefit at night but more importantly it did not increase temperatures.

The findings from this analysis are consistent with other findings in the research field. Research examining the response from vegetation during the European 2003 heat wave found that different vegetation types respond differently due to extreme heat [122]. The research found that short herbaceous vegetation such as grassland had an increase in evapotranspiration (ET) whereas ET decreased in forested land from increased temperatures. This change in ET caused forested land temperatures to be twice as high during the day

as over grasslands and the increased ET from grassland helped to attenuate an increase in temperature. Forested land's coping strategies to deal with extreme heat and drought conditions regulates the stomatal openings in order to conserve water. The increased ET from grasslands may provide short term cooling benefits but the vegetation land cover cannot maintain this cooling benefit over sustained time. The research showed that during the end of the heat wave the increase ET accelerated soil moisture depletion and resulted in grassland and crop failure causing an increase in heating. Agricultural responds similarly to grasslands by increasing its ET when temperature rise [123]. This increase in ET from agricultural land cover provides short-term resiliency but can dramatically increase vulnerability with prolong exposure to extreme heat. Tree canopy's conservation of water, on the other hand, prevents a system failure in the land atmosphere interaction.

This short-term benefit of increased ET leads to decrease soil moisture. To maintain the health and function of agricultural vegetation, it is vital that active management is undertaken to ensure sufficient soil moisture. The larger agriculture research world (beyond urban agriculture) is arguing for similar responses. Soil water content must be monitored and maintained at an adequate level during extreme heat periods to sustain the vegetation productivity and functions in order to not only reduce heat stress on plants but continue to provide cooling benefits to local communities during extreme heat conditions [124]. Active management of green infrastructure and specifically agricultural lands during extreme heat should become a priority to cities and local communities.

Water supply is an integral ingredient in maintaining agriculture's cooling potential. Potable water is a precious commodity and water shortages and droughts across the US and the world complicates this solution to agriculture resiliency. Municipal water supplies are already taxed and energy intensive. In 2009 California passed its Water conservation Act calling for a 20% reduction of urban water use, where 60% of use is attributed to outdoor irrigation [125]. Since municipal water supplies are already strained and rain fed agriculture is not sufficient or resilient, water efficiency practices such as water harvesting,

water reuse and improved irrigation through drip irrigation are all important measures to investigate. Specifically water harvesting techniques should be designed and collocated with urban agriculture in order to make urban agriculture more resilient especially during extreme climatic events.

Water harvesting techniques include grey water harvesting, storm water harvesting, and water retention systems such as basins and swales. Constructed wetlands have also been implemented for capture and filtration for peri-urban agriculture in places such as Australia [126]. Grey water harvesting includes the reuse of household generated water that do not contain high levels of contamination such as from bathing and washing clothes. Utilization of grey water harvest may need bio filters or natural pre-filtration treatment from hydrophilic plants before use. Between 8,000 -13,000 gallons of water a year is estimated to be recovered from a community wide grey water reuse project in Almeda County, California. This grey water harvesting generates reusable water from shower and laundry water for irrigation use [127].

Water harvesting techniques primarily focuses on maximizing storm water collection. Water catchment from storm water run off can provide a win-win for cities and urban agriculture. The overabundance of storm water from heavy rainfalls burdens municipal collection systems and waste water treatment facilities leading to flash floods in urban areas damaging the built environment and endangering lives. Excess storm water is a serious problem for many large metropolitan areas, especially in Atlanta, GA. The vast amounts of impervious surfaces from roads, parking lots and buildings not only contribute to the heat island but they also cut off the hydrological cycle by preventing water retention and infiltration, thereby increasing the speed and quantity of rain from a development. Water harvesting can reduce storm water runoff while simultaneously provide for food production.

Addressing the problem of storm water runoff for cities can provide a viable solution for agriculture irrigation. Storm water harvesting collects runoff from impervious surfaces

using surfaces such as roofs as catchment areas and funnels the water to collection systems such as rain barrels or cisterns. A case study looking at Roanoake VA, identified roofs for catchment near all current urban agricultural land and estimated that approximately 500,000 m3/year could be generated for agriculture use [128]. The water collection could reduce load, cost, and strain on infrastructure while providing a necessary agricultural input.

Water recovery from air conditioning systems is an overlooked water harvesting technique in urban environments. For example, the Grand Hyatt hotel in Atlanta recovers over 5000 gallons of water per day from its air handlers and ice machines. Atmospheric water vapor is ubiquitous and vast as it represents as much water as all of the unfrozen freshwater supply on earth. An AC system dehumidifies air during the cooling process generating condensation. This condensation can be a potential source for water reclamation. As air conditioning is the primary prevention for overheating during heat waves, the increase in use provide an excess of water as a byproduct, which could be harvested for agricultural irrigation. Increasing AC use has negative impacts such as increasing energy demand and generating waste heat, which further warms the built environment. Converting atmospheric vapor pressure to condensate is an energy intensive process, more intensive than reverse osmosis for desalination releasing latent heat and increasing waste heat [129]. Moisture harvesting index (MHI) is used to estimate energy requirements based on climate conditions around the world in order to ascertain the potential for this water source [129]. AC condensate cannot be used directly because of bacteria contamination causing public health concerns. Legionella is an airborne bacteria responsible for causing legionnaires disease which is a form of pneumonia. Water must be pretreated or applied through subsurface irrigation to limit exposure.

The cooling potential of agriculture during extreme heat is an important public health component of this type of green infrastructure. Active management of urban agriculture by ensuring adequate available water supply is imperative during extreme heat events to

ensure that agriculture maintains its cooling potential. Agriculture's response to rising temperatures by decreasing stomatal resistance provide for more evaporative cooling and which may be a more effective green infrastructure approach to reducing urban residents vulnerability to heat related mortality.

CHAPTER 6

PHASE 2: CITY LEVEL ANALYSIS OF URBAN FORM

RQ4: *How does urban form change the relationship between urban agriculture and local climate?*

RQ5: *How much land area must be converted to urban agriculture in order to see a local climate benefit?*

At the city scale, I am investigating how the urban form of an area changes the relationship between urban agriculture and local temperature. I specifically analyze whether there is an interaction effect between the urban form of a neighborhood and the use of urban agriculture as a heat mitigation strategy. I am comparing how temperatures vary depending on whether urban agriculture is implemented in one urban form condition, like a dense downtown area, as compared to another urban form condition like a single-family residential area. In order to conduct this investigation, I create urban form typologies based on Atlanta's urban morphology. Additionally in this analysis, I am investigating how much land must be converted to agriculture in order to see a cooling effect. Will a small backyard garden be a sufficient amount of area or will we need to implement a much larger urban farm?

The city level analysis will investigate how different patterns of urbanization mediate the influence of urban agriculture on local climate. A pilot study conducted for my dissertation proposal defense illustrated that the urban form of the built environment may be mediating the effect of agricultural lands on local climate. Using a local climate model to convert vacant lands to urban agriculture, I showed that an urban agriculture intervention in dense urban areas produced a 13% larger effect size in cooling than in a residential area. This illustrates that not only is it important that we place agriculture in cities but the agricul-

tural lands may provide stronger cooling potentials in different parts of the cities depending on the urban form. Therefore it will be important for policy makers and stakeholders to not only prioritize agricultural lands as part of their resiliency toolbox but to also think about the location of agriculture in cities.

In the previous chapters, the MSA analysis illustrates two main problems when conducting empirical urban agriculture land cover analysis. These problems deal with challenges of multicollinearity between different land cover variables and the lack of urban agricultural observations in urban areas. To address the former problem, urban form typologies are used to control for urban land covers that are often highly correlated. As I illustrated in the previous chapter, impervious and tree canopy are highly correlated land covers but we cannot adequately investigate the effect of UHI mitigation strategies without controlling for both of these land covers. Combining land covers in a typology or an index integrates all land covers into a single measurement so that when included in a statistical model, it does not create problems due to multicollinearity. To address the lack of urban agriculture observation in urban areas, I create an urban agricultural land cover proxy. This land cover proxy will, in essence, identify land covers in urban environments that behave similarly to urban agriculture from a radiometric perspective and therefore are likely to have similar cooling properties. By identifying the urban agriculture proxy, I can investigate the effectiveness of agricultural lands in urban areas, even if they are not currently present, in order to advance the discussion of urban agriculture as a heat management strategies.

6.1   Methods

In the previous chapters, I show that agricultural lands can create a statistically significant decrease in nighttime temperatures and that agricultural lands outperform tree canopy in cooling nighttime temperatures. In this chapter, I am investigating whether the urban form of a neighborhood impact the cooling potential of urban agriculture. Do we see the same temperature reduction from agricultural lands in a downtown neighborhood as in a resi-
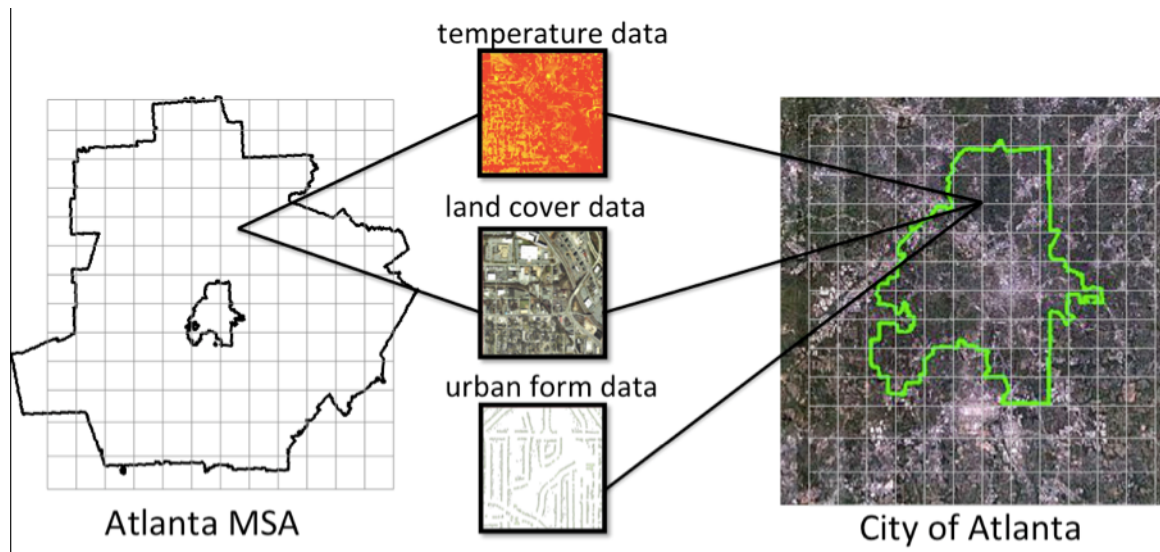
Figure 6.1: The city level analysis is similar to the MSA analysis into that it includes land cover and temperature data but it differs from the MSA analysis with its inclusion of urban form data.

dential one? The city level analysis differs from the MSA level analysis in that it includes urban form data (See Figure 6.1). The data needed to construct urban form typologies is only available at the city level. In addition to the urban form data, the analysis uses higher spatial resolution land cover data than the NLCD to better identify urban vegetation and to develop an urban agricultural land cover proxy. As such, there are three main datasets in this analysis: MODIS nighttime temperature data (the dependent variable), urban agricultural land cover data, and urban form data (See Table 6.1). The urban form data is composited into urban form typologies. Utilizing a similar grid as used in the MSA analysis, each variable will be aggregated to each of the grid cells and will be an observation in the statistical analysis.

6.1.1   Land Cover and Irrigated Urban Agriculture Proxy

For the city level analysis, I use high-resolution land cover data from the Quickbird satellite sensor. The Quickbird data was acquired for the city of Atlanta through Georgia Tech's Center for Geographic Information Systems. The data has a spatial resolution of 2 feet

Table 6.1: Variables needed for the analysis.

Variable Type	Variable Description	Data Source
Dependent	Surface Temperature	MODIS Satellite Data
Independent	Urban agriculture proxy	Quickbird satellite data
	Urban form typology	ArcGIS shapefile –City of Atlanta
		Quickbird land cover data
		LiDAR data – City of Atlanta
		SVF data – SVF simulation software
Control	Elevation	USGS 30 meter DEM
	Seasonal & Diurnal	Timing and day selection

for the 4 band multispectral imagery (Visible and NIR spectrum). The Quickbird data was used to identify land cover at a high resolution and to develop the irrigated urban agriculture proxy. The Quickbird land cover data was acquired as unclassified and in multiple scenes. I used ArcMAP to both mosaic the raster images into one raster and to classify the resulting land cover raster. To classify the Quickbird image, I did a supervised classification using ArcMAP's spatial analysis extension. I generated training sites for Trees, Grass/shrub, Roads, Buildings, Bare and Water and created a signature file from these training sites. When classifying the entire image, I used the maximum likelihood classification and the resulting signature file.

The supervised classification in general did a good job representing the actual land cover but, as with any classification, there were some misrepresentations. Water was the most frequently misclassified land cover. The classified image often labeled shadowed areas as water. Since there is not a lot of water in the city of Atlanta, I opted to exclude water from the classification. This mainly affects the grid cell containing Piedmont Park and the wastewater treatment plant at Hemphill and 10th. Buildings and roads were also misclassified for each other. Since I am only interested in the total amount of impervious land cover and since buildings and roads were often interchanged, I reclassified the road and building land cover into one impervious land cover class. The total vegetative land cover

was classified well. The trees land cover class was often over classified - inhabiting areas that were grass. I compared my classified image to a classified image done with the same dataset for the City of Atlanta (CoA). The visual comparison appeared close except that in general the CoA classification slightly under-classified trees and my classification slightly over-classified trees. My resulting image has a classification of "impervious", "non-tree vegetation", "trees", and "bare."

Irrigated Agriculture Proxy

Identifying cropland that is irrigated is an important process in agriculture research and practice. Researchers often need to know how much agricultural land is irrigated to determine the impact of droughts as well as the cost for agriculture production. To identify irrigated agriculture, researchers often use a threshold based on the agricultural land cover's Normalized Difference Vegetative Index (NDVI) [130, 131, 132].

NDVI is a vegetation index that measures the health, maturity, and leaf density of plants and a plant's NDVI will vary depending on these measures. For example, crops will have a higher NDVI later in the growing season such as in summer than in springtime. NDVI reflects how well a plant absorbs red visible light and reflects infrared light. The pigment, chlorophyll, in plants absorbs visible (red) light in the spectral range of 0.4-0.7 micrometer for energy in photosynthesis, but the leaf structure reflects infrared radiation. NDVI values range from -1 to +1 and land covers with low vegetation such as bare land cover will have a NDVI approaching -1.

The more leaves that are present and the healthier the plant then the more visible light will be absorbed and more infrared reflected. High NDVI values represent dense vegetation as well as agricultural crops that are at their peak growing period. NDVI has been shown to be correlated with biomass and LAI as well as with increase precipitation [133, 134, 135, 136]. When available water increases so does the NDVI for grass, shrubs and crop land covers [136]. NDVI plays an important role in identifying vegetation, healthy vegetation

and even irrigated agriculture. For example to identify irrigated agriculture in Nebraska after one of the worse droughts on record, researchers used remote sensing data in their identification process [131]. They first identified all cropland in the area of interest then calculated the NDVI for the cropland. Next, they calculated NDVI values for known irrigated agriculture locations. They developed a NDVI threshold based on these training sites and verified that any agricultural land with NDVI values exceeding the NDVI threshold were irrigated agriculture.

In my research, I use a similar approach as Dappen et al. [131] in order to create an irrigated agriculture land cover proxy. I identify all potential agriculture land cover and filter the land cover based on a locally derived NDVI threshold. The NDVI threshold is generated from current urban agriculture training sites located in the city of Atlanta. (See Appendix A for more detail) To begin this process, I first calculate the NDVI for the city of Atlanta. Eq. 6.1 represents the formula for NDVI. The Quickbird raster image is a 4 band multispectral imagery. Band 1 represents red visible light and Band 4 represents near infrared. Eq 6.2 substitutes the band numbers in the NDVI equation.

$$NDVI = (NIR{-}VIS)/(NIR+VIS) \tag{6.1}$$

$$NDVI = (Band4 - Band1)/(Band4 + Band1) \tag{6.2}$$

Next, I identify all of the "agricultural lands"in the city. Since agricultural lands are not prevalent throughout the urban environment, I develop an agriculture proxy, which is based on the assumption that grass and agriculture have similar climate-impacting properties and can be interchangeable. Researchers have used grass to represent agriculture in climate studies because they have similar properties that affect the heat balance as well as the hydrological and carbon cycle [35, 137]. Though grassland can be exchangeable for crops and pastures because of their similar properties, they are not a perfect substitution.

Grasslands have a smaller LAI and surface roughness compared to agriculture and do not have increased soil moisture due to irrigation [49]. Using grass as a substitution for agriculture will not fully capture the cooling potential of agriculture, as land cover change from agriculture to grass has been shown to increase local temperatures [49]. It is important to realize that this definition of urban agriculture will create a negative bias by underestimating the agriculture parameter. As such, I assume that all non-tree vegetation has the potential to be agriculture. To identify agricultural lands, I isolate all of the non-tree vegetation land cover into a separate raster. Using the non-tree vegetation land cover raster as a mask, I then extract the NDVI that corresponds with this land cover type.

I next identify irrigated agriculture based on a local NDVI threshold. Agricultural researchers have derived different NDVI thresholds for identifying irrigated agriculture [138, 139, 132]. These thresholds vary across studies because they are based on contextual conditions and therefore do not hold up across irrigated agriculture projects in different locations. Using a similar approach as Dappen et al. [131], I develop a threshold based on the NDVI values for known urban agricultural training sites. I locate irrigated agriculture land in the city of Atlanta and sample from these locations in order to develop a localized NDVI threshold.

Urban agriculture did not take off in Atlanta until after the year 2010 leaving me with the challenge of identifying suitable agriculture locations. As there is no current and exhaustive repository of urban agriculture sites in the city of Atlanta, I used a myriad of sources. To compile my list of agricultural sites in Atlanta, I used directories from Park Pride, Georgia Organics,Food Well Alliance and Local Harvest.org (an online "yellow pages"for urban agriculture). From this analysis, I identified six urban agriculture locations in the City of Atlanta: Habesha Gardens/Rosa Burney Park Community Garden, Peachtree Hills Community Garden, Good Shephard Garden (located on Lawson St and associated with the Good Shephard Community Church), an "Outdoor Activity Center"Community Garden (located from Park Pride), Blue Heron Community Garden and Gaia Gardens. Af-

Figure 6.2: Satellite image of Gaia Gardens (left panel). The grey area represents the irrigated agriculture proxy (right panel).

ter identifying urban agricultural training sites, I digitized and geocoded their locations in ArcGIS.

Misclassification between trees and grass created some bias in the analysis by under-representing high potential agricultural sites. When examining Gaia gardens (See Figure 6.2), we can see that some of the very "green"and lush agriculture land cover is being classified as trees in the remote sensing classification. The left image is of Gaia gardens, the right image is Gaia gardens with the grass layer overlaid. You can see that some of the bare areas are removed (which is good) but not all of it and some of the lush areas at the bottom which is obviously crops are not included in the grass/agriculture land cover raster as they are instead classified as trees.

Now that I have identified my urban agricultural training sites, I next calculate the values of the NDVI for each of the training sites. To do this I use the spatial analysis tool "zonal statistics as table"to aggregate the NDVI values for each of the urban agriculture training sites. The table below (Table 6.2) lists the irrigated agriculture sites and their associated NDVI descriptive statistics. The low minimum NDVI for many of the gardens indicate that much like Gaia Gardens, bare land is included in the agriculture land cover. To set the NDVI threshold, I average the mean NDVI for each site. The average NDVI across all six training sites equaled to 0.41 and is the NDVI threshold I use to identify irrigated

Table 6.2: A list of the irrigated agricultural training sites and the associated NDVI descriptive statistics.

Name	Count	Area	Min	Max	Range	Mean	StD	Sum
Peachtree Hills Garden	441	1708.87	0.05	0.51	0.45	0.42	0.09	187.03
Habesha	1541	5971.36	0.17	0.55	0.38	0.43	0.05	655.37
Good Shepherd Farm	4237	16,418.34	0.05	0.62	0.57	0.43	0.08	1809.36
Outdoor Activity Center	728	2820.99	0.19	0.53	0.34	0.45	0.05	326.66
Blue Heron Community Garden	1108	4293.49	0.23	0.40	0.17	0.31	0.03	342.12
Gaia Gardens	15,835	61,360.50	0.20	0.62	0.41	0.43	0.06	6858.81

agriculture across the city of Atlanta. In essence, if any non-tree vegetative land cover has an NDVI greater than 0.41 then it will be identified as the irrigated agriculture land cover proxy.

Using the "*reclass*" tool located within the spatial analysis toolbox, I reclassify the raster so that all pixels with a NDVI value above 0.41 are classified as irrigated agriculture. I used the Zonal Histogram tool to calculate how much of the area of each grid cell has irrigated agriculture. To examine the effect of patch size I also compute the average area of each irrigated agriculture patch within a grid cell.

Figure 6.3 illustrates the classification of the raster imagery. The image has a transparent fill over all of the impervious land cover giving it a red hue. The vegetative land cover of grass, shrubs and trees that has been classified is able to clearly show through. Image A and C illustrate the irrigated agriculture that is classified in each of the scenes.

Inspecting the classified irrigated agriculture proxy showed that there are many patches in the dataset that are only comprised of one pixel. These isolated irrigated agriculture pixels would skew the average by having many 1 square pixels in the grid cells. I choose to leave these pixels as they were but these isolated pixels may create too much noise in the dataset to see an effect from the size of the urban agriculture. I discuss this problem more in detail in below.
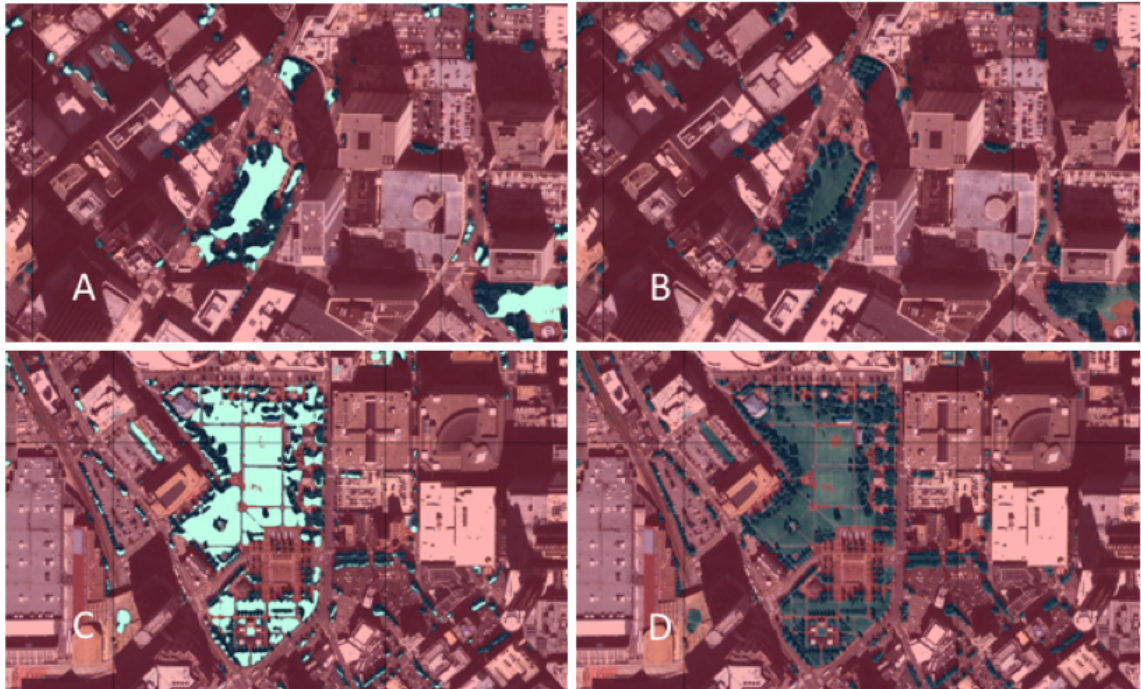
Figure 6.3: Vegetative and agricultural land cover. Images A & B are taken of Five Points in downtown Atlanta with Woodruff Park in the middle of the Image. Images C & D are taken of Centennial Olympic Park. The dark green in the image represents all vegetative land cover that was classified in the images. The bright overlay represents what the land cover that is classified as the irrigated agriculture proxy.

6.1.2   Urban Form – Local Climate Zones

This section briefly discusses different metrics used to measure urban form when investigating a variety of outcomes. When creating urban form typologies for this study, it is important to include urban form parameters that directly impact local temperatures. When analyzing the urban morphology of a city different parameters are well established in the literature to have impacts on various activities including transportation, walkability and building energy; but these parameters do not necessarily translate to impacts on local temperatures. For example, land use mix, residential density and street connectivity have all been shown to be directly correlated with walking [140, 141, 142, 143]. Design criteria such as small blocks and complete sidewalk systems are demonstrated to increase pedestrian travel three times more than sites that had large block sizes and incomplete systems [143]. Urban form thresholds effecting walkability have also been documented stating that areas with at least 6 dwellings per acre and at least thirty intersections per square kilometer were considered to be more walkable [142].

Urban form and urban infrastructure can also have a significant effect on transportation patterns. Researchers have shown that density and compact development have a strong relationship between vehicle miles traveled. For example, comparing fuel consumption to vehicle miles traveled, researchers have demonstrated that a thirty person per hectare threshold and a residential to employment ratio of around 20 per hectare threshold in developments can significantly decrease miles traveled by vehicles [144].

The urban form parameters of mixed land use and accessibility to commercial activities are also important urban form components for both work and non-work trips [145]. Mixed use is especially important in order to break up high-density, single land use areas of employment found in many cities' centers. The availability of transportation infrastructure, such as transit, interstates, parking, road capacity, etc, also has a significant effect on transportation patterns, as does neighborhood design for non-work trips. Neighborhood designs such as 4-way intersections and on-street parking, can have strong influences on

mode choice for non-work travel behavior [145]. The design of the urban environment plays a large role in helping to explain travel patterns, which cannot be explained solely with economic effects of fuel costs [146, 144, 145].

The urban form and the design of buildings have also been shown to effect a city's energy consumption by as much as fifty percent [147, 148]. The urban morphology parameters of density, land use, building size and building typology have been shown to be large drivers to energy efficiency [147, 148, 149, 150]. Studies have found that urban geometry accounted for 10% of the variation in building energy consumption between European cities [148]. A mixture of density has been shown to be a more beneficial urban form strategy then having a consistently high dense area in order to maximize solar radiation for heating and lighting purposes [149] and a mixed land use urban design has also been shown to be more efficient for energy distribution.

Land use research in England has shown that residential buildings use the majority of their energy for space heating whereas air conditioning and lighting contribute to the majority of energy use in office buildings [147]. Detached single-family homes as compared to attached multifamily homes, consume 54% and 26% more energy for space heating and cooling, respectively. As for American single-family homes, there is a 16% and 13% increase in the amount of energy consumed due to heating and cooling for each additional 1000 square foot in housing size [150]. Larger single-family homes are more readily found in sprawling developments and therefore these development types consume more residential energy [150]. Researchers have established building depth thresholds of 33-40 feet, obstruction angles of less than 30 degrees, and 81 dwellings per acre density threshold in order maximize their energy efficiency [147, 148].

There are myriad urban form metrics utilized to understand the performance of the built environment. Land use mix, density, street connectivity, small blocks, complete sidewalk systems, intersection density, residential to employment ratio, accessibility to commercial activities, transit, interstates, road capacity, 4-way intersections, on-street parking, build-

ing size, building typology, build depth, and obstruction angles are just some of the urban form metrics used to access the impact on walkability, transportation and energy efficiency. Therefore when deciding how to create the urban form typologies for this analysis, it was important to select urban form parameters that have been documented to impact temperatures and the cooling efficiency for urban form. Fortunately, there has been extensive urban climate literature illustrating the direct impact of urban morphology on land cover on temperatures.

In order to investigate whether the urban form of a neighborhood impacts the cooling potential of urban agriculture, I create urban form typologies for the city of Atlanta. My urban form typologies are based on Stewart & Oke's Local Climate Zones and the urban form characteristics I use in the creation of these typologies are those characteristics that have been used to define "Local Climate Zones" [151].

Local climate zones were developed to create consistencies in referring to what is "urban"and what is "rural"when measuring urban heat islands. The temperature in cities varies depending on the local urban morphological conditions. For example, temperatures in downtown Atlanta will be hotter than temperatures in a forested historic residential neighborhood. Since the urban landscape varies dramatically within and between cities, the local climate zones were developed to more accurately describe the surrounding physical landscape by using a set of physical characteristics to classify the urban form into specific typologies. These physical characteristics have been shown to directly impact near surface air temperatures, and the specific combination of these characteristics into zones have been shown to relatively impact temperatures consistently across cities. Therefore the morphological characteristics used to define the urban typologies for Atlanta are those that have been found by urban climatologist to directly influence near surface air temperatures. These characteristics primarily refer to the structure of the surfaces such as building height and spacing and the cover of the surface such as whether the surface is covered by impervious or pervious material. "*Surface structure* affects local climate through its modification of

100

airflow, atmospheric heat transport, and shortwave and longwave radiation balances, while *surface cover* modifies the albedo, moisture availability, and heating/cooling potential of the ground"[151].

Oke has argued that the primary drivers of the urban heat island effect can be directly tied to "the urban modification of the surface energy and radiation balance"[152]. From urban climatological research, Steward and Oke have developed ten Local Climate Zones which are defined by seven surface cover and geometric properties of the urban form (See Figure 6.4). In my classification, I use five of the seven properties to identify urban form typologies. The urban form characteristics I include in my urban form typologies include the roughness height, sky view factor, building surface fraction (% building footprint), impervious surface fraction (% impervious surface), and pervious surface fraction (% pervious). The roughness height in urban areas refers to the height of buildings and the sky view factor is a measurement to describe the geometry of urban canyons and refers to the amount of the sky that is visible from the ground. For the local climate zones, both of these measurements are averaged across the grid cell. Once urban typologies are created for Atlanta, I incorporate the typologies into the regression model as categorical dummy variables, and investigate whether there is a difference in effect size when agriculture is implemented in different urban form context.

To calculate the LCZs, I calculate the following parameters:

- **Sky view factor**:Sky view factor is the "ratio of the amount of sky hemisphere visible from ground level to that of an unobstructed hemisphere."To calculate sky view factor, I use the Viewsphere software program developed by Georgia Tech's Perry Yang. I use building height data, building footprints, terrain data, and observation points to calculate the average sky view factor for each grid cell. This process is described in more detail in section 6.1.2.

- **Building Surface fraction**: Building surface fraction is the "ratio of building plan area to plan area (%)."To calculate the building surface fraction, I use building foot-
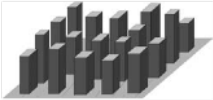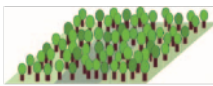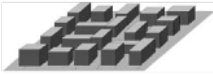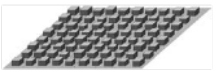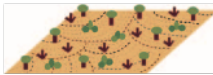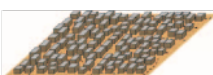
Built types	Definition	Land cover types	Definition
1. Compact high-rise	Dense mix of tall buildings to tens of stories. Few or no trees. Land cover mostly paved. Concrete, steel, stone, and glass construction materials.	A. Dense trees	Heavily wooded landscape of deciduous and/or evergreen trees. Land cover mostly pervious (low plants). Zone function is natural forest, tree cultivation, or urban park.
2. Compact midrise	Dense mix of midrise buildings (3–9 stories). Few or no trees. Land cover mostly paved. Stone, brick, tile, and concrete construction materials.	B. Scattered trees	Lightly wooded landscape of deciduous and/or evergreen trees. Land cover mostly pervious (low plants). Zone function is natural forest, tree cultivation, or urban park.
3. Compact low-rise	Dense mix of low-rise buildings (1–3 stories). Few or no trees. Land cover mostly paved. Stone, brick, tile, and concrete construction materials.	C. Bush, scrub	Open arrangement of bushes, shrubs, and short, woody trees. Land cover mostly pervious (bare soil or sand). Zone function is natural scrubland or agriculture.
4. Open high-rise	Open arrangement of tall buildings to tens of stories. Abundance of pervious land cover (low plants, scattered trees). Concrete, steel, stone, and glass construction materials.	D. Low plants	Featureless landscape of grass or herbaceous plants/crops. Few or no trees. Zone function is natural grassland, agriculture, or urban park.
5. Open midrise	Open arrangement of midrise buildings (3–9 stories). Abundance of pervious land cover (low plants, scattered trees). Concrete, steel, stone, and glass construction materials.	E. Bare rock or paved	Featureless landscape of rock or paved cover. Few or no trees or plants. Zone function is natural desert (rock) or urban transportation.
6. Open low-rise	Open arrangement of low-rise buildings (1–3 stories). Abundance of pervious land cover (low plants, scattered trees). Wood, brick, stone, tile, and concrete construction materials.	F. Bare soil or sand	Featureless landscape of soil or sand cover. Few or no trees or plants. Zone function is natural desert or agriculture.
7. Lightweight low-rise	Dense mix of single-story buildings. Few or no trees. Land cover mostly hard-packed. Lightweight construction materials (e.g., wood, thatch, corrugated metal).	G. Water	Large, open water bodies such as seas and lakes, or small bodies such as rivers, reservoirs, and lagoons.

VARIABLE LAND COVER PROPERTIES

Variable or ephemeral land cover properties that change significantly with synoptic weather patterns, agricultural practices, and/or seasonal cycles.

Built types	Definition	Land cover types	Definition
8. Large low-rise	Open arrangement of large low-rise buildings (1–3 stories). Few or no trees. Land cover mostly paved. Steel, concrete, metal, and stone construction materials.		
9. Sparsely built	Sparse arrangement of small or medium-sized buildings in a natural setting. Abundance of pervious land cover (low plants, scattered trees).	b. bare trees	Leafless deciduous trees (e.g., winter). Increased sky view factor. Reduced albedo.
		s. snow cover	Snow cover >10 cm in depth. Low admittance. High albedo.
10. Heavy industry	Low-rise and midrise industrial structures (towers, tanks, stacks). Few or no trees. Land cover mostly paved or hard-packed. Metal, steel, and concrete construction materials.	d. dry ground	Parched soil. Low admittance. Large Bowen ratio. Increased albedo.
		w. wet ground	Waterlogged soil. High admittance. Small Bowen ratio. Reduced albedo.

Figure 6.4: Local climate zones defined by Stewart and Oke. Local climate zone 1-9 is based on Oke's urban climate zones [153].

print data in the form of ArcGIS shapefile. The building footprint data was received from the City of Atlanta's planning department. Through ArcMAP, I calculate the percent area of each grid cell that is covered by buildings. I use the intersect tool to split buildings that cross the grid cell boundaries and to associate the building footprints with the corresponding grid cell.

- **Impervious surface fraction**: The impervious surface fraction is the "ratio of impervious plan area to total area (%)." The classified Quickbird data discussed above provided the data for the impervious surface fraction. I used the ArcMAP's "Zonal Statistics as Table"tool located within the Spatial Analysis extension to calculate the percentage of the grid that is impervious. Using the zonal statistics tool, I then summed the pixels within each grid. The sum demonstrated the number of pixels per grid that were vegetated land cover.

- **Pervious surface fraction**: The pervious surface fraction is the "ratio of pervious plan area to total plan area (%)."The classified Quickbird raster provides the data for this parameter. I use a similar approach to calculate pervious fraction as I used for the impervious surface fraction. I use the "Zonal Statistics as Table" tool to count total number of pixels that are classified as vegetation. The land cover data is classified by grass and tree canopy. I reclassified the raster data so that grass and tree canopy equaled 1 and all other land covers equaled 0. I then use the zonal statistics tool to sum the pixels which returns the number of pixels per grid that are classified as vegetation.

I check to ensure the zonal statistics tool and the join function ran correctly in ArcGIS for both the pervious and impervious surface fraction calculations. To check the accuracy of the tool, I located the grid with the most impervious land cover. Grid ID 621 had 98.5% and of the grid cell as impervious and the remaining as vegetation. Visually inspecting the grid confirmed this calculation.

- **Height of roughness element**: The height of roughness element is for LCZ 1-10 is the "geometric average of building heights." I calculated the building height from LiDAR data. These heights were joined with the building footprint shapefile used to calculate the Building Surface Fraction parameter. For a full description of the building height calculations see Section 6.1.2 entitled LiDAR.

For my urban form typologies I did not include the Aspect ratio parameter nor the terrain roughness class into the typology creation. The **Aspect ratio** is defined as the "mean height to width ratio of street canyons, or building spacing". This parameter is inversely related to the sky view factor. Since these to variables are highly correlated, I chose to not include this variable. The **Terrain roughness class** is defined as a "Classification of effective terrain roughness (z0) for city and country landscapes". This is based on pre-calculated measurement by Davenport et al [154]. Since a zone is given the class once the zone is determined, it was not necessary to include this parameter.

Grid Scale: The size of a local climate zone can vary significantly in size. Stewart and Oke define zones as "regions of relatively uniform surface-air temperature distribution across horizontal scales of 10^2 to 10^4 meters."According to Stewart and Oke, the LCZs should between 100s and 1000s of meters. From a LCZ demonstration video conducted by WUDAPT, researchers indicated that optimal scales for what they call their training sites should be a minimum side of 250 meters and that the optimal distance on a side is 500 meter. Unger et al. [155] also use a grid size of 0.5km x 0.5km for the LCZ classification. MODIS nighttime temperature data, which is used for the dependent variable, is only available at a 1 km resolution. Following WUDAPT and Unger et al. (2011) I used a grid size of 0.5km x 0.5km for my urban form typologies. Using this grid size results in a sub-grid of my 1km temperature data. Dividing the original 1km grid results in grid cells that are 500 meters to a side. For pattern recognition purposes- in their paper [156] WUDAPT had to pick their training sites to be smaller around 100-150 meters but they said this was not optimal for LCZs final classification and had to do some reclassifications after the pattern

recognition, though they did not explain exactly what they did. To subdivide the original grid created from the 1km MODIS temperature raster, I used the fishnet tool in ArcGIS.

LiDAR – Building Height Data

The roughness height parameter is derived from building height data. For local climate zones 1-10, the roughness height parameter represents the average building height per grid cell. To derive building height data, I used three primary datasets: the building footprint shapefile discussed above which I used to generate the building surface fraction parameter; a digital elevation model (DEM), and Light Detection and Ranging (LiDAR) data (See Appendix B for more detail). The LiDAR data was produced for and acquired from the City of Atlanta's planning department. LiDAR is a remote sensing technique used to map both natural and man-made elements on the earth's surface. The LiDAR data is comprised of unclassified point cloud data, has a spatial resolution of 1.5 ft., and did not cover the entire city limits for Atlanta. See Figure 6.5 for the boundary area of the LiDAR data. Since the LiDAR data is only available in this area, this boundary becomes the area of the study for the city level analysis.

To generate building height data, I use LiDAR and DEM data to create a normalized digital surface model (nDSM), which is joined with the building footprints shapefile. An nDSM represents the height of the surface above the ground layer and is created by subtracting a DEM from a digital surface model (DSM). Since the point cloud data is unclassified, I use a DEM from USGS to represent the base layer and the LiDAR data to create a DSM. I use ArcGIS's ArcMAP and ArcCatalog to process the LiDAR and USGS DEM data. Using ArcMAP's conversion tool, I convert the LiDAR dataset to a raster image. Each pixel in the raster is given an elevation value from the converted dataset. I use ArcMAP's raster calculator to create the nDSM by subtracting the DEM raster from the DSM raster and join this raster data with building footprint data. Figure 6.6 illustrates an elevation of downtown Atlanta generated from the LiDAR data. For visualization purposes, I create
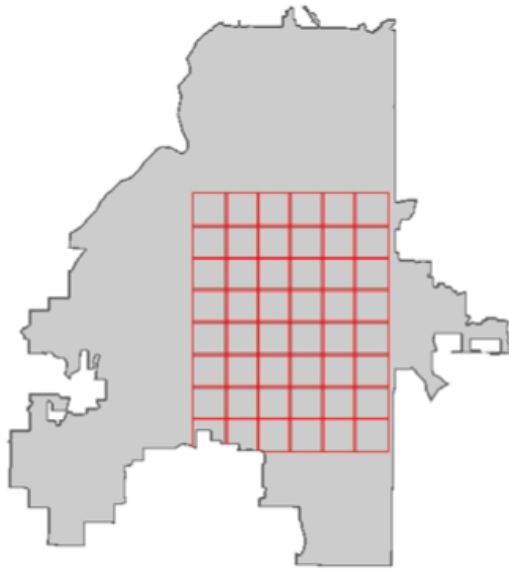
Figure 6.5: LiDAR Boundary Area.
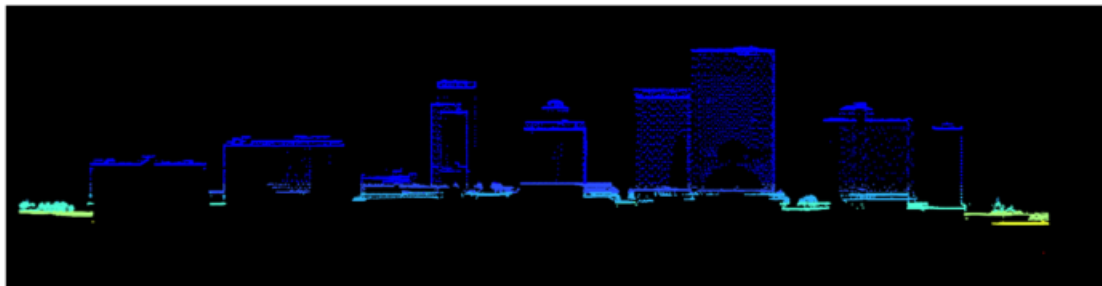
Figure 6.6: Elevation of downtown Atlanta created from the LiDAR data.

a hillshade plan view using the Image Analysis extension in ArcGIS to create an easy to interpret elevation dataset (See Figure 6.7).

Using the USGS DEM data and the first returns from the LiDAR data to generate building height data, I was able to generate accurate building heights. For example, checking residential neighborhoods, single story single-family residential buildings had heights approximately 14 feet tall. When checking the downtown area, buildings near five points were all quite accurate. For example, my process estimated an elevation height of 842 feet for the SunTrust building. The SunTrust Wikipedia page indicates the building is 869 feet.
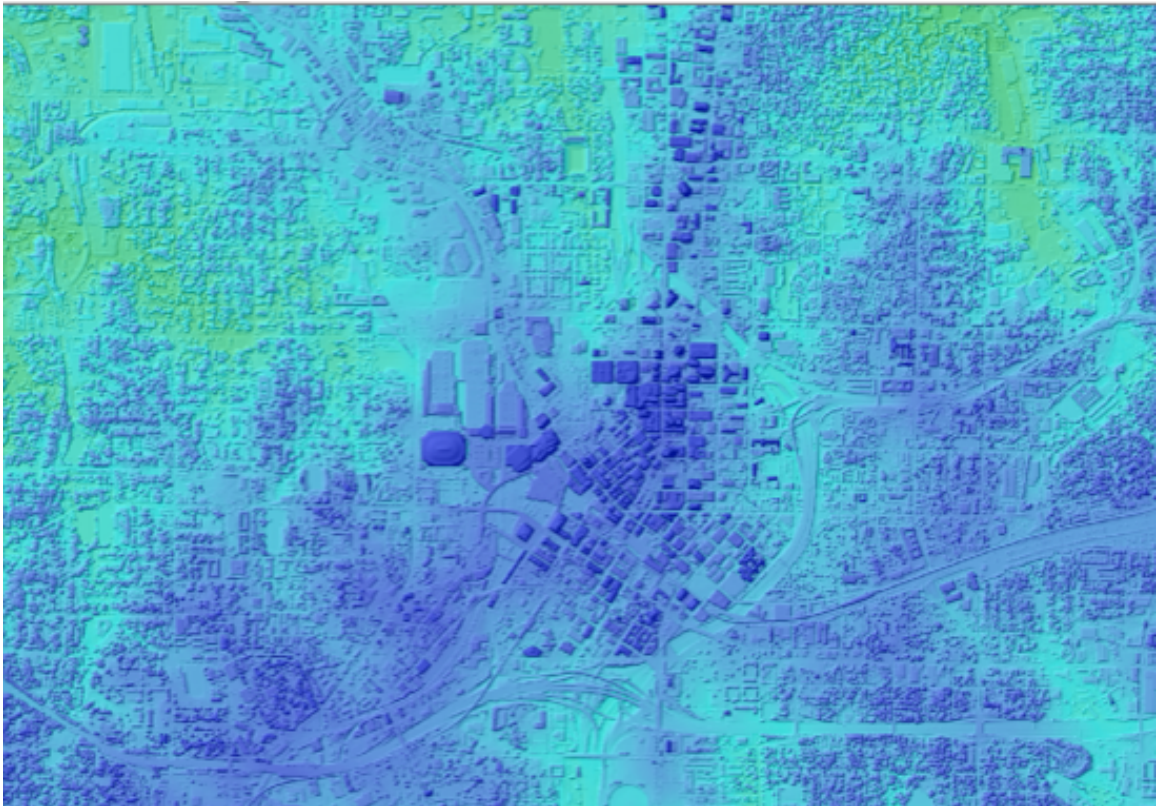
Figure 6.7: Hillshade plan view of Atlanta's elevation data generated from LiDAR data.
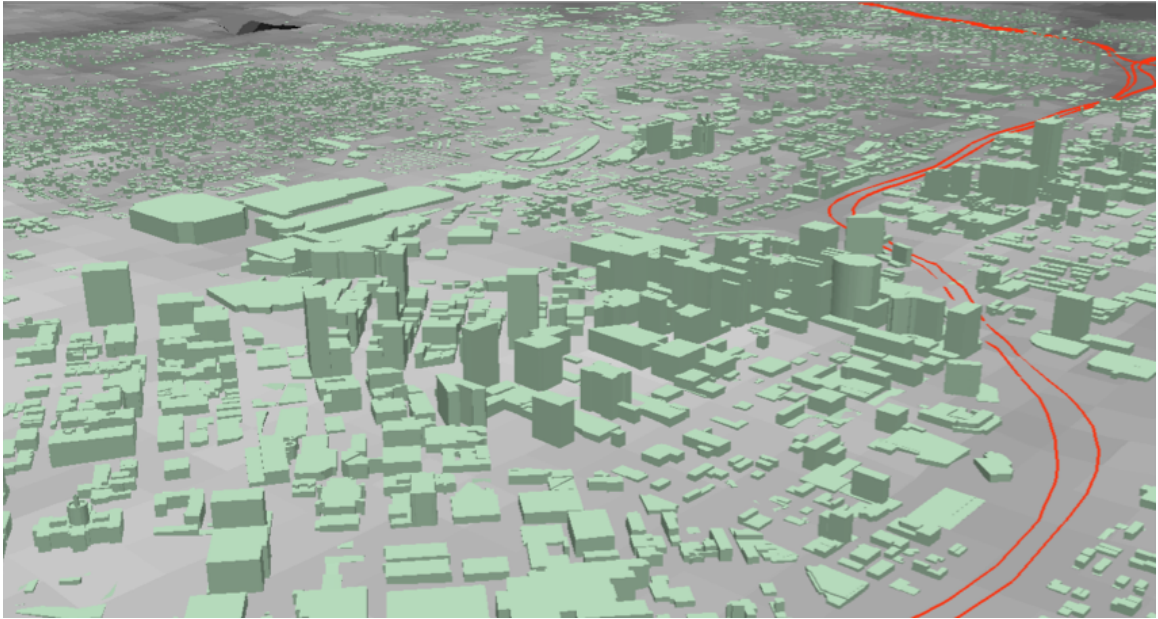
Figure 6.8: 3D Model of the constructed building height data for the study area.

Given the varied height of the building top, this is a reasonable estimation. Figure 6.8 is a visualization of a 3d model created in ArcScene of the constructed building height data.

Sky View Factor

Sky view factor is the final parameter for the urban form typologies. The sky view factor (SVF) represents the percentage of sky that is visible from a specific observation point. SVF is a ratio that ranges from 0 to 1. Zero indicating that no sky is visible and 1 indicating that 100% of the sky is visible. An open greenspace such as a park or golf course will have a SVF approaching 1 whereas urban canyons created from closely clustered tall buildings often found in historic downtowns will have a SVF closer to zero. To calculate the sky view factor for my urban form typologies, I use Viewsphere [157]. Viewsphere is a GIS-base software application created to measure the 3D visibility of differing urban forms. ArcGIS' ArcScene is used to run Viewsphere. Because of the programing platform for the Viewsphere software, an older version of ArcGIS (v9.3) is needed to run the software. To calculate the SVF through Viewphere, the user needs three datasets, a 3D surface topography file saved as a TIN file, building footprint data with building height in its as-

Figure 6.9: Observation points for sky view factor calculations.

sociated attribute table, and observation points which indicate where to calculate the SVF (See Appendix C for more detail).

For the observation points needed to create the SVF, I created them from the nodes in a street shapefile. The points are located approximately midblock as well as close to street intersections. This approach was an efficient method to locate observations in street canyons that are evenly dispersed throughout each grid cell and throughout the study area. Figure 10 illustrates the street shapefile overlaid on top of an areal image of downtown Atlanta. The yellow dots represent the observation points from which the SVF is calculated. I clean the observation point data by removing any observation points that intersect a building footprint. Also I removed any nodes that were more than the maximum buffer distance from a building. This buffer limit is set by the "max radius"field in the viewsphere dialogue box with a default value of 300 feet. Ninety-five percent of these nodes were located along the interstate.

To create the 3D surface topography file, I use a USGS 10-meter resolution DEM. I crossed checked this elevation data with 2ft topographic contour lines for the city of Atlanta to ensure the accuracy of the data. The 3D Analyst Tools located in ArcMAP is
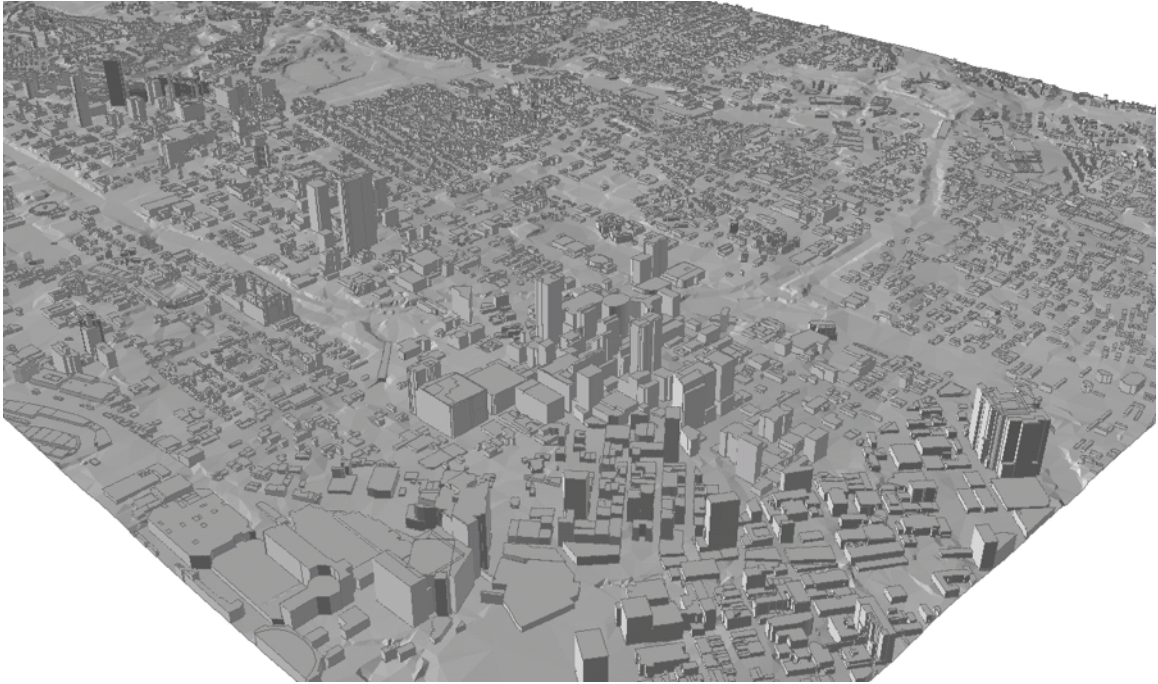
Figure 6.10: The study area with the 3D buildings added to the topographic TIN data.

used to convert the DEM to the necessary TIN file. Next I add three-dimensional buildings to the surface topography with an ArcScene plugin tool, "Add Bldgs to TIN". I use the building footprint heights and shapefile created from LiDAR data as discussed in the previous section. Figure 6.10 illustrates my area of study with the 3D buildings added to the topographic TIN data.

Using the observation points and the 3D surface TIN file, I calculate the SVF for each observation with Viewsphere. In the Viewsphere dialogue box I set the Z offset for the observer to be 1.5 meter, Initial Radius to 300 feet, the rooftop buffer to 0.3 feet, and I left default settings for everything else. I join the SVF output file with the observation point shapefile and average the SVF of each observation point to their corresponding grid cell.

For a more detailed examination of my SVF calculations, I created a subset of my data for one grid cell in downtown Atlanta in the Five Points district (See Figure 6.11). Checking the SFV for the area, the observation points had a SVF range from 0.1814 to 0.7716. The points with the higher SVF (more sky visible) were located along Peachtree Road and

Woodruff Park and the smallest SVF were located inside of Fairlie Poplar. The average for these 11 points is 0.44. The high SVF calculations along Woodruff parks positively skews the SFV average so that it has a higher average than if the park was not present.

Classifying Urban Form Typologies

As previously discussed, my urban form typologies are based on Stewart & Oke (2012) Local Climate Zones [151]. The urban form parameters used in the typology classification are based on the parameters used to classify LCZs. To classify my urban form typologies, I used the definitions and parameter ranges for each LCZ as a guideline for my classification process. The LCZ classes are not easily generalizable to other cities as there is not a seamless process to recreate Stewart & Oke's LCZ exactly how they define their zones. First of all, none of the classes are mutually exclusive. All of the class parameter ranges run into adjacent classes. In addition, there is no first order priorities given to the different the urban form parameters. Because of these challenges, there is no pre-established way to create a decision tree in order to classify grids into their respective classes in order to match exactly how Stewart & Oke classified their LCZs. Also, many of the classes that should be classified as a specific zone by definition did not have urban form parameter values that matched the associated parameter ranges as defined in Figure 6.4. This problem will be discussed more below.

Stewart and Oke understand this challenge and in their seminal paper on LCZs they discussed that the LCZ classes are not perfect representations of urban environments. They explain that the metadata detailing the surface properties for each LCZ will not match perfectly with real world examples. LCZ metadata "should lead users to the best, not necessarily exact, match of their field sites with LCZ classes"(pg 1891)[151]. They explain that it is important to have a person with good local knowledge involved when classifying the LCZs. The creation of subclasses, that is the combination of different LCZs, may be necessary in order to best classify the urban form. Though this may be a more accurate
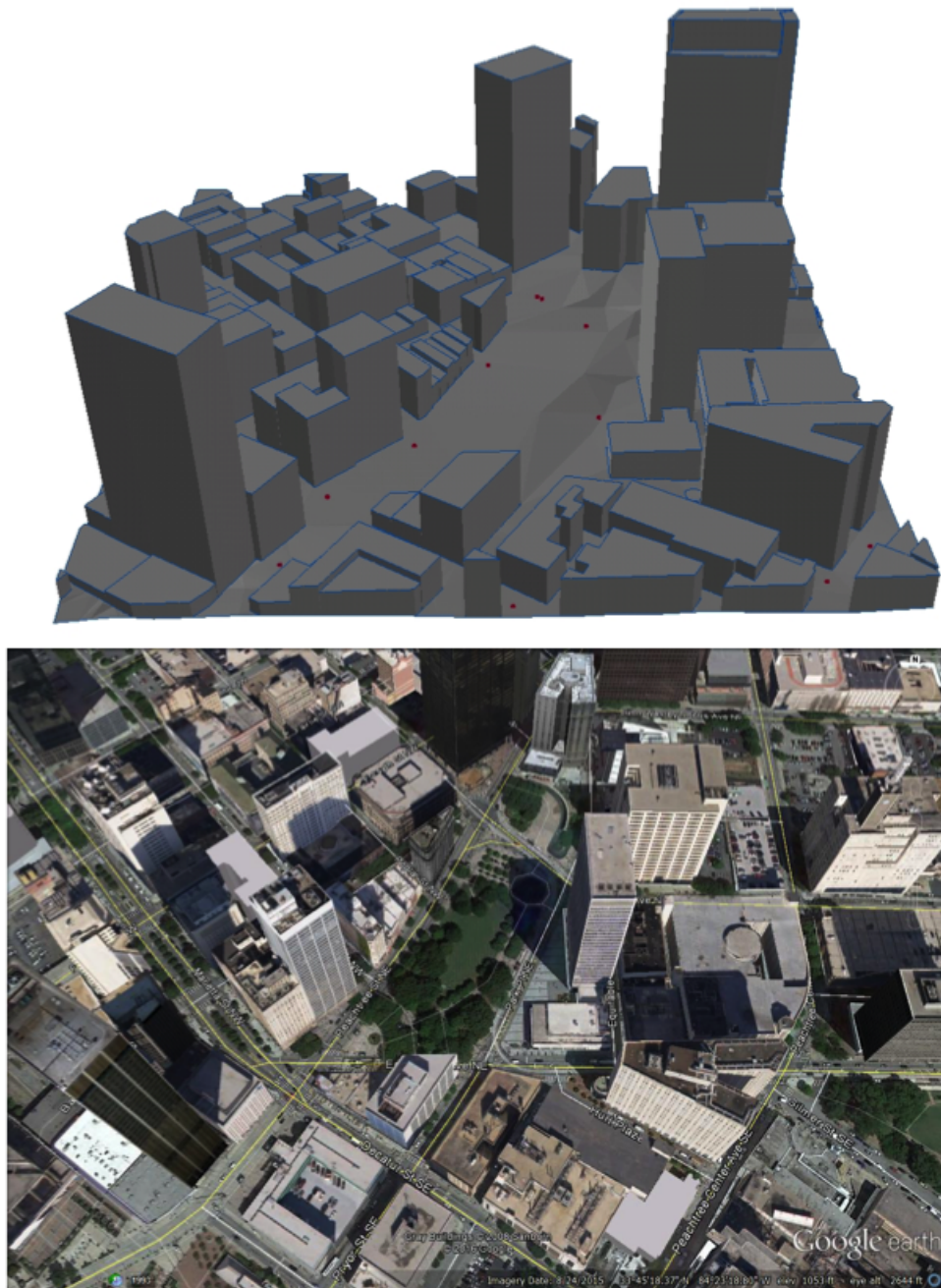
Figure 6.11: A detailed look at one grid cell in the Five Points/Fairlie Poplar district. The top image is a screen shot of the 3D rendering of the building height data with the observation points for the sky view factor calculations. The bottom image is a screen shot from Google Earth to give more context for the area and to also validate the 3D model.

classification approach, there are definite tradeoffs for creating LCZ subclasses. Too many subclasses may create too much variability between local climate zones and make it even more difficult to generalize LCZs to other cities.

To classify my urban form typologies I developed a method based on the work of the World Urban Database and Access Portal Tools (WUDAPT). WUDAPT has the most publications, information, and research presence on the actual classification of LCZs. Their aim is to create LCZs for cities across the world. Instead of using the predetermined parameter ranges for LCZ identification from Stewart & Oke, the researchers establish their own parameter ranges from a city's present urban form. Their method creates training sites, where the researcher identifies sites in all LCZ categories that are present in their region of interest (ROI). In order to identify appropriate LCZ classes for the training sites, WUDAPT argues that researchers identifying these training sites should be a person with good local knowledge of the area. They use Landsat 8 data, Google Earth and SAGA GIS (opensource GIS platform). They create their training sites in Google Earth and then import these sites into SAGA. WUDAPT uses limited urban form data for their classification as their purpose is to develop a universal process that anyone can conduct. They use Landsat 8 landcover data, but does not generate other variables such as roughness height or sky view factor. They then put the sites into a preprogram pattern recognition application in SAGA where they classify the rest of the ROI based on the properties in each training site. The input training data must be in raster format for the pattern recognition application. They do not discuss the limitations of excluding many of the other urban form metrics.

Building from their work, I devise a similar methodology to identify my urban form typologies for Atlanta, GA. I first create training sites in ArcGIS. To create training sites, I identify grids which are good representations of the individual Local Climate Zones. In some cases, I had to create LCZs subclasses to best classify the urban morphology distinct to Atlanta. After training sites were identified, I then derive the statistics for the urban form properties for all sites associated with each LCZ (average, min and max, std). I then create

new threshold values for each LCZ to represent the conditions in Atlanta, GA and classify the remaining grids according to these values using ArcGIS attribute functions. Left over grids that did not have parameters to fall within the zone parameter were either grouped into new classes or nudged into the preexisting classes.

Mixed Local Climate Zones

For my classification process, I have selected "training sites for the different local climate zones in Atlanta. In order to generate statistics from the training sites, I need to first identify the LCZs that are present in Atlanta, GA. Atlanta's urban form did not easily fit into the predefined LCZ classes. A use of mixed zones was necessary to accurately classify the urban form. To illustrate the need for mixed zones, I use the LCZ1 as an example. LCZ 1 represents compact high-rise development and is a development type typically located in historic downtowns. A simplified illustration of LCZ 1 is represented in Figure 6.12

According to the parameter ranges for LCZ 1, Atlanta did not have any LCZ 1 in the city. At first, this was surprising finding giving the distribution of tall buildings and large amounts of impervious surfaces in the downtown and midtown neighborhoods. Though Atlanta has many tall buildings in their downtown neighborhood, they are not tightly nestled together creating a continuous area of tall buildings that would be necessary for LCZ 1 (compact high-rise). Many of the tall buildings are adjacent to smaller buildings and to open spaces creating a more spread out urban form in Atlanta's downtown and midtown neighborhoods. The open spaces are not necessarily green space but more often are represented by large spans of impervious surfaces. These neighborhoods have a lot of surface parking lots distributed throughout them. In addition, the interstate (I-75/85 and I-20) cuts right through the downtown area. Atlanta's dense urban areas have some tall buildings but there exist a lot of space between buildings because of parking lots and transportation infrastructure like interstates. Atlanta's urban morphology creates a problem with the roughness height, building surface fraction and sky view factor parameters values necessary for a LCZ 1 classification.
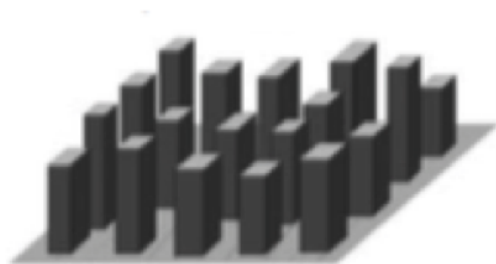
Figure 6.12: This image is a simplified generalization of the urban morphology for LCZ 1.

Figure 14 illustrates the problem associated with the roughness height parameter, which translates into building heights. In this image, I have selected grid cells that have an average building height greater than 80 feet (the lower height threshold for LCZ1). I have also highlighted in yellow the buildings that are greater than 80 feet. In these grid cells, the tall buildings do not represent more than 50% of the buildings in their corresponding grid cell. The building height variable for these grids has a positively skewed distribution with the majority of building height frequency falling around 50 feet. These grid cells have large variances in the building height variable and have large standard deviations with some larger than the mean. The mix of tall buildings (greater than 80 feet) and medium height buildings (50-80 feet) is better represented by creating a subclass. Instead of representing a standard LCZ 1, these grid cells are better represented with a LCZ subclass, which would be a mix between compact high rise and compact midrise.

Building Fraction

The building fraction parameter is another variable that does not fit well with Stewart & Oke definition for both LCZ 1 and LCZ 2. The building fraction represents the percentage of the grid cell that is covered by building footprints. In Atlanta, the dense urban neighborhoods do not have a building fraction as high as the LCZs would suggest they would have. Figure 6.14 is an image of Midtown Atlanta and is located just north of the Ponce de Leon Avenue and the Peachtree intersection and includes the Fox Theatre. This midtown cell only has a building fraction of 0.372. I recalculated the building footprints for this grid cell to ensure the accuracy of the parameter measure. The parameter value is so low because of the multiple surface parking lots located in the grid cell. I found similar problems throughout the study area and especially in the grid cells located

115

Figure 6.13: Roughness height example for Atlanta. The top images represent south Midtown at the intersection of I75/85 and North Avenue. The bottom images represent north Midtown at the intersection of 14th Street and Peachtree Street.
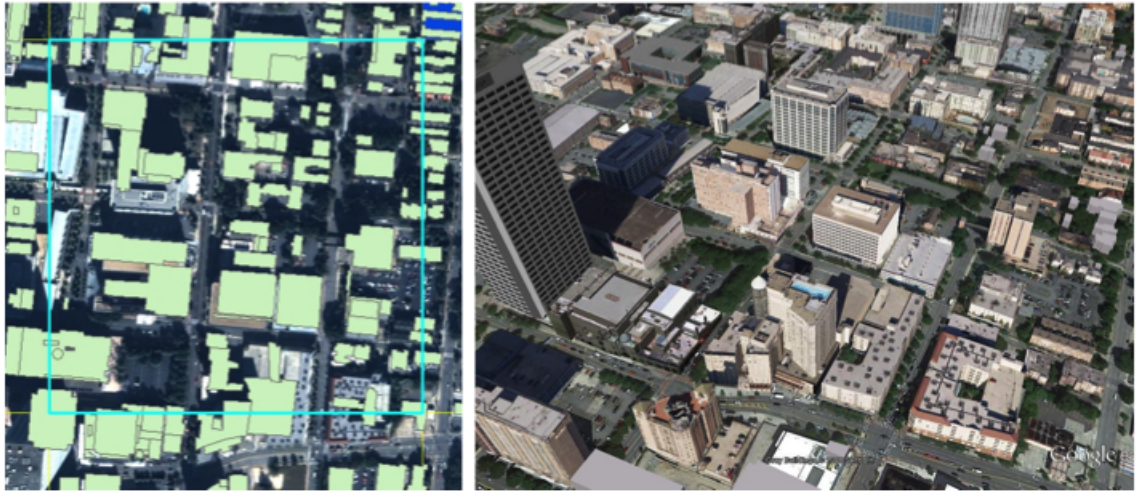
Figure 6.14: An image of midtown Atlanta illustrating the low building fraction in Atlanta's high dense neighborhoods.

along the instate connector.

Sky View Factor

In addition, the sky view factor parameter also did not match up with the real world observations in Atlanta, GA. For example, the downtown SVF example at the end of Section 6.1.2 did not fit into the LCZ 1 category. This grid cell which is located in the Fairlie Poplar and Five Points neighborhood had an average sky view factor greater than 0.4 whereas the SVF range for LCZ 1 is 0.2-0.4. The location of Woodruff Park in the grid cell contributed to a higher mean value. In fact none of the grid cells in my study area had a sky view factor within the LCZ 1 range, which meant that none of the grid cells could be classified as LCZ 1 in my analysis according to Stewart & Oke.

Since the SVF variable is an average metric, the distribution of observation nodes could potentially skew the mean value. Since I generated these observations from street nodes, I selected a handful of grids to ensure that the placement of the observations were not biasing the results (i.e., if there were many observations located along a park or parking lot compared to in an urban canyon) and were relatively evenly distributed throughout the grid cells. Figure 16 illustrates two examples of Midtown grid cells. The two images represent south midtown (just south of the fox) and north midtown (colony square). One can see that the observation nodes are pretty well distributed. There

are a few more observations located along North Avenue for the south midtown grid and along 14th Street for the north Midtown cell. Removing a few of these nodes and recalculating the average did not substantially change the average SVF outcome in any particular direction. For Atlanta, neighborhoods do not have consistently low sky view factors even for the downtown and midtown areas. As such, there is little variability in the sky view factor metric. This limited SVF variance is a result of the measurement itself and the sprawling character of Atlanta's urban area, even in the more dense downtown areas.

Comments on Parameters

Certain parameters had limitations when used to define the urban form typologies. For example, some had higher explanation power, others had limited variance, and others had operationalization problems. First of all, the parameters for the local climate zones were not equally important to all zones. Certain parameters were more important than others in defining zones. Some of this importance is attributed to the parameters variance and range of observations. For example, the sky view factor and the building height parameter did not have large variances in their distribution range and as such they are not very useful parameters for distinguishing between all zones. They were most helpful in identifying the zones with the most building density (the compact high/midrise and the open midrise zones). Beyond these two urban form typologies, the lack of variance in the data made it less useful in distinguishing between other typologies. In addition, the building fraction parameter had operational problems. Getting reliable building footprint shapefile data is difficult. Buildings change frequently and the shapefile data is not updated often enough to accurately represent the adding or demolishing of buildings throughout the city. In addition, the way the building footprints are drawn also creates problems. Often complex buildings are drawn with multiple overlapping polygons to represent the building footprint instead of having a single polygon to represent the perimeter of the building. This operationalization process creates problems when calculating building fraction but also with other variables that need the building footprint data such as building height and sky view factor data. The Stewart and Oke classification did not maximize all variables needed in order to classify their zones, as such additional variables were needed for better identification. For example, average building size was a useful urban form parameter for distinguishing between the large low and midrise development pattern. In some examples, these development patterns had

118
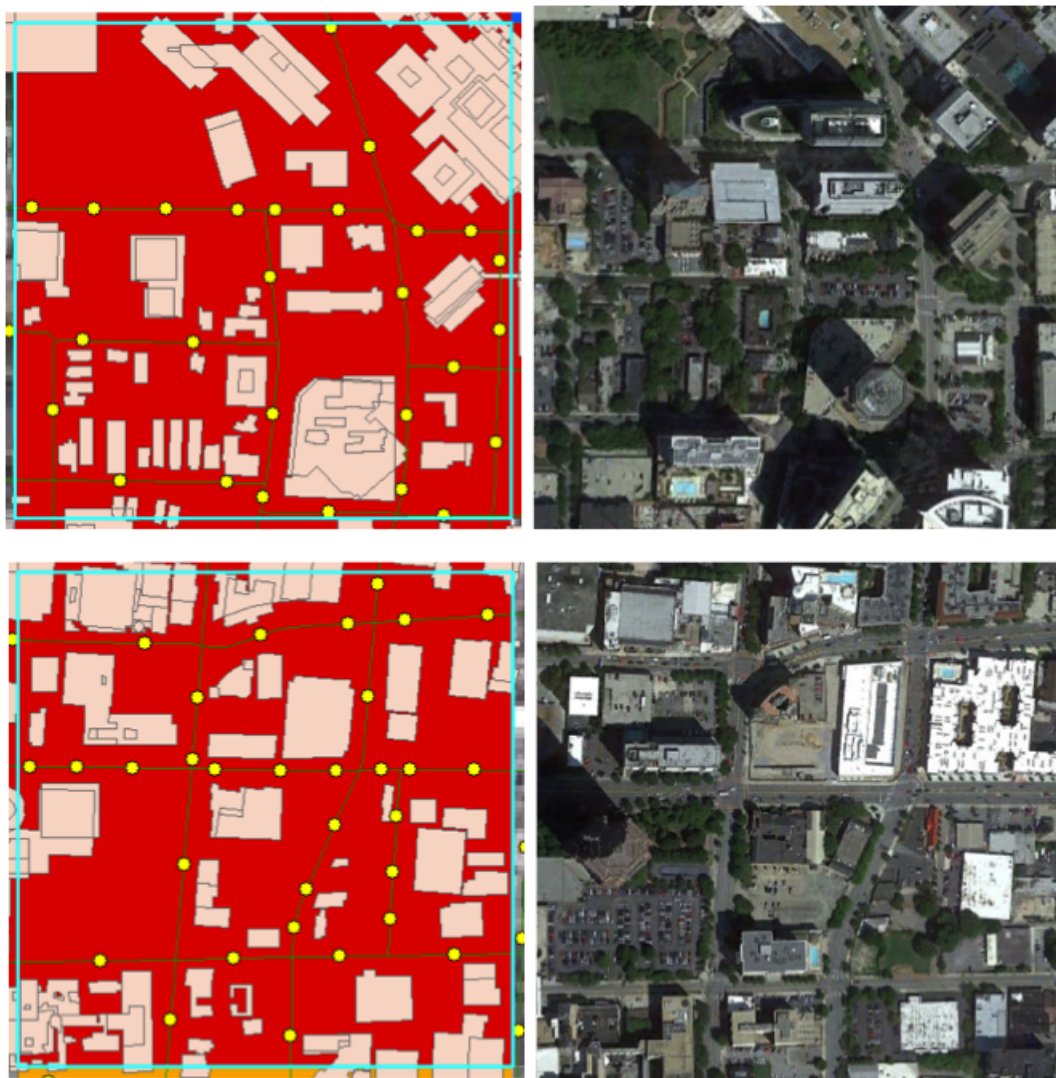
Figure 6.15: Illustrate the observation nodes for SVF calculations in north Midtown (above) and south Midtown (below).

similar impervious surface coverage, and building fraction but the average size of the buildings help to distinguish the typologies. Geletic et al. [158] also supplement the LCZ classification with number of buildings when identifying LCZs in two European cities.

Urban Form Classes

Atlanta had seven main urban form classes. These urban form classes include both LCZs and LCZ subclasses. The urban form classes include: compact high/midrise, open midrise, large low-rise, infrastructure, open mid/low-rise, open low-rise, and sparsely built (See Figure 6.16). Three of these urban form classes are subclasses I created by combining two or more LCZs. They include: Compact High/Midrise, Open Midrise, and Open Mid/Lowrise. Open Low-Rise, Large low-rise, Open Low-Rise, Sparsely Built and Infrastructure were based on Stewart & Oke's previously defined LCZs (6,8,9, & E). In addition to the seven main urban form classes, most of these classes have additional subclasses depending on whether there is substantial amount of infrastructure located within the grid or a substantial amount green space located within the grid. In addition, there are two other categories that do not fit well in the urban form typology one is "Greenspace- a grid that is predominantly green- and the second is LargeLow Residential.

The compact high/midrise zone is mainly located in downtown and midtown and is combination of LCZ 1 & 2. Combining the two zones provides for a better urban form typology where there are no consistently tall buildings in Atlanta even on a smaller grid scale. As previously noted, most tall buildings are combined with tall midrise buildings between 32' and 82' – and vice versus – most midrise buildings are combined with some tall buildings (greater than 82'). This urban form class takes place only in midtown and downtown. The grid cell that includes Ponce City Market is the one exception. The sky view factor is much higher in this category than in Stewart and Oke's classification parameter and this difference is because Atlanta has an extensive amount of parking lots and is due to the interstate cutting right along/through the most dense areas of the city – namely through downtown and midtown.

The next two subclasses both combine the infrastructure class into their definitions. As discussed, Atlanta's non-residential core is very impervious but these areas do not have densely clustered buildings. The "open"categories for both midrise and low-rise development do a good job at
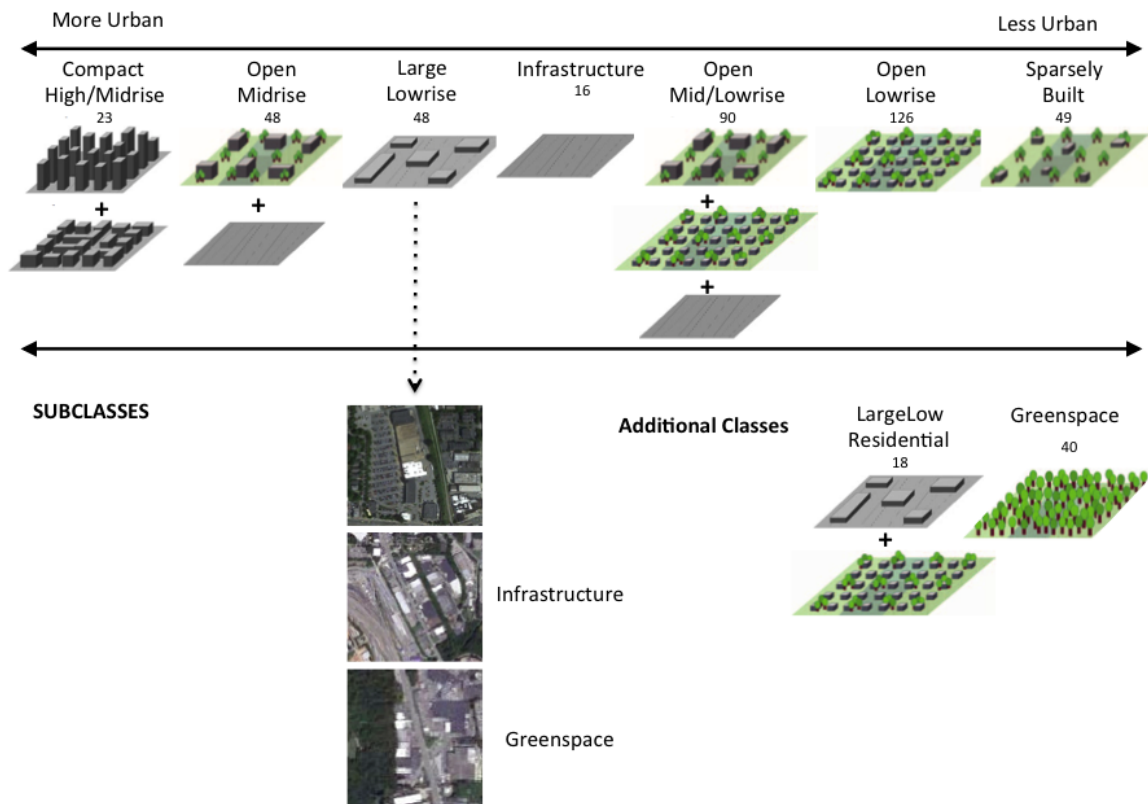
Figure 6.16: Urban form classes and subclasses classified for Atlanta's city center.

representing different areas of Atlanta but Stewart and Oke indicate that this openness is created by pervious surfaces and green space as we see with modernist/Corbusier development theory which can translate into office parks or different large scale public housing projects around the world. But in Atlanta's more historic core, historic buildings have been torn down and replaced by impervious transportation infrastructure such as surface parking lots, interstates and rail yards. For example, the open midrise class is combined with the infrastructure class because of the substantial about of impervious surfaces located in these areas. As per Stewart and Oke's description, this class has medium tall buildings that are spread out in the grid cell but instead of pervious land cover such as green space being the predominant land cover creating the openness of the urban form it is due to impervious surfaces such as parking lots and transportation infrastructure such as railroads and interstates. The Open Mid/Low-rise subclass combines both midrise and low-rise buildings that are spread out and thus do not have a high building surface ratio. As with the open midrise class, this urban form class also included infrastructure in its definition because of the lower amount of pervious coverage and the predominance of parking lots and other impervious land covers.

By identifying seven main urban form classes, distinguishing between outlier development typologies, and classifying green/infrastructure subclasses, creates a higher fidelity in the urban form classification scheme. Increased fidelity creates more classes, but it allows me to analyze only the zones that are better representative of their urban form definition.

6.2   Analysis

In this city level analysis, I am examining the impact of urban form on the cooling potential of agriculture. In order to explore this research question, I investigate whether there is an interaction effect between urban form and irrigated agriculture in relationship to the dependent variable of nighttime temperature. I am asking whether the relationship between urban agriculture and nighttime temperature changes depending on the surrounding urban morphological conditions in which the agriculture is implemented. Additionally, do we see that the size and amount of agriculture has an impact on the local temperature.

From Chapter 4, I illustrate that each additional increase in 10 acres of agricultural land can, on average, decrease night time temperatures by approximately 0.65°F for every 1 km grid cell. In

Chapter 5, I illustrate that the presence of a heat wave moderates the cooling potential of agriculture. In this chapter, I am questioning whether there is an interaction effect with urban form and agriculture and if there is a threshold effect when it comes to the size of the urban agricultural implementation. Is there a threshold value where the predicted behavior of the independent variable changes once this threshold is exceeded? For example, we may see that urban agriculture provides little to no cooling benefit to an area unless a certain amount of agriculture is implemented which exceeds the critical threshold value. Below the threshold value there will be little to no effect and above the threshold value there is a statistical significant impact. In order to investigate these two research questions, I create an interaction term between the categorical variable of urban form and the proxy measure of irrigated agriculture. I then group the observations by the agricultural land present in each of the zones to investigate a potential threshold value.

Local climate zone classification is used to create the categorical variable in the statistical model. The LCZs distinguishes between urban form typologies that should theoretically vary by temperature. Looking at the urban form typologies I created for Atlanta, GA, one can see that the temperatures are varying across the differing typologies. Figure 6.17 illustrates that the urban form classifications created are robust enough to see temperature variation between zones. The "Compact High/Midrise"typology has the highest average temperatures and the "Sparsely Built"has the lowest average temperatures. Infrastructure typology falls right in the middle but it also has the least number of observations with the largest standard deviation. The order of zones by temperature falls well in line with other documentation of LCZ temperatures (Stewart & Oke, 2011) There is a $2°C$ difference between the coolest zone and the warmest zone.

To confirm a statistical difference between the LCZ temperatures, I conduct a one-way ANOVA and employ Tukey's post hoc pairwise comparisons. The Sparsely Built zone is statistically different from all other zones. Compact High/Midrise and Open Midrise are not significantly different from each other but are significantly different from all other LCZs. The Infrastructure zone showed the least difference between zones. It was only statistically different from Compact High/Midrise, Open Midrise, and Sparsely Built. Infrastructure has the largest variance and smallest sample size of all the zones. As previously discussed, it was difficult to select zones that were completely comprised of impervious infrastructure as infrastructure was often coupled with large amounts of green space.
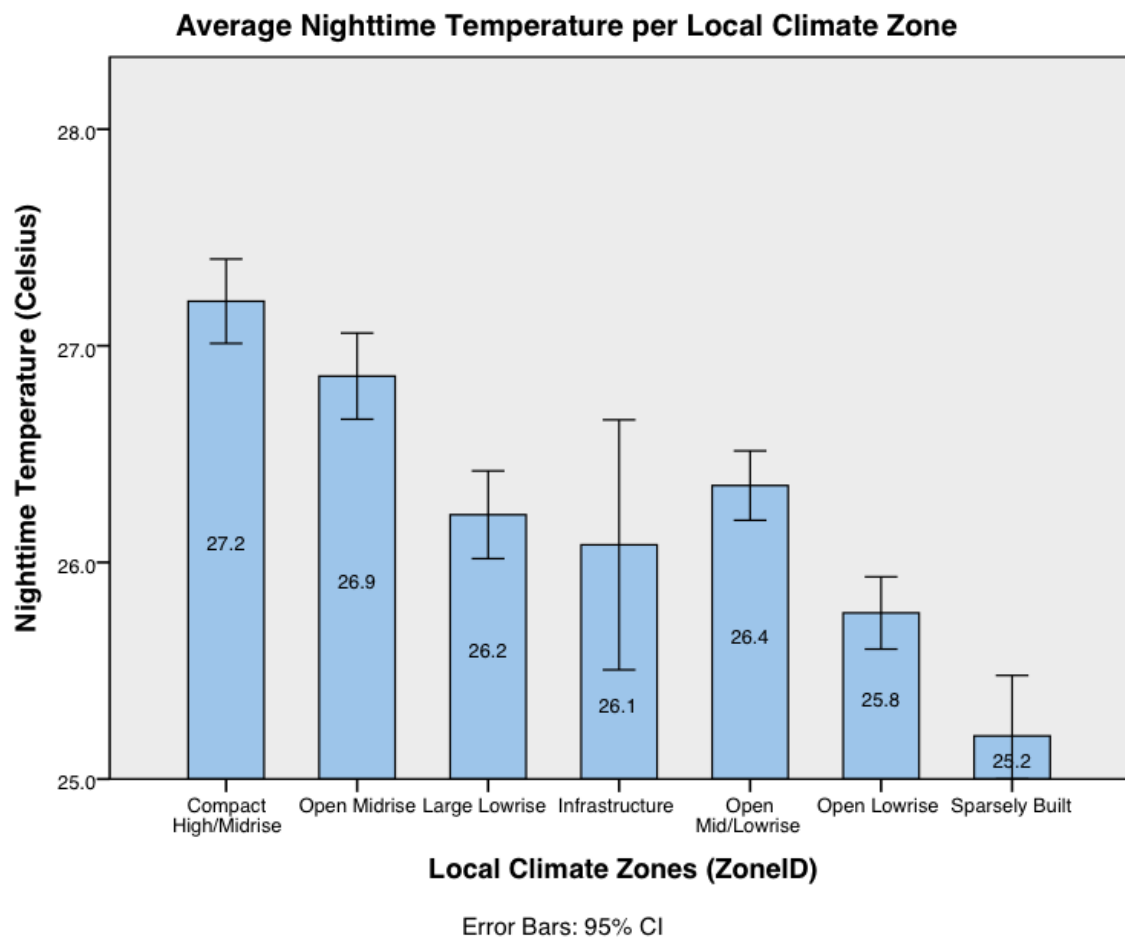
Figure 6.17: Average Nighttime Temperature per Local Climate Zone.

As with the nature of urban morphology, local climate zones are not evenly distributed within a city. Therefore certain urban typologies have a larger representation than others. For example the Compact Highrise and the Open Midrise zones have 23 and 48 observations respectfully whereas Open Lowrise has 126 observations. When analyzing categorical variables, equal sample sizes makes for better research design and is beneficial for statistical controls. In order to analyze a larger temperature difference and to make the sample sizes more evenly distributed, I combined the two densest zones (Compact Highrise and OpenMidrise). These two zones are morphologically similar, exist only in downtown and midtown Atlanta and have the two highest temperatures from all other urban typologies. Additionally the temperature differential between these two zones is not statistically significantly different (see Figure 6.17). I compare them against the predominantly residential zone of Open Lowrise in order to assess whether there is change in effect size if agriculture is implemented in a dense downtown neighborhood versus a sylvan historic residential neighborhood. For this comparison, I create a binary dummy coded categorical variable. Since the residential typology has the largest observations, I coded it with a zero.

To test for an interaction effect between urban form and agriculture, I use SPSS's Advance Models, I conduct an univariate General Linear Model (GLM) in order to test for an interaction effect between the urban form and agriculture independent variables. For my design, I am measuring temperature for each 1km x 1km grid cell during a non heat wave period (June 10th). I run a full factorial model to control for all covariate and fix factor main effects and to obtain the between subject and covariate interactions. I use a Type III method for calculating the sum of squares in the model (as it is the most commonly used sum of squares method and the most encompassing for different model designs (SPSS Manual 17.0).

6.3 Results

To test for an interaction effect between urban form and agriculture, I run a univariate General Linear Model (GLM). The interaction is tested during a summer night but not during a heat wave. I include LCZs (urban vs residential) as a fixed factor, urban agriculture area as a covariate and the interaction of LCZ and agriculture into the model. Testing the main effects showed that though LCZ and agriculture were both significant the interaction between the two independent variables was not

Tests of Between-Subjects Effects

Dependent Variable: Night Temperature (Non-Heat Wave)

Source	Type III Sum of Squares	df	Mean Square	F	Sig.
Corrected Model	29.215[a]	3	9.738	10.383	.000
Intercept	14843.965	1	14843.965	15827.286	.000
LCZ	5.853	1	5.853	6.241	.013
Agriculture Size	5.656	1	5.656	6.030	.015
LCZ * Agriculture Size	1.512	1	1.512	1.612	.206
Error	181.009	193	.938		
Total	92766.918	197			
Corrected Total	210.224	196			

Figure 6.18: Univariate General Linear Model. Testing for an interaction effect during a non-heat wave period.

significant (See 6.18). We can assume that agriculture effects temperatures similarly in both urban form typologies.

Since Chapter 5 illustrated that heat waves can modify the cooling potential of agriculture, I then test for the interaction effect between urban form and agriculture during a heat wave period (July 20th). I run the same univariate GLM model but with the temperature dependent variable measured during a heat wave. This GLM model indicates that there is an interaction effect between urban agriculture and urban form (See Figure 6.19).This model illustrates that not only do we see the relationship between agriculture and temperature change depending on the urban form but that this interaction is based on the presence of a heat wave.

In order to examine whether there is a 3-way interaction effect between urban form, agriculture and heat waves, I run a Repeated Measure GLM to test for a 3 –way interaction. The GLM is a mixed factorial analysis including both within factors (temperature and timing) and between factors (LCZ and agriculture). In the GLM Repeated Measures procedure, I create a "timing"factor with two levels. The first level is defined as June 10th and the second level defined as July 20th. To

Tests of Between-Subjects Effects

Dependent Variable: Night Temperature (Heat Wave)

Source	Type III Sum of Squares	df	Mean Square	F	Sig.
Corrected Model	1.274	3	.425	2.708	.046
Intercept	15872.502	1	15872.502	101193.461	.000
LCZ	1.222	1	1.222	7.792	.006
Agriculture Size	.063	1	.063	.402	.527
LCZ * Agriculture Size	1.069	1	1.069	6.813	.010
Error	30.273	193	.157		
Total	103203.192	197			
Corrected Total	31.547	196			

Figure 6.19: Univariate General Linear Model. Testing for an interaction effect during a heat wave period.

examine the trends in agriculture, I create a categorical variable of irrigated agriculture size by grouping agriculture into 3 size classes. The breaks for the classes were based on the percentiles of the distribution of agriculture land. More than three classes are not used in the analysis because of small group size. Using the "rank cases"function in SPSS, I rank all of my observations by total amount of agriculture land present in each grid cell and then I grouped the observations into three even percentile groups.

The results of the Repeated Measures GLM model indicates that the 3-way interaction is significant, which asserts that agriculture impacts temperatures differently in different urban form conditions but only during a heat wave (See Figure 6.20). To compare the estimated marginal means in the model, I create separate profile (interaction) plots for heat wave and non heat wave events. The profile plot shows that the estimated marginal means for temperature decreases similarly across the different levels of agriculture size during a non-heat wave event. These approximately parallel lines support the first univariate GLM model that found no interaction between urban agriculture and urban form during a non-heat wave period. On the other hand, the non-parallel lines in the heat

Repeated Measures GLM: Multivariate Tests

Effect		Value	F	Hypothesis df	Error df	Sig.
Timing	Pillai's Trace	.555	238.684[b]	1.000	191.000	.000
	Wilks' Lambda	.445	238.684[b]	1.000	191.000	.000
	Hotelling's Trace	1.250	238.684[b]	1.000	191.000	.000
	Roy's Largest Root	1.250	238.684[b]	1.000	191.000	.000
Timing * Ag Size * LCZ	Pillai's Trace	.223	10.964[b]	5.000	191.000	.000
	Wilks' Lambda	.777	10.964[b]	5.000	191.000	.000
	Hotelling's Trace	.287	10.964[b]	5.000	191.000	.000
	Roy's Largest Root	.287	10.964[b]	5.000	191.000	.000

Figure 6.20: Repeated Measures General Linear Model. Testing for a 3-way interaction effect.

wave profile plot support the assumption that an interaction effect is occurring (See Figure 6.21).

Since finding an interaction between the main effects, I next carry out a test of simple main effects by comparing the size of agriculture within each urban form group. To test the simple main effects during a heat wave, I conduct a univariate GLM with LCZ and Agriculture as fixed factors. I use the "emmeans" and "compare" syntax commands to generate pairwise comparisons of the simple main effects while holding the main effects constant and use SIDAK to adjust the confidence interval. Figure 6.22 shows the test of simple main effects. First, we can see that there is no significant difference in temperature across the different agriculture sizes in the residential zone during a heat wave. For urban areas, we see that there is a difference in temperature between the second size group and the third size group (See Figure 6.22). For visualization purposes, I plot the temperature change per agriculture size and per LCZ with five agriculture size groupings instead of 3. The graphs look to be reasonably consistent as the overall pattern still holds (See Figure 6.23).

128
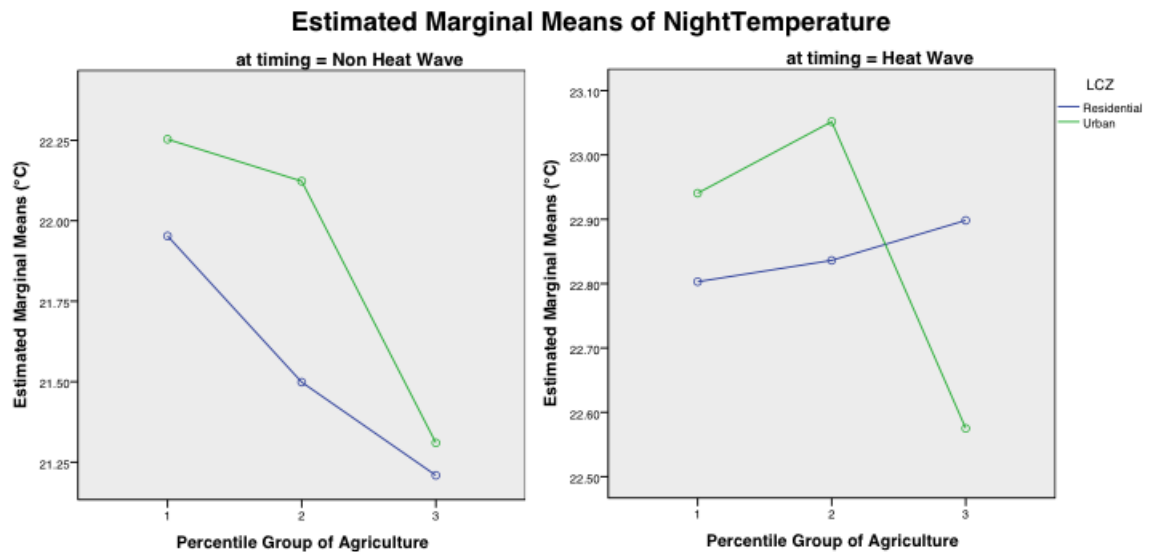
Figure 6.21: Profile plots. The plot on the left is during a non heat wave and the plot on the right is during a heat wave.

Pairwise Comparisons

Dependent Variable: Night Temperature during a Heat Wave

LCZ	(I) Percentile Group of Agriculture	(J) Percentile Group of Agriculture	Mean Difference (I-J)	Std. Error	Sig.	95% Confidence Interval for Difference Lower Bound	Upper Bound
Residential	1	2	-.033	.116	.989	-.313	.247
		3	-.095	.115	.792	-.372	.181
	2	1	.033	.116	.989	-.247	.313
		3	-.062	.076	.796	-.244	.120
	3	1	.095	.115	.792	-.181	.372
		2	.062	.076	.796	-.120	.244
Urban	1	2	-.111	.120	.732	-.400	.178
		3	.366	.160	.069	-.020	.751
	2	1	.111	.120	.732	-.178	.400
		3	.477*	.184	.030	.034	.919
	3	1	-.366	.160	.069	-.751	.020
		2	-.477*	.184	.030	-.919	-.034

Figure 6.22: Pairwise comparisons evaluating the temperature difference between the simple main effects of agriculture size.

129
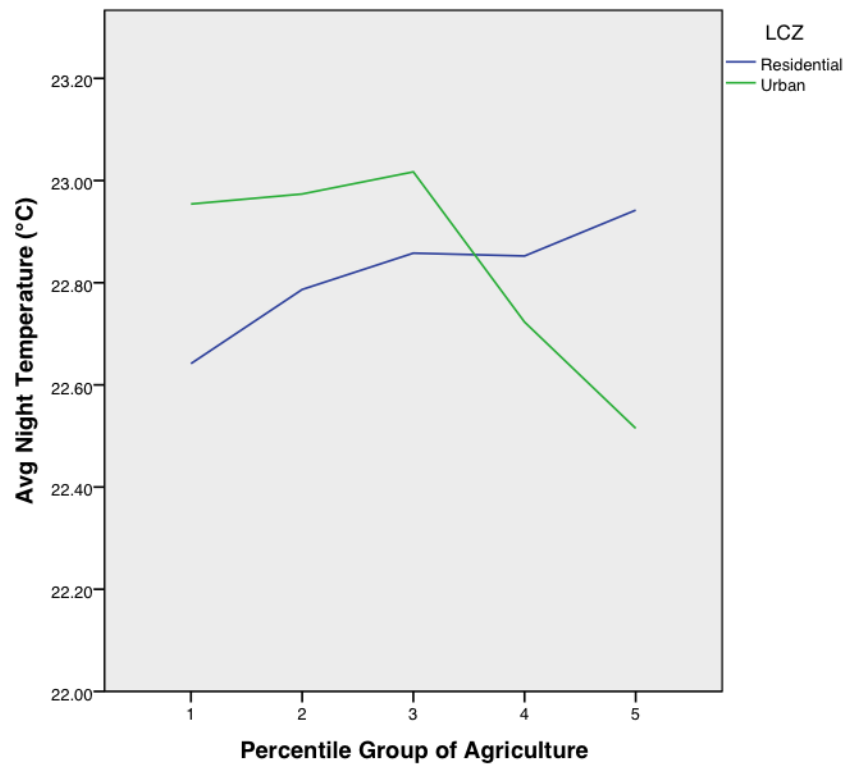
Figure 6.23: Graph illustrating the temperature change across quintile groups for agriculture size.

# of Breaks	Statistic (acres)	Group 1	Group 2	Group 3	Group 4	Group 5
3	Min	0.22	4.74	7.55	*	*
	Max	4.67	7.39	15.0	*	*
	Avg.	3.14	6.27	8.77	*	*
5	Min	0.22	3.33	5.81	7.06	8.42
	Max	3.26	5.71	7.05	8.42	14.95
	Avg.	2.25	4.33	6.29	7.76	9.77

Figure 6.24: Table illustrate the descriptive statistics for each agriculture group size.

6.4 Discussion

From this analysis we see that an interaction effect exists between urban form and urban agriculture when a heat wave is present. Chapter 4 illustrates the cooling potential of agriculture to cool nighttime temperatures. Chapter 5 furthers the discussion by addressing the impact that heat waves may have on urban agriculture's cooling potential. Chapter 5 showed that agriculture still maintains the ability to cool local nighttime temperatures but that this cooling potential is dramatically reduced during heat waves. In this chapter, when analyzing the interaction effect between urban form and agriculture during a non heat wave period, no interaction occurred. Therefore, we can assume that agriculture impacts local nighttime temperatures similarly across urban and residential zones. When examining the interaction effect during a heat wave, I find an interaction effect between urban form and agriculture. A further investigation into this interaction effect by conducting pairwise comparisons between the simple main effects of agriculture size, showed no difference in temperature change across agriculture size in the residential zone. However, it did show a significant change in temperatures in urban zones. Specifically the change in temperature is statistically significant when comparing between groups 2 and 3. This simple main effect supports the idea that a statistically significant change of temperatures during heat waves can occur in urban areas when agriculture is implemented at larger scales.

A significant difference in temperature was found between the second and third percentile groups while controlling for urban form and heat waves. Graphing the temperature data across five

size groups instead of 3 (see Figure 6.23), shows a similar temperature pattern with temperatures deceasing between group 3 and 4. The graphs imply the presence of a threshold effect occurring at or around 7 acres of irrigated agriculture within a 1 km grid (see Figure 6.24 for descriptive statistics). For the urban areas, there is a temperature decline from the implementation of medium to large amounts of agricultural lands, which translates to implementing at least seven acres of agricultural lands in a neighborhood and as much as 15 acres of land. From Chapter 4, we saw that on average an increase in 10 acres of agricultural lands could decrease the temperatures at the local 1km scale by an average of 0.65°F. From the 2 x 3 factorial GLM analysis, we see that an implementation of agriculture at the city scale between 7.5 and 15 acres, will statistical decrease temperatures by approximately 0.48°C (0.86°F). This result seems to be on par with the findings from Chapter 4, especially when one takes into consideration that Chapter 4 results are averaging across the entire MSA and that much of the agricultural land analyzed for Research Question 1 are located in less urban environments.

How difficult would it be to implement 15 acres of agricultural lands in a dense urban neighborhood like Atlanta's midtown and downtown neighborhoods? In Chapter 4, I illustrated that 10 acres represents approximately 5% of the 1 km grid cell. I used Gia Gardens to illustrate how an existing urban agricultural typology fits within the city of Atlanta. But how would agricultural land currently fit into these dense urban typologies? In order to explore this question, I map the vacant parcels in my study area. I acquired the vacant parcel shapefile from the City of Atlanta. The Department of Planning defines "vacant"as any parcel that is not built on, which represents green space, parking lots, and completely empty parcels. Using ArcGIS Identity and Dissolve functions, I summed the total amount of vacant land in grids cells defined as Compact Highrise and Open Midrise. Each of these grid cells had an excess of 14 acres of vacant land. Atlanta's poor urban design with an over emphasis on single occupancy transportation infrastructure provides a spatial opportunity for these neighborhoods. As previously discussed, even in Atlanta's most dense urban form typologies, these typologies did not fit well within Stewart & Oke's LCZs class. From a local perspective, the urban form of the city of Atlanta is quite spread out due to an abundance of surface parking lots and interstates and railyards that cut through the city. An abundance of these parcels are parking lots, which could be utilized has agricultural land. Truly Living Well an urban farm in Atlanta's historic

black downtown neighborhood was a great example of transitioning impervious vacant land to a functioning downtown urban farm.

This research argues for the potential of vacant parcels in cities to be used for both agricultural and heat mitigation strategies. Cities are often plagued with vacant and distressed land parcels resulting from economic recessions and, on much larger scales, due to shrinking cities (i.e. Detroit, Michigan). Agricultural land is often a difficult land use category to designate inside city limits due to the high cost of inner city land. It is simply too expensive to justify using urban land for agriculture. However, when cities find themselves burdened with an over abundance of vacant or distressed parcels, they should investigate the possibilities of banking these parcels for uses like agriculture, that are often pushed outside of the city in a booming economy. Cities should utilize community land trusts and land banks to reserve and preserve land for future agricultural uses in their city centers. Land banks can play an important role in holding and maintaining land for agricultural uses in urban environments.

This analysis does not address patch configuration, only total size. The patch configuration of agricultural land is an important discussion point, which my dissertation does not address. 10 acres of agricultural land may only represent 5% of the 1km grid cell, but if this area needs to be contiguous then this translates into a huge urban farm. The largest urban farms in the US are approximately 6 acres in area and there are only a handful of existing farms in this size. If urban agriculture needs to be contiguous instead of consisting of several separate parcels, then this becomes problematic for cities.

6.4.1 Analysis Limitations

As in any research analysis there are inherent limitations to this study. The spatial resolution for the MODIS nighttime data is definitely one of these limitations. The large spatial resolution limited the amount of temperature variation within the city of Atlanta that may be possible to see with higher spatial resolution data. Since the study area needed to be smaller to deal with data availability for the urban form typology, the low spatial resolution limited the number of observations analyzed in the study. The lower spatial resolution also created difficulties with analyzing the urban form typologies. Though there is no set standard for Local Climate Zone sizes and a 1 km grid fit within

the allowable size according to Stewart & Oke, this grid size was not ideal for the city of Atlanta. Though the local climate zones showed distinct temperature differentials as seen in Figure 6.17, these differentials may be more distinct with higher resolution data. As mentioned previously, MODIS nighttime data was important to use because of the importance of negative health effects, the unique contribution agricultural lands may provide at lowering nighttime temperature due to larger sky view factors, and the enhanced increase in nighttime temperatures due to the urban heat island effect.

Since Chapter 4 addressed the cooling potential of agricultural lands at night, I previously considered using daytime temperature data in order to maximize spatial resolution. What I found was that not only is there a limitation with the resolution of nighttime data, but the availability of higher spatial resolution such as Landsat data is quite limited. To investigate the potential of daytime temperature data, I downloaded Landsat TM data from USGS Glovis (glovis.usgs.gov). I pulled all scenes with a cloud cover equal to or less than 20% for the entire summer months. There were only 5 scenes between May and September that met the 20% requirement for the city of Atlanta (there were no scenes in March, April, October, or November).

One of the scenes needed to be discarded. Scene 07/24 could not be included in the study because its data looked to be grossly inaccurate. In Figure 21, Scene 07/24 is the image on the right. The four remaining scenes look similar to the image on the left. There were no data flags in the metadata that would contribute to these inaccurate data. Therefore there were only four scenes during the summer months and one of the scenes is during a heat wave. Cloud cover contamination limits the amount of viable scenes needed to conduct urban heat island research. Reducing cloud cover contamination was one of the big advantages of using MODIS 8-day average temperature data in Chapter 4.
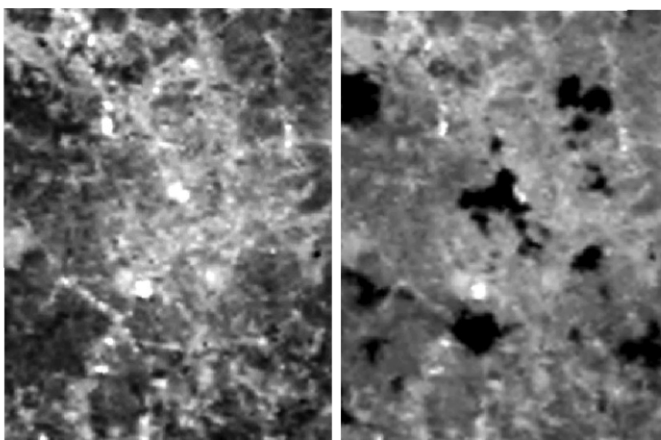
Figure 6.25: The image on the right is taken from 05/05. This is typically what a temperature should look like for the Atlanta. The image on the right is taken on 07/24. The black wholes represent missing data from the scenes.

CHAPTER 7

CONCLUSION: AGRICULTURE ON THE RISE

Urban agriculture has been growing in popularity across US cities over the past decade. Urban farms and community gardens are popping up in large cities across the country. Rust belt cities have seen an explosion in urban agriculture due to economic decline generating large amounts of vacant land providing access to land for urban farming. For example, in 2004 Detroit had 80 community gardens and in 2015 had approximately 1400 community gardens involved in the city's Garden Resource Program with more than 20,000 Detroit residents involved with these urban agriculture projects. Cleveland, Ohio another rust belt city, which has experienced recent economic declined, has also experienced a recent a surge in urban agriculture. In 2014, Cleveland had over 40 for profit urban farms including one of the largest and continuous urban farms in the country – Ohio's City Farm - generating food production on over 6 acres of agricultural space. Rustbelt cities are not the only US cities experiencing this resurgence in urban agriculture. Cities like Atlanta, Austin, Portland, and Seattle are among the list of burgeoning markets. The densest city in the US, New York City, is argued to have the largest urban agriculture movement with over 600 community gardens on parklands affiliated with its Parks and Recreation Department alone.

Not only is there a surge in the building of new urban farms and community gardens but also there is growth in the support and resources for urban agriculture. Many states and local communities have issued new policies to help urban agriculture flourish in their regions. In Michigan, the Urban Agriculture Act was introduced to Congress in 2016. The legislation aims to strengthen agriculture in Michigan cities by establishing "an Office of Urban Agriculture within the Department of Agriculture (USDA) and make urban agricultural activities eligible to receive funding from various USDA programs." This act is designed to provide funding, information and training to farmers and growers. In 2014, California passed the Urban Agriculture Incentive Zone Act (Assembly Bill 551) to allow landowners to receive a tax break if they allow their land to be farmed for at least 5 years. Atlanta, Austin, Chattanooga, Cleveland, Milwaukee, Nashville, and Portland are some of the cities that have all amended their zoning ordinances to allow for agricultural lands in their city limits. In

2015, the City of Atlanta hired a Director of Urban Agriculture, a position located in their Office of Sustainability. This appointment marks the first time this position has been held in Atlanta or any other major US city.

At the federal level, support for urban agriculture has also increased with the United States Department of Agriculture (USDA). In 2016, the USDA provided funding for 12 urban farms, the most to date and released its new toolkit for urban agriculture. The toolkit is a resource depository designed to help farmers apply for grants and get training and education on topics such as how to use hoop houses, green houses, or garden on roofs. In 2013, the USDA also started its microloans programs. These smaller loans (up to 50,000 dollars) are more geared toward urban farms and of the 23,000 loans granted, it is estimated that 70% of these loans went to new farmers who were primarily in urban areas. In addition to federal policies, the University of the District of Columbia has created educational curriculum centered on urban farming. Through its Center for Urban Agriculture and Gardening Education, its mission "seeks to expand academic and public knowledge of sustainable farming techniques that improve food and water security, health and wellness by providing research and education on urban and peri-urban agroecology and gardening techniques to residents and organizations in Washington, DC, and beyond."

7.1 Contributions to the Gap in the Research Community

The research community also reflects this popularity with increasing trend in urban agriculture research. To identify the global trend in urban agriculture research, I used the Web of Science database to track trends in publications. Using Web of Science query functions I identified all publications from 1900 to present. The keyword "urban agriculture" was used in the search query. The basic search function was utilized in order to identify all published items. As seen in Figure 7.1, there has been an exponential increase in urban agriculture research over the past decade. In 2006, there were 16 publications and by 2016 there were over 160. This tenfold increase in publication in just 10 years is another illustration of the growing interest in urban agriculture research.

In addition to an increasing trend in urban agriculture research, there has also been an increase in UHI research over the past decade. Figure 7.2 illustrates the upward trend in UHI publications over time from the Web of Science database. The findings illustrate that in 2006 there were 75
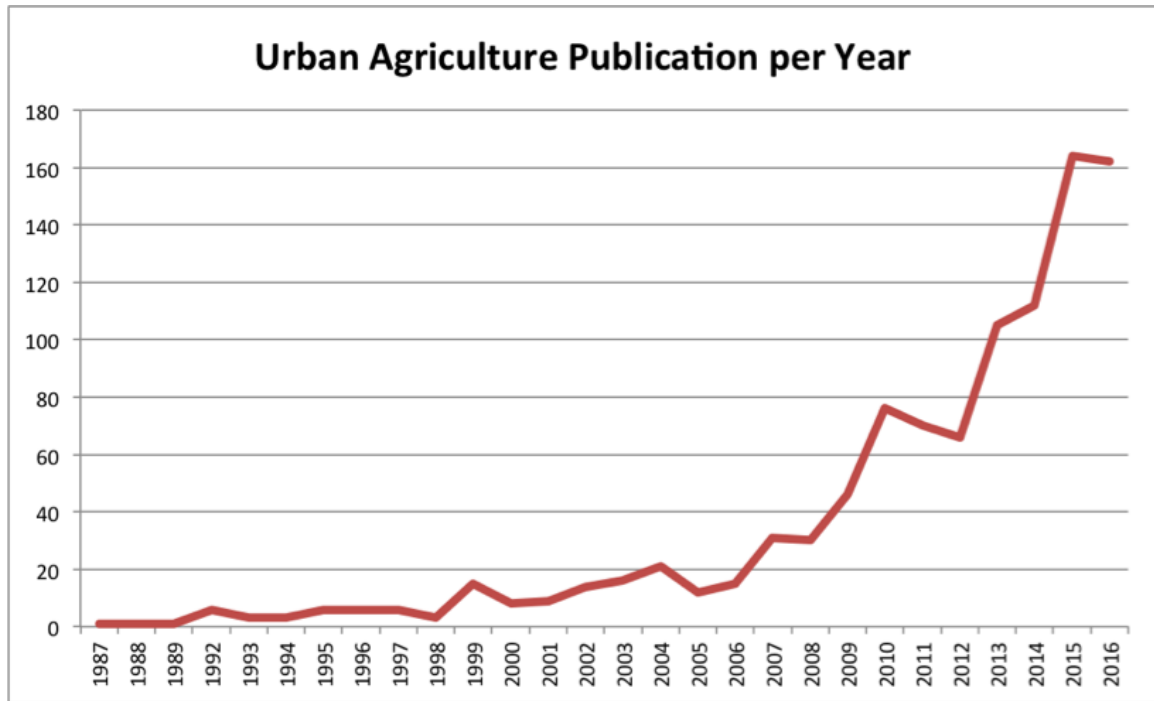
Figure 7.1: This graph, plotting the number of publications per year based on the Web of Science database, illustrates the increase in interest and popularity surrounding the urban agriculture research domain.

publications referencing UHIs and by 2016 there were over 500 publications.

Though there has been a growing emphasis on both urban agriculture and urban heat island research, there has been very little research attention to the overlap of these two research domains. Refining the Web of Science search to include both urban agriculture and urban heat island as two separate keywords returned twelve total publications. Only one of these publications examined the temperature impact from agriculture land cover in the urban environment. This publication was conducted in the Middle East and urban agriculture was a subset of the work- contributing mainly to a discussion of peri-urban agriculture.

Not only is there little research published at the intersection of urban agriculture and urban heat islands (none conducted in the United States), the research community has failed to uncover this gap in the literature. My investigation establishing this gap in the literature revealed that the research community already perceives a link between urban agriculture and urban heat island mitigation. Several papers cite urban agriculture's cooling potential [159, 160, 161] but none of these articles reference papers that actually demonstrate the cooling effect from urban agriculture. Papers refer-
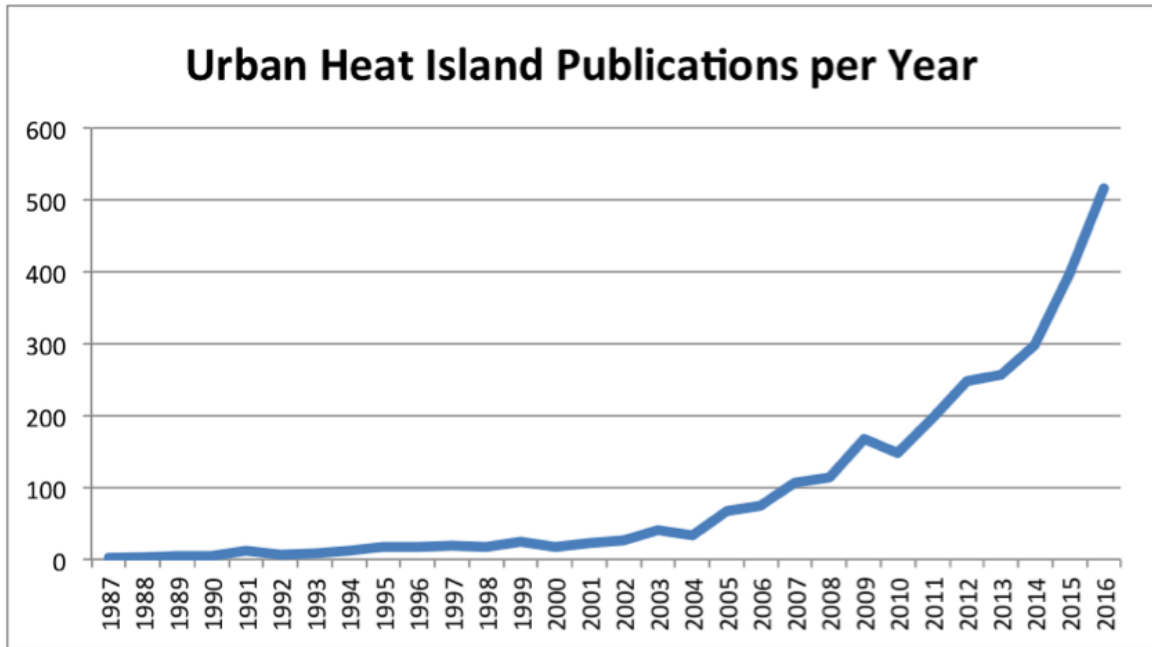
Figure 7.2: This graph, plotting the number of publications per year based on the Web of Science database, illustrates the increase in interest and popularity surrounding the urban heat island research domain.

ence general vegetative UHI research but none of these citations examine the potential for urban agriculture to act as a successful UHI mitigation strategy. Papers are citing themselves for work illustrating this impact. They are making cyclical arguments, which had no validated proof to begin with. Not only has the work not been done, but the community does not realize this gap in the literature and as such does not understand the complexity that surrounds this research topic. My work attempts to address this research gap and shed light on some of these issues.

7.2 Research Limitations

When conducting urban agriculture research there are inherent limitations with the domain that is important to recognize. One of the main limitations with an empirical land cover investigation into urban agriculture is the lack of observational data that is available. As discussed in the previous chapter, data acquisition for high-resolution nighttime temperature data was problematic. The highest resolution temperature data that is available is MODIS data which has a spatial resolution of 1km. Landsat temperature data is available at a higher spatial resolution (30 meters) but this tem-

perature dataset is only available during the daytime for the southeastern United States. Acquisition time is directly related to the temporal resolution of the satellite. MODIS on the other hand has a much a higher temporal resolution than Landsat and can provide both day and night temperature data but there is a trade-off with the spatial resolution. Since I am examining the potential for urban agriculture to mitigate the UHI effect and because I am interested in the impact on public health it is important for my research to analyze nighttime temperature. Minimum temperatures which are temperatures that occur in the evening and early mornings have been shown to be a better temperature metric for the impact of heat-related mortality [118]. While high daytime and nighttime temperature both stress physiological functions associated with cardiovascular and respiratory systems; it is the consistently high temperatures during the evenings that have a stronger association with an increase in physiological stress [78, 59].

High-resolution temperature data is important for an urban analysis because of both the interest of scale and implementation. Examining urban agriculture, I am interested in the potential of agriculture to impact local temperatures. My research differs from regional land cover analysis because of this focus on scale and a focus on the urban environment. Since a 1km grid cell will not be comprise solely of agriculture in an urban environment this lower spatial resolution presents the mixed-pixel problem. This occurs when the pixel is mixed with multiple land covers. If I could obtain higher resolution temperature data then I could directly relate temperature to grid cells comprised solely of agriculture. Instead the analysis must control for all other land covers that are present in the grid cell. This mixed pixel problem muddies the analysis and statistical controls are necessary to assess the relationship between agriculture and temperature.

Higher resolution temperature data would also allow for a better assessment of the temperature impact from parcel level implementation. Parcel level implementation is important from a policy point of view and from an urban agriculture typology point of view. Urban agriculture exists on much smaller scales than traditional industrial agriculture. Individual and community gardens are often located on single-family residential parcels with many urban agriculture sites taking place on forgotten parcels peppered throughout the city. Urban farms are implemented on much smaller scales than a traditional farm. Even the largest urban farms in the United States are miniscule compared to the industrial agriculture sector. Baltimore's largest farm, Real Food Farm is located

on 6 acres as is Cleveland's largest farm, Ohio City Farm. Atlanta's Aluma Farm, located on the Beltline, and Gaia Gardens are both located on approximately 4 acres of land. And Seattle's largest farm, Rainier Beach Urban Farm and Wetlands, is located on 7.2 acres of land where approximately half is dedicated to food production and the other half is a wetland restoration project. On the other hand, according to the USDA 2007 census, the average farm size in the United States was approximately 450 acres with the largest farms totaling in size over 2,000 acres. This farm size does not represent just an outlier; over 27,000 farms fell in this size bracket. The discrepancy in agriculture size illustrates why high-resolution temperature data is so important for urban agriculture research. It is much easier to assess agricultural impact on regional temperatures due to sheer size and presence of traditional agriculture.

Controlling for contextual variables can be problematic in urban agricultural research. For example, the mixed pixel problem also creates problems with multicollinearity in the MSA analysis where the impervious land cover and the tree canopy were highly correlated ($>.9$). Multicollinearity problems with urban form metrics are not new problems when dealing with urban variables. The walkability index and the sprawl index are both urban form indices that were created to handle the problem of multicollinearity between different urban form measures, (i.e., high density is highly correlated with mixed use and residential density is highly correlated with intersection density)[145, 142, 162]. In these examples, factor analysis is used to handle multicollinearity problems. Combining the variables into a single measure allows for one to control for the variation of the different variables without them contaminating the model. The Local Climate Zones (LCZs) created for the city-level analysis addressed this challenge. The creation of urban form typologies through LCZs allowed for the combination of both impervious and vegetative land cover while not creating problems of multicollinearity. As discussed in Chapter 6, though they were an effective mechanism for dealing with correlated variables, the LCZs were not sufficient in describing all urban form typologies especially those found in post automobile American cities.

Another difficulty in conducting empirical agricultural land cover analysis is that urban agriculture is not ubiquitous throughout the urban environment. In order to assess how temperatures vary with land cover, multiple observations are necessary in order to access cooling trends. I use the NLCD, which identifies agricultural land cover across the US, to assess impact from agricultural

land cover at the MSA level. This investigation further emphasized the lack of agricultural land cover present in the Atlanta, MSA. In addition, the agriculture movement in Atlanta, GA did not gain significant movement until after 2010. It is difficult to assess the impact from agriculture on temperature when it is not abundant through the urban environment.

To deal with this problem, and tease out the potential temperature impact from urban agriculture without using a simulation model, I develop what I call an irrigated agriculture proxy. Using multispectral land cover data and a local NDVI threshold developed from existing urban agriculture training sites, I identify land cover that approximates the physical characteristics of urban agriculture. I estimate irrigated agriculture by assuming all non-tree vegetation with NDVI values above 0.41 to be irrigated agriculture.

NDVI is used in the research community to differentiate irrigated agriculture from non-irrigated agriculture [130, 131]. The USDA consistently surveys farm lands and documents the location of large scale agricultural sites. Therefore when researchers derive solutions to identify agriculture that is irrigated they start with the agricultural location as a given and then they differentiate irrigated agriculture using NDVI thresholds. For my methodology, I assume that all non-tree vegetation in the urban environment is "agriculture" and I use the NDVI threshold to distinguish between irrigated and non-irrigated. Grass has been used as a proxy for agriculture in global climate models in previous studies that assess the impact of agricultural land on climate [35, 137]. Grass, however, is not a perfect substitution for agriculture as it varies in its biophysical parameters (i.e. has a lower leaf area index and roughness height than agriculture). NDVI is used in the agriculture research community because irrigated agriculture and non-irrigated agriculture have different peak NDVI values. Peak NDVI values are tied to crop type and to location. Additionally, NDVI values are more differentiated during drought conditions [130].

NDVI is the most widely used vegetation index when it comes to assessing vegetative land cover [163]. NDVI is used to measure the health of vegetation, used as a predictor for vegetative biomass, and as a biophysical parameter used in calibrating models that monitor agriculture crops [134, 164, 163]. NDVI has been shown to be correlated with both biomass and LAI of different plant types [134, 134]. Though it is correlated with biomass and LAI these relationships becomes less clear beyond certain values. For example, the relationship between LAI and NDVI follows

an exponential curve. Once NDVI increases above approximately 0.8 then the relationship between LAI and NDVI becomes saturated as one value of NDVI can have multiple LAI values and therefore increasing the prediction error. The relationship between LAI and NDVI is further complicated by context. The relationship between LAI and NDVI is dependent on contextual conditions such as location, plant type and timing (degree days from sowing).

Land covers have differing NDVI values. For example, barren rock and sand have low NDVI values of 0.1 or below; soil has NDVI values between 0.1 and 0.2, grasslands and shrubs have NDVI values between 0.2 and 0.3; dense vegetation canopy is typically between 0.3 an 0.8 and temperate and tropical forests have NDVI values between 0.6 and 0.8 [165]. Irrigating these land covers increases their NDVI values. For example, turf can have NDVI values as high 0.8 due to intense irrigation and fertilization [166]. Biophysical parameters (such as LAI, biomass, etc.) vary across differing types of agriculture and these parameters are dependent on site as well as growth cycles [133]. As such, it is difficult to derive one vegetative metric that represents all of the different types of agricultural land covers.

In addition, to a lack of observational urban agriculture data, there is also a lack of urban agriculture tracking. In Atlanta, and in other burgeoning markets, a consistent problem includes a lack of a governing body to track all urban agriculture in their city area. A central repository could facilitate urban agriculture research by providing location, area, and other farm characteristics to researchers.

7.3   Terminology Clarification

The research I have conducted, including the extensive literature review, revealed important terminology that is either not understood or is glossed over in urban agriculture research. In this section, I aim to shed light on three of these issues: urban agriculture typology and their potential to impact the UHI effect; vegetative physiological characteristics, and diurnal temperature variation.

First of all, there are many different urban agriculture typologies. There are in ground solutions which include backyard gardens, community gardens and urban farms. Raised beds are included in this typology group. On the other hand there are typologies that are engineered through some sort of technology. These include rooftop gardening, greenhouses, hydroponics and vertical agri-

Agriculture Parameter	Effects
Leaf Area Index (LAI) (-)	Canopy (-)
Albedo (+)	Solar radiation (-)
Surface Roughness (-)	Atmospheric Mixing (-)
Soil Moisture (+)	Evapotranspiration (+)
Stomatal Resistance (-)	Water availability (+)
Skyview factor (+)	Nocturnal max
	Park Cool Island (+)

Figure 7.3: This table list the how the parameters of agriculture compares to forested land (+ or -) and the impact the parameter has on associated effects. For example, agriculture has less leaf area index than forested land and therefore has less canopy.

culture. When asserting urban agriculture can either combat climate change or mitigate the UHI effect it is important that researchers distinguish between UA typologies. With the exception of roof top gardening, all other technological engineered solutions will not have a cooling impact on local temperatures. These UA typologies are basically agriculture inside buildings. UHI research will treat UA high tech typologies as buildings. The research can examine the impact from waste heat generated by the building, the albedo of the roof material, the heat storage capacity and any impact on the urban form's sky view factor. In general though, one can assume this UA typology will increase local temperatures. Though this may seem like a straightforward argument, in the literature researchers are too quick to assert that UA can mitigate the UHI and at the same time push for vertical agriculture. The two do not equate. As the UA movement continues to progress the current trajectory is toward vertical/high tech agriculture which will need its own separate investigation on the impact to local temperatures. Another important terminology for the research community to understand is that of the physiological structure of agriculture that differentiates it from other vegetation. Agriculture's different biogeophysical parameters accounts for why agricultural land can outperform forested land cover in lowering temperatures in urban environments. Some of these vegetation parameters include surface albedo, surface roughness length, soil moisture, leaf area index, stomatal resistance, and sky view factor (See Figure 7.3 and See Chapter 2 for further discussion). Changes in these parameters affect the climate in two main ways: first by changing the radiative forces of the land, which primarily results from the surface albedo change and second, by partitioning surface energy between sensible and latent heat through the altering of available water for evapotranspiration [30, 29, 34].

Soil moisture, stomatal resistance and sky view factor are three parameters that play an important role in contributing to agriculture's cooling effect in the evening. Soil moisture and stomatal resistance directly impacts the amount of water available for evapotranspiration. The irrigation practice associated with agriculture provides for higher soil moisture and in turn higher rates of evapotranspiration as does the lower stomatal resistance. The stomatal resistance of agriculture is approximately 40s/m as compared to 125 s/m for evergreens. A lower stomatal resistance inhibits the release of water less than a higher stomatal resistance value. This increases water availability for evapotranspiration and leading to higher cooling effect. [51]. The lower stomatal resistance also plays an important role during extreme heat conditions. As temperatures increase stomatal resistance for agriculture decreases allowing for more soil moisture to be evaporated through transpiration. Stomatal resistance for trees, on the other hand, increases in order to conserve water. This parameter for agriculture is important for two reasons, first it is promising that agriculture can continue to cool local temperatures even during extreme heat conditions, but that it is important that agriculture is actively managed through irrigation during heat waves.

The final parameter, sky view factor, represents the percentage of the sky that is visible. Agriculture has a higher svf as compared to forested land. The large canopy of trees contributes to a lower sky view factor but it is the large tree canopy that provides significant amounts of cooling from shade during the day. During the evening, the large canopies of trees provide a negative cooling feedback by inhibiting the emission of long wave radiation to the atmosphere. This trapping of heat contributes to temperature being higher under a tree than in an open green space. Due to the difference in sky view factors, forested parks have a different timing in their maxi- mum "park cool island" (PCI) effect (which is synonymous to the oasis effect) as compared to gardens or open grass parks. A forested park is coolest relative to its surroundings during the afternoon, therefore having an afternoon maximum PCI, whereas gardens or open grass parks have a nocturnal maximum PCI [54].

This difference between nighttime and daytime cooling leads directly into the final terminology, which is the diurnal temperature variation. The diurnal temperature variation describes how temperature changes throughout the day. Throughout a 24-hour period, the temperature varies depending on the incoming solar radiation. Temperatures are highest during the afternoon and lowest

during the evening when the sun goes down. Throughout the day impervious surfaces store solar radiation and during the evening slowing releases the stored radiation as longwave radiation back into the atmosphere. This slow release of radiation is why we see peak measurements of the UHI in the evening. It is also this same process which causes tree canopies to trap outgoing radiation and create areas of higher temperature compared to open green space (cite china paper. This diurnal pattern is important for researchers to understand. This pattern is why mortality effects are higher in the evening and why high quality nighttime temperature metrics are so important. But this diurnal pattern also explains that different vegetation patterns have diurnal patterns in their cooling potential. Agriculture out performs forested land cover in the evening. Green roofs, another UHI vegetative mitigation strategy, may also exhibit similar diurnal patterns as green roofs do not provide the cooling benefit during the evening because of a decrease in evaporation during the night. David Sailor, an urban climatologist explains that "if you try to mitigate the urban heat by putting up green roofs, it will do some good for reducing temperatures during the day, but it might increase at night,"

7.4   Policy Approaches: Urban Agriculture as Green Infrastructure

I define Green Infrastructure as *a multipurpose, comprehensively designed network of green space with a primary function to make urban areas healthier and more resilient. Green Infrastructure is an integrative system that is optimally planned for in advance and in conjunction with other infrastructure systems in order to function holistically and systematically in the urban environment.*

From a policy point of view, urban agriculture would make cities more resilient if it is envisioned as green infrastructure (GI). The concept of green space and land conservation planning has been evolving since the 1980s with the concept of green infrastructure emerging over the past two decades [167]. Conservation was originally seen as solely related to parks and recreation planning with the main objective of active recreation and scenic enjoyment. The understanding of green space has shifted to one of a more holistic and systematic vision which can best be defined as GI. Green infrastructure integrates all of the past objectives from active and passive recreation, to hubs and corridors to urban wildlife and forestry protection, and to regional and state ecological systems [167]. Urban agriculture is a logical next addition into the evolving definition of green infrastructure.

146

GI is multipurpose – it functions as storm water management, habitat and wildlife preservation, recreation, climate mitigation, and food production. GI is comprehensive. It is planned for ahead of time and does not exist as an afterthought. It is not a compilation of piecemeal parcels, but instead an integrative planned system. GI functions best when it is planned for, and financed similarly as grey infrastructure. When agriculture is argued for in cities, one should not imagine the hundreds of acres of monoculture production as representative of traditional industrial agriculture. Instead one should plan for an agricultural system that functions like GI. Urban agriculture should integrate into the urban environment instead of existing despite of it.

Like GI, urban agriculture (UA) should be multipurpose. It should not maximize food production at the expense of the local environment. In their conceptual diagram, Foley et al. (2005) illustrate how agriculture can be conceptualized with a holistic and multipurpose approach to ecosystem services (See Figure 7.4). An intensive cropland land use maximizes crop production at the expense of all other ecosystem services. On the other hand, an integrated cropland design would allow for other ecosystems to function in line with agriculture. Though crop production is not maximized, the local environment and community reaps the benefit of other ecosystem services such as habitat protection, water quality regulation and climate controls. When arguing for urban agriculture, one should attempt to capture all of these ecosystem benefits.

My work supports the concept of UA as multipurpose. UA has myriad benefits from food production to community development. My work adds to the multipurpose function of UA by showing that UA cools local nighttime temperatures and can offset approximately 10% of the surface UHI assuming an even distribution across the MSA. The cooling potential of UA is an important ecosystem function which has yet to be explored in the literature and by supporting this climate benefit of agriculture, the multipurpose characteristic of UA as GI is strengthen.

Like GI, Urban agriculture should be comprehensive and forward looking. Today UA is too reactive and UA policy should be proactive. It should be planned for in comprehensive plans, sustainability plans and climate action plans. These planning processes represent a community's long-term vision and normative values. Though these plans can drastically vary in scope and implementation, by enumerating the vision of urban agriculture as a comprehensive network of greenspace defines it as a priority and goal for a community. As with sustainability planning and climate action plan-

147
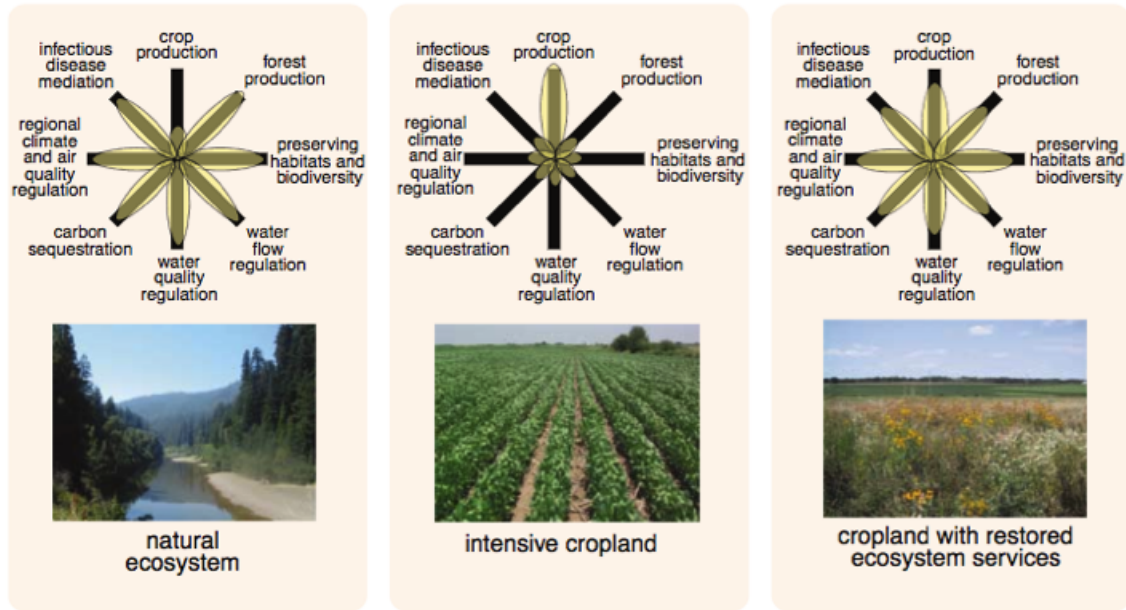
Figure 7.4: Image from Foley et al. [27] illustrates how agriculture can be designed to incorporate other ecosystem functions.

ning, there are myriad tools that communities and stakeholders can use to start integrating UA into their cities. Municipalities can use a variety of tools typically used for land conservation besides just land purchasing which include easements, floodplain management, smart growth management tools, conservation land development, public private partnerships, and land trusts.

For UA to function as GI it should be planned ahead of time instead of part of a piecemeal development. The comprehensiveness of UA is important in order to ensure that there is an adequate size of agriculture in neighborhoods to provide cooling benefits. My work suggests that a minimal amount of agriculture would be necessary before cooling benefits occur (approximately 7.5 acres per km^2). UA installations are typically not large. The majority of UA occupy land less than 1 acre in size with the largest examples of UA in the United States approximately 5-6 acres. Additionally, since my results suggest that UA provide larger cooling benefits to urban neighborhoods as compared to residential during extreme heat events then it is important to proactively plan for agriculture in dense urban areas where land prices may normally prohibit agriculture land use from occurring. Comprehensive planning could provide tools supporting neighborhoods to proactively convert underutilized land to agriculture when opportunities present themselves.

Urban agriculture as green infrastructure should be integrative. It should not only be comprehensive but it should be planned at the same time as other infrastructure projects in order to capture inherent synergies. One of the strongest synergies that exist with UA is between water harvesting and food production. Specifically water harvesting techniques should be designed and collocated with urban agriculture in order to maintain agriculture's cooling potential and to make urban agriculture more resilient especially during extreme climatic events. In my work, I utilize an irrigated agriculture proxy through the use of a locally derived NDVI threshold and show that non-tree vegetation with a NDVI of at least 0.41 continues to cool urban temperatures during a heat wave event. This irrigated agriculture proxy is attempting to capture the beneficial effects of irrigation. As other work supports the notion that agriculture continues to cool during heat waves and that irrigation can maintain this cooling ability, my work suggests that irrigation may be making this vegetative strategy more effective as a cooling mechanism during extreme heat conditions. Further investigation is needed to tease out how well the irrigated agriculture proxy is actually capturing the irrigated agriculture as a land cover and what other land covers are captured in the proxy as well as further investigate the climatic benefit of irrigation in urban areas.

When thought of as a climate mitigation strategy, UA should also be integrated with other climate adaptation strategies. My work shows that though agriculture continues to cool nighttime temperatures during heat waves, its cooling magnitude can decrease by as much as 75%. As such urban agriculture as a vegetative UHI mitigation strategy alone is not sufficient to protect urban residents from extreme heat conditions. As such UA should be planned in conjunction with other UHI mitigation strategies and should be considered for inclusion in local heat response plans. Heat response plans, in addition to pushing for UHI mitigation strategies, can focus on enhancing infrastructure resilience in order to proactively prevent infrastructure failure, from the transportation and energy sector, during intense heat waves. As air-conditioning is one of the most effective cooling strategies during heat waves, heat response plans can support the availability of public air-conditioned spaces, necessary to provide relief from future heat waves [112, 168]. Many regions have experienced blackouts during these critical times. Outdated electrical systems can subject populations to unnecessary heat exposures and can put larger numbers of people at risk for adverse health outcomes.

7.4.1 Water Harvesting and Urban Agriculture

In my dissertation, I examine the impact of heat waves on agriculture. Chapter 5 and Chapter 6 both show that heat waves are mitigating the cooling performance of agriculture at both the MSA and the city level. Specifically, I make the following contributions to the research community. In Chapter 5, I demonstrate that agriculture continues to cool local nighttime temperatures during a heat wave but that urban agriculture only retains 25% of its cooling potential. In Chapter 6, I demonstrate that there is an interaction effect between irrigated agriculture and urban form when a heat wave is present. One of the reasons why agriculture has been shown to reduce temperatures is because of the increase in soil moisture from irrigation, which my irrigated agriculture proxy attempts to capture at the city level. The results from this work suggests that cities should investigate the potential for the coupling of water harvesting techniques with its urban agriculture interventions.

Different vegetation types respond differently due to extreme heat. For example, short herbaceous vegetation such as grassland and agriculture showed an increase in evapotranspiration during the 2003 European heat wave whereas ET decreased in forested land from increased temperatures [122]. When temperatures increase, the stomatal resistance of agriculture decreases allowing for more water to be used in evapotranspiration than would otherwise be the case during non heat wave days [133]. The increased cooling from the reduction in stomatal resistance is only maintained as long as there is adequate soil moisture. But if urban agriculture is irrigated, the agricultural land has the potential to not only maintain its cooling potential but to also increase it. A call for active management of agriculture especially during heat waves is an important urban agriculture policy. Instead of implementing water restrictions for urban agriculture in cities during heat waves, cities should investigate the tradeoffs and opportunity costs in developing a network of distributed water harvesting infrastructure that can be used to irrigate agriculture during heat waves. The water harvesting infrastructure should have a goal to irrigate agriculture without impacting the drinking water supply nor put further strain on water supply during times of drought.

To maintain the health and function of agricultural vegetation, it is important that active management of vegetation is undertaken to ensure sufficient soil moisture. The larger agriculture research world (beyond urban agriculture) is arguing for similar responses. For example, The Nebraska

Agricultural Water Management Network (NAWMN) supports work to monitor and maintain soil moisture at an adequate level during extreme heat periods to sustain vegetation productivity and functions. This active management would not only reduce heat stress on plants but continue to provide cooling benefits to local communities during extreme heat conditions [169]. Active management of green infrastructure and specifically agricultural lands during extreme heat should be further investigated with the aim to be included into heat response plans.

One way to irrigate urban agriculture is through the harvesting of water in urban environments. Water harvesting techniques include grey water harvesting, storm water harvesting, and water retention systems such as basins and swales. See Chapter 5 for an in-depth discussion on water harvesting techniques. Since the evidence from my work supports that urban agriculture cools nighttime temperatures, then communities should explore the potential of designing water harvesting infrastructure in conjunction with urban agriculture in order to maximize the cooling potential of this vegetative strategy. To accomplish this task, cities should make it easier for individuals to harvest water, allow for collective reuse and design for collective storage and design for subsurface irrigation. UA designed comprehensively and integrated with water harvesting can make for more resilient communities.

Governments should make it easier for individuals to harvest water on site. There are many steps that governments can take to enhance water harvesting in their cities. Water harvesting needs to be legal, water needs to be priced appropriately, individuals need to be incentivized, and governments should have different strategies for pre and post developments. The first is to make water harvesting legal. Harvesting of rainwater has been problematic throughout the US especially in water scarce areas like the west because of inconsistencies of regulations. The state of Colorado for example explicitly banned water harvesting and just recently relaxed this restriction in the past year. Rainwater is primarily governed by administrative laws and therefore it is important that building and municipal codes are augmented to explicitly allow rain water harvesting to be incorporating into plumbing codes [170]. Eleven states, including Georgia, have revised their building, planning and landscaping codes to include active rain water harvesting measures [170]. Most regulations restrict water harvesting for potable use. The state of Ohio and the city of Atlanta, GA are two exceptions with Atlanta, GA having one of the first potable rainwater harvesting ordinances in the US enacted

in 2012.

The EPA has also argued that the low cost of water in the United States has created a barrier to water harvesting and they argue that water costs should reflect the full cost of using potable water. The US has the fourth lowest water cost when compared to all developed countries. Germany and Denmark's water costs are more than three times higher than the cost of water in the US. Atlanta, GA not only has one of the first potable rainwater harvesting ordinances in the US but it also has one of the highest water costs of any US metropolitan area due to the cost of separating its combined overflow sewage system . As such, Atlanta is well positioned to become a leader in water harvesting and reuse amongst cities in the US and the next logical step is for Atlanta to design policies to connect this water supply to urban agriculture.

Water harvesting incentives can be an effective policy for encouraging the coupling of water harvesting and agriculture in cities. Incentives can be implemented at the state or the local level, that is, if the states do not prohibit it. Incentives can be in the form of tax credits or even lower water bills. The state of Rhode Island, New York (pending) and Virginia are incentivizing individuals and businesses through income tax credits [171] . The tax credits are for green infrastructure investments and would credit up to a certain percentage of construction costs. Though Atlanta has developed a comprehensive rainwater harvesting ordinance, Atlanta makes residents pay an annual fee based on the water harvesting collection size. The ordinance stipulates lower annual fees if harvested water is used for irrigation. One way to augment current policies is to give a larger rebate and tax credit if property owners allow their water collection to be used for agriculture purposes.

Policies should also be amended to allow for the collective reuse of water for agriculture purposes, specifically allowing for reuse on land where the water was not originally collected. Colorado for example explicitly prohibits this type of collective reuse by restricting the use of water only to be used on the collecting parcel. It is imperative that policies allow for collective reuse for agriculture so that urban agriculture can be irrigated from water harvested from adjacent impervious surfaces. Small-scale nongovernmental buildings such as single family and commercial buildings can provide a significant amount of harvested water for urban agriculture. For example, a case study looking at Roanoke VA, identified roofs for catchment near all current urban agricultural land and estimated that approximately 500,000 m3/year could be generated for agriculture use [128]. This

152

water potential can only exist if state and local policy allow for txhis function. It is possible to harvest, treat and store storm water from dense urban areas and reuse it to produce food [172]. A case study looking at urban agriculture and storm water in Australia, demonstrate the potential for storm water to be collected from roofs of single-family housing, collectively channeled to a constructed wetlands project for treatment and then used for agriculture purposes. A distributed infrastructure stormwater design at the neighborhood level could provide the necessary irrigation for local urban agriculture, providing win-win-win for the city, property owners and farmers. The city reduces its stormwater load, individuals get cheaper water bills, and farmers get access to reused water.

Collective harvesting and collective reuse, either from a few large buildings or many small houses, will take planning and financing to lay pipes and design collection systems (natural wetlands or cisterns). As with any infrastructure planning, co-locating water harvesting with UA takes time, is easier to implement pre-development and can be costly. Additionally guidelines and landscaping codes should standardized the channeling of harvested water for subsurface irrigation. Subsurface irrigation benefits crops in many ways, but from a public health and safety point of view irrigation below surface can reduce and/or limit the need for water treatment. Irrigation is a permitted use of harvested water because it assumes that the water is used primarily for lawns and grass and will have limited exposure to people but this is not the case when irrigating agriculture. Research is still needed to better understand if and how much water should be treated before it can be used for urban agriculture. For example, water harvested from air conditioning units need to be pretreated for bacteria contamination. From a public health policy perspective, the simplest thing to do is to restrict harvesting and reuse of water across the board in an effort to minimize human contact with grey water. However, taking this naïve approach hinders the ability for developments to take full advantage of available natural resources. Alternatively, crafting policy to encourage safe and efficient treatment of harvested water should take precedence.

7.4.2 Size Matters

In Chapter 6, I explore whether the size of agriculture makes a difference on its impact on lowering local temperatures. I make a contribution to the research field by showing that the size of agriculture does impact its cooling ability when examining urban neighborhoods during a heat wave. My

research shows that temperatures in urban neighborhoods were only statistically lower if agriculture was implemented at sizes greater than 7.5 acres. Agriculture implemented at the city scale between 7.5 and 15 acres, statistical decrease temperatures by approximately 0.48°C (0.86°F). If agriculture was implemented at smaller scales in the local urban environment no change in temperature was detected. Therefore in order to see local nighttime temperatures decrease in urban environments during heat waves because of urban agriculture, cities should ensure that there is sufficient amount of land available for agricultural uses in their neighborhoods. Though my dissertation does not directly address whether this implementation needs to be contiguous, it does suggest that several acres are necessary to start seeing a cooling effect. Therefore my research supports policies that aim to transition large amounts of land into agricultural uses. One of the more immediate ways for cities to transition enough land to support urban agriculture is by leveraging underutilized public lands.

Urban farms are not large in US cities. The largest farms are between 5- 6 acres and only a handful of urban farms across the country are in this size category. In order to convert large areas of land into agriculture, cities can leverage their public land for agriculture use. The urban agriculture movement in Cuba provides a great example of government offering public land for private agriculture use. Though it provides a great case study of public land for private use, Cuba is an anomaly in this regard because of its unique economic and public health crisis. Instead of the Cuba model, US cities are creating public private partnership between their parks departments and nonprofit groups to allow for public parks to be farmed by communities and managed by private entities (Atlanta, Cleveland, NYC all have example of this partnership). Park Pride is Atlanta's nonprofit example with a mission to manage community gardens on public parklands.

Though parklands have proven an effective mechanism for providing public land for community use, cities need to look past their parklands and utilize this same public/private mechanism to allow for farming on non-park public land. For example, I led the creation of the first community garden in Atlanta that was located on public land outside of the parks department. Under my guidance for the neighborhood of Cabbagetown, I worked with Atlanta's city council and Park Pride to pass city council legislation to allow for such a creation. Cabbagetown's community garden represents the first community garden in Atlanta located on public land that is not located in a park. This garden created the pathway for the creation of other community gardens located on public non-park

land. Because local governments often own underutilized land, policies are needed to allow for community stewardship of public lands.

Philadelphia is a great example of how to leverage underutilized public land for community and agricultural use. Currently there are tens of thousands of vacant parcels in the city of Philadelphia. Of these vacant parcels, over twenty-five percent are publicly owed. To deal with this vacant public land, Philadelphia has created a citizen toolkit to help transition underutilized public lands into community stewardships. The "Vacant Land Toolkit" is a toolkit for citizens to learn how they can access vacant land throughout the city of Philadelphia. The toolkit supports the community management of open spaces with urban agriculture as one of its highest priority uses. A self-guided toolkit, it aims to train community members on how to work within the government to get access to vacant land through advocacy. The toolkit identifies vacant land throughout the city, the department that manages the land, and answers questions about access, tenure, use, and zoning (cite "grounded in Philly). The "Vacant Land Toolkit" serves as an example for how policy can be used to empower citizens to take control of their local environment. Philadelphia is not the only city to use a citizen toolkit to support community drive action in transforming vacant land into agriculture. Los Angeles and Pittsburgh also have similar programs.

7.4.3 Urban Agriculture needs to be Urban

In Chapter 6, I investigate the extent to which the local urban form impacts the cooling effect of agriculture. I make a contribution to the research field by illustrating that the urban form does change the impact that agriculture has on temperatures when a heat wave is present. Agriculture cools temperatures similarly in both residential and downtown areas but this relationship changes during a heat wave. In urban areas we see that agriculture continues to cool local temperatures during heat waves but it does not impact temperatures in residential areas. The outcome that agriculture maintains a cooling impact in urban areas supports policies that implement agriculture in highly urbanized areas such as downtown and midtown Atlanta. When planning urban agriculture as green infrastructure, cities should prioritize location in these areas.

Zoning is an effective tool to support agriculture in cities. Many large cities across the country, from Atlanta to Portland, have amended their zoning ordinances to allow for agriculture in their city

limits. But unfortunately these zoning regulations may be working against the notion of agriculture in dense urban areas. For example, Philadelphia's zoning ordinance designates where urban agriculture is allowed to be implemented. It divides urban agriculture into four typologies based on the purpose of the agriculture. The "Market or Community Supported Farm" typology is not allowed in downtown, city center commercial districts as well as in other highly urbanized areas of Philadelphia. My research argues that these dense downtown places could benefit the most from urban agriculture as a nighttime cooling mechanism. Instead of making it illegal for urban agriculture to exist in city centers, zoning should be amended to support the creation of urban farms in these urban neighborhoods.

Land in downtown and midtown neighborhoods are often too expensive to support agriculture. Access to and longevity of high quality land is one of the biggest barriers to urban agriculture especially in highly urbanized areas. This is why we see an explosion of urban agriculture in shrinking cities that have an abundance of vacant land in their cities. Many large metropolitan areas around the county have a dearth of underutilized, vacant, and/or foreclosed properties resulting from economic downturns, such as the housing market collapse of 2008 or deindustrialization in rustbelt cities. Land banks are an important mechanism for acquiring land while it is cheap and keeping it for future use.

Cities should create community land banks and/or create partnerships with nonprofit land banks in order to acquire land while it is cheap for the future use of agriculture. Philadelphia's created the Philadelphia Land Bank. The land bank was created to help transition vacant and delinquently taxed property into functioning uses throughout the city. Urban agriculture is one of their main priorities for transitional uses. It is not enough for land to be acquire but it is important that it be held in perpetuity for food production. Cities must devise policy to prevent land from being developed once a local economy rebounds. For example, Truly Living Well was the most high profile urban farm in Atlanta. Located in the historic African American district of Auburn Avenue, Truly Living Well (TLW) was a successful and active farm. But in 2015, TLW was forced to relocate because the landowners chose to develop the land. The relocation of TLW is a prime example of why land needs to be held in perpetuity in order to preserve their future use. Philadelphia's Neighborhood garden Trust (NGT) does exactly that. It preserves existing gardens and farms in order to keep them from

being developed.

7.5 Summary

The urban agriculture research field involves many players and all from different pedagogical and epistemological backgrounds. Planning is the most dominant research domain associated with urban agriculture. The planning discipline has decided to play an active role in this research agenda, which is fitting, and as such the planning community needs to understand not only the lack of research in this domain but also understand the complexity that surrounds this research agenda. Vegetative UHI research is not so simple that you can substitute one vegetative approach for another with complete authority.

My work attempts to bring awareness to the UHI/UA research gap and begins addressing some fundamental research questions regarding urban agriculture as a UHI mitigation strategy. Specifically, my research bridges two built environment and health research areas: urban heat islands (UHI) and urban agriculture. I investigate the potential for urban agriculture to act as an urban heat island mitigation strategy at the neighborhood scale. I have five research objectives:

1. to examine the potential for urban agriculture to cool the local climate by lowering temperatures in urban areas;

2. to compare the performance of urban agriculture to the UHI mitigation strategy of urban forestation;

3. to quantify the amount of land that needs to be converted to urban agriculture in order to receive a measurable local climate benefit;

4. to investigate how different patterns of urbanization mediate the influence of urban agriculture on local climate;

5. to investigate whether urban agriculture as a heat mitigation strategy is as effective during extreme heat conditions.

My research shows that urban agriculture decreases high nighttime temperatures during summer months, which is an important public health finding as nighttime temperatures are a better metric

157

for capturing negative health effects from extreme heat than daytime temperatures. At the local level, an increase of 10-acres per km^2 in agricultural land cover can reduce nighttime temperatures by approximately 0.65°F accounting for approximately 10% of Atlanta's UHI effect. Agricultural lands outperformed forested land cover as a nighttime cooling mechanism. Where agricultural lands exhibited a statistically significant cooling effect, tree canopy, though statistically significant, contributed to a slight increase in local temperatures at night. Though agricultural lands can act as a heat mitigation strategy by lowering nighttime temperatures, their cooling effect is not maintained during heat waves. Though urban agriculture still contributes to cooling local temperature during extreme heat conditions, the cooling effect decreases by as much as 75%. As such, I argue for an active management strategy to ensure that urban agriculture maintains its cooling potential during extreme heat conditions.

In addition, when investigating whether the urban form of a neighborhood plays an important role in how well vegetative strategies perform in reducing temperatures, I illustrate there is an interaction effect at play. The interaction effects describes that the urban form at the neighborhood scale impacts the relationship between urban agriculture and local temperatures when a heat wave is present. For example, agricultural implementations in dense urban neighborhoods decrease temperatures more than in the residential areas. I also found that a minimum of seven acres of agricultural lands needs to be implemented before cooling effects will occur. As such, I argue that urban agriculture should not only be placed in cities but that the morphology of the built environment should be taken into consideration when selecting locations for urban agriculture.

Appendices

APPENDIX A

DEVELOPING AN IRRIGATED AGRICULTURE PROXY

In my research, I use a similar approach as Dappen et al.[131] in order to identify an irrigated agriculture land cover proxy. I identify all potential agriculture land cover and filter the agriculture land cover based on a NDVI threshold in order to identify irrigated agriculture. The NDVI threshold is generated from current urban agriculture training sites located in the city of Atlanta.

Equation A.1 is the formula for NDVI. The Quickbird raster image is a 4 band multispectral imagery. Band 1 represents red visible light and Band 4 represents near infrared. Equation A.2 substitutes the band numbers in the NDVI equation.

$$NDVI = (NIR - VIS)/(NIR + VIS) \qquad \text{(A.1)}$$

$$NDVI = (Band4 - Band1)/(Band4 + Band1) \qquad \text{(A.2)}$$

To generate NDVI data, I to calculate an index by using the raster calculator found in ArcMAP's spatial analysis extension. The raster calculator is used to process Band 1 (red) and Band 4 (NIR) according to Equation A.2. Once the NDVI is generated, I ensure that data range is from –1 to +1. Any values below or above this range indicates that the calculation is incorrect. A higher NDVI value indicates that the land cover is emitting more infrared and negative values indicated that land cover that is absorbing infrared.

Next I identify all of the "agricultural lands" in the city and extract their NDVI values. Since grass has often been used in climate models to represent agricultural land and since agricultural lands are not prevalent throughout the city, I assume that all grass/shrub land cover represent agriculture land [35]. To isolate all of the grass/shrub land cover from the classified land cover raster, I reclassify the raster image to be either grass/shrub (1) or not grass (0) and extract the grass/land cover so that it is the only info in the raster. Using the grass/shrub land cover raster as a mask, I then extract the NDVI that corresponds with the grass land cover.

I identify 6 urban agriculture sites in Atlanta. I create a new urban agriculture shapefile and draw polygons to represent the location and boundaries of the urban agriculture training sites. I calculate the NDVI for each of the training sites. To do this I use the spatial analysis tool "zonal statistics as table" to aggregate the NDVI values for each of the urban agriculture training sites. I calculate the average NDVI for all 6 sites and use this value as the threshold to select irrigated agriculture from "agriculture land." The average NDVI is = 0.41. Using the "reclass" tool located within the spatial analysis toolbox, I reclassify the raster so that all pixels with a NDVI value above 0.41 are classified as irrigated agriculture. I used the Zonal Histogram tool to sum the number of irrigated agriculture pixels for each grid in order to calculate the total area of irrigated agriculture in each grid cell. I also compute the average area of each irrigated agriculture patch within a grid cell to examine the effect of patch size.

To calculate the average size, I convert the irrigated agriculture pixels from a raster dataset to a vector dataset using the ArcMAP conversion tools (Raster to Polygon tool). I then use the identity tool to both assign the agricultural patches to a grid ID number and to divide the agricultural patches when it crossed a grid boundary. Using the dissolve tool, I then aggregate descriptive statistics of the agricultural patches to each grid cell. Descriptive statistics included the number of patches, the total area of agricultural land, the range of patch area, the max and min of patch area, and the average area of patch.

APPENDIX B

GENERATING BUILDING HEIGHT DATA FROM LIDAR

The roughness height parameter is derived from building height data. For local climate zones 1–10 it represents the average building height per zone. To derive building height data, I used three primary datasets: the building footprint shapefile discussed above and used to generate the building surface fraction parameter; a digital elevation model (DEM) and Light Detection and Ranging (LiDAR) data. The LiDAR data was produced for and acquired from the City of Atlanta's planning department. LiDAR is a remote sensing technique used to map both natural and man-made elements on the earth's surface. A LiDAR sensor sits aboard an aircraft such as an airplane or helicopter and measures the varying distance from the earth's surface. Using both GPS receiver and a scanner in conjunction with the laser, one can estimate a model of the earth's surface. LiDAR data is distributed in what is known as point cloud data. The point cloud data can be classified by the number of returns from the pulsing laser. Basically one laser beam can be returned back to the sensor multiple times depending on what is happening at the surface. The first return is always the highest structure such as a building or tree canopy, then subsequent returns are reflected by lower structures and the final return is usually the ground. The first return can also represent the ground layer if there is no other structure present. The LiDAR data I acquired for the city of Atlanta was unclassified, had a spatial resolution of 1.5 ft and did not cover the entire city limits for Atlanta. See Figure B.1 for the boundary area of the LiDAR data. Since the LiDAR data is only available in this area, this boundary becomes the area of the study for the city level analysis.

In order to generate building height data, you must create a normalized digital surface model (nDSM) and join this data with building footprints. An nDSM represents the height of the surface above the ground layer and is created by subtracting a digital elevation model (DEM) from a digital surface model (DSM). To create an nDSM you subtract the highest point (or the first return in the LiDAR point cloud data) from the base floor layer. You could do this process in two methods, first you can classify the point cloud data to identify the base layer from the first returns, or you can use a second approach which is to subtract the first returns from a already generated DEM. Using ArcGIS
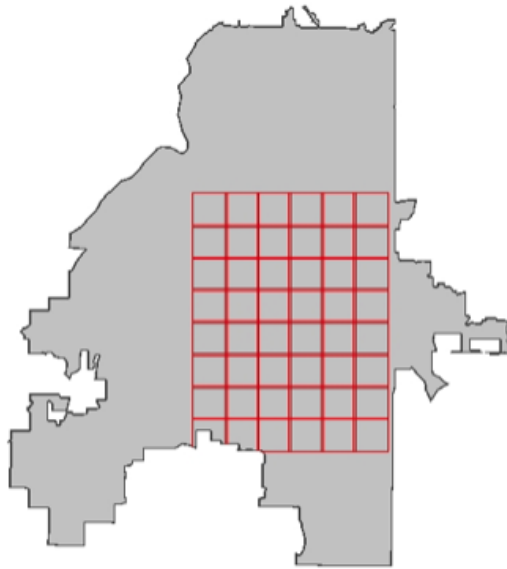
Figure B.1: LiDAR Boundary Area

and a third party software extension in ArcMAP called LP360, I attempted to classify the LiDAR data. I used the software application LP360 to classify the ground points but the classification process was not successful because the LiDAR data did not have adequate ground returns for the entire image. In theory the last returns from the laser should represent the ground level and this was not the case for a large area of the dataset. I checked the data by correlating last returns with ground features. Since the point cloud data is unclassified, I used a DEM data from the USGS to represent the base layer and the LiDAR data to create a DSM.

I use ArcGIS's ArcMAP and ArcCatalog to process the LiDAR and the USGS DEM data in order to create the nDSM. Since ArcGIS does not automatically recognize LAS files, I used Arc-Catalog to create a LAS dataset so that ArcGIS would recognize the LiDAR data. Using the "LAS dataset toolbar" I created a raster surface model that consists of only the first returns to create a DSM. This process creates a LAS dataset layer file which contains only a subset of the LAS points by filtering out all other returns, so that the dataset only contains first returns. Using ArcMAP's conversion tool, I convert the LAS dataset to a raster image so that each pixel in the raster will be given the elevation value from the filtered LAS dataset. For visualization purposes, I used the hill shade tool from the Image Analysis extension to create an easier to interpret elevation dataset.

I used ArcMap's raster calculator to subtract the DEM raster from the DSM raster. I also used the raster calculator to change the USGS elevation data into the same units as the LiDAR data. I created the nDSM which generates heights of features relative to the building height data. After the nDSM is created, I join this raster data with building footprint data. I used zonal statistics table to join the nDSM with footprint shapefile and calculated all statistics which include both average and max height. I used ObjectID as my identifying field and then joined the resulting table with the building footprint shapefile.

Using the USGS DEM data and the first returns from the LiDAR data to generate building height data, I was able to generate accurate building heights. For example, checking residential neighborhoods, single story single-family residential buildings had heights approximately 14 feet tall. When checking the downtown area, buildings near five points were all quite accurate. For example, my process estimated an elevation height of 842 feet for the SunTrust building. The SunTrust Wikipedia page indicates the building is 869 feet. Given the varied height of the building top, this is a reasonable estimation. In ArcScene,I created a 3D model of the generated building height data.

APPENDIX C

SKY VIEW FACTOR

To calculate the sky view factor for my urban form typologies, I use Viewsphere [157]. Viewsphere is a GIS–base software application created to measure the 3D visibility of differing urban forms. ArcGIS' ArcScene is used to run Viewsphere. Because of the programing platform for the Viewsphere software, an older version of ArcGIS (v9.3) is needed to run the software. To calculate the SVF through Viewphere, the user needs three datasets, a 3D surface topography file saved as a TIN file, building footprint data with building height in its associated attribute table, and observation points which indicate where to calculate the SVF.

To create the 3D surface TIN file, I use the 3D Analyst Tools located in ArcMAP. I use USGS 10–meter resolution DEM. I crossed checked this elevation data with 2ft. topographic contour lines for the city of Atlanta and the data lined up well. I chose not to use the 2ft. contour topography because the computational cost was too high as the Viewsphere Analysis software would most likely not be able to handle the high resolution. I created the TIN in an older version of ArcGIS (9.3). I used the 3D Analyst Tool to convert the DEM raster to a TIN. Next I used an ArcScene plugin tool, "Add Bldgs to TIN" created by the same researchers who created Viewsphere to use in conjunction with the Viewsphere software. The tool does exactly as it is named. It adds a 3D representation of buildings to a TIN surface file. I used the building footprint shapefile with building heights estimated from LiDAR data as discussed in the LiDAR section.

Once the observations are created and the buildings added to the topographic data, then you can begin calculating the SVF for each observation with Viewsphere. To run Viewsphere, there area a few adjustments I needed to make in order to run the program without returning error messages. First, Viewsphere requires there to be a rooftop buffer. It requires that the resulting TIN file (one with both topographic and building data) not have a vertical surface. Therefore you must offset the roof inward in order to make the outer building wall slightly sloped. The smaller the buffer the better the SVF estimates. If the buffer is too small, the process will fail; if it is too large, the estimates will be less accurate. The Viewsphere dialogue box sets the default rooftop buffer to be

0.5 (unit is based on the unit of the file). After running a set of trial simulations, I determined that a rooftop buffer of 0.3 was optimal for my dataset. This in essence means that the top of the roof has a slight inset of 0.3 feet from the base of the building.

The observation data points also need to be cleaned before running the program. First, all observations that intersect a building footprint need to be removed. In theory, a road should never intersect a building but often GIS shapefile data are not true to reality. Therefore it is important to clean the data as much as possible. I selected any node that intersected the building shapefile (select by location tool) and deleted these nodes from the shapefile. Second, the Viewshere program sets a buffer maximum. This number is the maximum distance an observation point can be from a structure before calculations will not run. This creates two problems with the observation data, first the observations cannot be too close to the edge of the TIN file and second the observations cannot be too far away from a building. This buffer limit is set by the "max radius" field in the Viewsphere dialogue box. If one point is too close to the edge, then the entire process will not run. The program would also fail if there were any nodes that were more than 300 feet from a building (this is the default value set in the program to determine the max radius for the SVF calculations). To clean this data, I selected all nodes more than 300 feet from a building (I ran select by location- set the buffer distance to be 300 feet – and then reverse the selection in the attribute table). 95% of these nodes were located along the interstate. I decide to delete all of these nodes and rerun the analysis. To sum up, I ran my analysis by first ensuring no nodes intersected with building footprints and deleted nodes that were not within a certain distance from buildings. In the Viewsphere dialogue box, I set the Z offset for the observer to be 1.5 meter, Initial Radius to 300 feet (which is the buffer radius range for the SVF calculations) and I left default settings for everything else.

Viewsphere software outputs a .csv file for each session. The CSV file is organized by point number. The point number represents the order in which the nodes are analyzed. The nodes are ordered by the order they are in in the shapefile. For example, point 1 is equal to a node with an FID =0. Therefore when joining the SVF .CSV file with the observation point shapefile, you need to create a new attribute in the shapefile with an ID that equals to FID +1. I ensure I had the same number of points in the CSV as in the attribute table. I joined the SVF CSV table to the observation point shapefile based on the new ID number.

REFERENCES

[1] CDC, *Extreme heat: A prevention guide to promote your personal health and safety. centers for disease control and prevention website*, 2004.

[2] *National hazard statistics*, 2011.

[3] ——, "Heat-related deaths–united states, 1999-2003", *MMWR: Morbidity and mortality weekly report*, vol. 55, no. 29, pp. 796–798, 2006.

[4] S. H. Wainwright, S. D. Buchanan, M Mainzer, R. G. Parrish, and T. H. Sinks, "Cardiovascular mortality—the hidden peril of heat waves", *Prehospital and disaster medicine*, vol. 14, no. 04, pp. 18–27, 1999.

[5] G. Luber and M. McGeehin, "Climate change and extreme heat events", *American journal of preventive medicine*, vol. 35, no. 5, pp. 429–435, 2008.

[6] M. A. Palecki, S. A. Changnon, and K. E. Kunkel, "The nature and impacts of the july 1999 heat wave in the midwestern united states: Learning from the lessons of 1995", *Bulletin of the American Meteorological Society*, vol. 82, no. 7, pp. 1353–1367, 2001.

[7] B. Revich and D. Shaposhnikov, "Climate change, heat waves, and cold spells as risk factors for increased mortality in some regions of russia", *Studies on Russian Economic Development*, vol. 23, no. 2, p. 195, 2012.

[8] J.-M. Robine, S. L. K. Cheung, S. Le Roy, H. Van Oyen, C. Griffiths, J.-P. Michel, and F. R. Herrmann, "Death toll exceeded 70,000 in europe during the summer of 2003", *Comptes rendus biologies*, vol. 331, no. 2, pp. 171–178, 2008.

[9] T. R. Oke, *Boundary layer climates*. New York, NY: Routledge, 1987.

[10] B. Stone, J. Vargo, and D. Habeeb, "Managing climate change in cities: Will climate action plans work?", *Landscape and Urban Planning*, vol. 107, no. 3, pp. 263–271, 2012.

[11] D. Habeeb, J. Vargo, and B. Stone Jr, "Rising heat wave trends in large us cities", *Natural Hazards*, vol. 76, no. 3, pp. 1651–1665, 2015.

[12] "World urbanization prospects: The 2008 revision", *United Nations, Department of Economic and Social Affairs (DESA), Population Division, Population Estimates and Projections Section, New York*, 2008.

[13] H. Akbari, S. Menon, and A. Rosenfeld, "Global cooling: Increasing world-wide urban albedos to offset co 2", *Climatic Change*, vol. 94, no. 3, pp. 275–286, 2009.

[14] K. W. Oleson, G. B. Bonan, and J Feddema, "Effects of white roofs on urban temperature in a global climate model", *Geophysical Research Letters*, vol. 37, no. 3, 2010.

[15] B. H. Lynn, T. N. Carlson, C. Rosenzweig, R. Goldberg, L. Druyan, J. Cox, S. Gaffin, L. Parshall, and K. Civerolo, "A modification to the noah lsm to simulate heat mitigation strategies in the new york city metropolitan area", *Journal of Applied Meteorology and Climatology*, vol. 48, no. 2, pp. 199–216, 2009.

[16] Y. Zhou and J. M. Shepherd, "Atlanta's urban heat island under extreme heat conditions and potential mitigation strategies", *Natural Hazards*, vol. 52, no. 3, pp. 639–668, 2010.

[17] T. Carter and L. Fowler, "Establishing green roof infrastructure through environmental policy instruments", *Environmental management*, vol. 42, no. 1, pp. 151–164, 2008.

[18] S Johnston and J. Coffee, "Green building and climate in chicago", *Sustainable Chicago*, 2008.

[19] E. G. McPherson, J. R. Simpson, Q. Xiao, and C. Wu, "Million trees los angeles canopy cover and benefit assessment", *Landscape and Urban Planning*, vol. 99, no. 1, pp. 40–50, 2011.

[20] C. J. LaCroix, "Urban agriculture and other green uses: Remaking the shrinking city", *The Urban Lawyer*, pp. 225–285, 2010.

[21] J. Hansen, R. Ruedy, M. Sato, and K. Lo, "Global surface temperature change", *Reviews of Geophysics*, vol. 48, no. 4, 2010.

[22] D. L. Hartmann, *Global physical climatology*. Newnes, 1994, vol. 103.

[23] R. Pachauri and L. Meyer, "Ipcc, 2014: Climate change 2014: Synthesis report. contribution of working groups i, ii and iii to the fifth assessment report of the intergovernmental panel on climate change", p. 151, 2014, Geneva, Switzerland.

[24] J. Salzman and B. H. Thompson, *Environmental law and policy*. Foundation Press New York, 2003.

[25] S. G. Philander, *Is the temperature rising?: The uncertain science of global warming*. Princeton University Press, 1998.

[26] N. Ramankutty and J. A. Foley, "Estimating historical changes in global land cover: Croplands from 1700 to 1992", *Global biogeochemical cycles*, vol. 13, no. 4, pp. 997–1027, 1999.

[27] J. A. Foley, R. DeFries, G. P. Asner, C. Barford, G. Bonan, S. R. Carpenter, F. S. Chapin, M. T. Coe, G. C. Daily, H. K. Gibbs, *et al.*, "Global consequences of land use", *science*, vol. 309, no. 5734, pp. 570–574, 2005.

[28] R. A. Pielke, "Land use and climate change", *Science*, vol. 310, no. 5754, pp. 1625–1626, 2005.

[29] R. A. Pielke, G. Marland, R. A. Betts, T. N. Chase, J. L. Eastman, J. O. Niles, S. W. Running, *et al.*, "The influence of land-use change and landscape dynamics on the climate system: Relevance to climate-change policy beyond the radiative effect of greenhouse gases", *Philosophical Transactions of the Royal Society of London A: Mathematical, Physical and Engineering Sciences*, vol. 360, no. 1797, pp. 1705–1719, 2002.

[30] T. N. Chase, R. A. Pielke, T. G. Kittel, R. Nemani, and S. W. Running, "Sensitivity of a general circulation model to global changes in leaf area index", *Journal of Geophysical Research. D. Atmospheres*, vol. 101, pp. 7393–7408, 1996.

[31] V. Meher-Homji, "Probable impact of deforestation on hydrological processes", in *Tropical forests and climate*, Springer, 1991, pp. 163–173.

[32] J. J. Feddema, K. W. Oleson, G. B. Bonan, L. O. Mearns, L. E. Buja, G. A. Meehl, and W. M. Washington, "The importance of land-cover change in simulating future climates", *Science*, vol. 310, no. 5754, pp. 1674–1678, 2005.

[33] R. Houghton, J. Hobbie, J. M. Melillo, B Moore, B. Peterson, G. Shaver, and G. Woodwell, "Changes in the carbon content of terrestrial biota and soils between 1860 and 1980: A net release of co" 2 to the atmosphere", *Ecological monographs*, vol. 53, no. 3, pp. 235–262, 1983.

[34] M. Zhao, A. Pitman, and T. Chase, "The impact of land cover change on the atmospheric circulation", *Climate Dynamics*, vol. 17, no. 5, pp. 467–477, 2001.

[35] V. Brovkin, A. Ganopolski, M. Claussen, C. Kubatzki, and V. Petoukhov, "Modelling climate response to historical land cover change", *Global Ecology and Biogeography*, vol. 8, no. 6, pp. 509–517, 1999.

[36] G. B. Bonan, "Effects of land use on the climate of the united states", *Climatic Change*, vol. 37, no. 3, pp. 449–486, 1997.

[37] P. Snyder, C Delire, and J. Foley, "Evaluating the influence of different vegetation biomes on the global climate", *Climate Dynamics*, vol. 23, no. 3-4, pp. 279–302, 2004.

[38] G. B. Bonan and D. Pollard, "Vegetation on global climate", *Nature*, vol. 359, pp. 716–718, 1992.

[39] M. H. Costa and J. A. Foley, "Combined effects of deforestation and doubled atmospheric co2 concentrations on the climate of amazonia", *Journal of Climate*, vol. 13, no. 1, pp. 18–34, 2000.

[40] C. A. Nobre, P. J. Sellers, and J. Shukla, "Amazonian deforestation and regional climate change", *Journal of Climate*, vol. 4, no. 10, pp. 957–988, 1991.

[41] G. Bala, K Caldeira, M Wickett, T. Phillips, D. Lobell, C Delire, and A Mirin, "Combined climate and carbon-cycle effects of large-scale deforestation", *Proceedings of the National Academy of Sciences*, vol. 104, no. 16, pp. 6550–6555, 2007.

[42] G. B. Bonan, "Forests and climate change: Forcings, feedbacks, and the climate benefits of forests", *science*, vol. 320, no. 5882, pp. 1444–1449, 2008.

[43] T. N. Chase, R. A. Pielke, T. Kittel, M Zhao, A. Pitman, S. W. Running, and R. R. Nemani, "Relative climatic effects of landcover change and elevated carbon dioxide combined with aerosols: A comparison of model results and observations", *Journal of Geophysical Research: Atmospheres*, vol. 106, no. D23, pp. 31 685–31 691, 2001.

[44] K. K. Goldewijk, "Estimating global land use change over the past 300 years: The hyde database", *Global Biogeochemical Cycles*, vol. 15, no. 2, pp. 417–433, 2001.

[45] E. Kalnay and M. Cai, "Impact of urbanization and land-use change on climate", *Nature*, vol. 423, no. 6939, pp. 528–531, 2003.

[46] S. Fall, D. Niyogi, A. Gluhovsky, R. A. Pielke, E. Kalnay, and G. Rochon, "Impacts of land use land cover on temperature trends over the continental united states: Assessment using the north american regional reanalysis", *International Journal of Climatology*, vol. 30, no. 13, pp. 1980–1993, 2010.

[47] D. B. Lobell and C. Bonfils, "The effect of irrigation on regional temperatures: A spatial and temporal analysis of trends in california, 1934–2002", *Journal of Climate*, vol. 21, no. 10, pp. 2063–2071, 2008.

[48] R. Mahmood, S. A. Foster, T. Keeling, K. G. Hubbard, C. Carlson, and R. Leeper, "Impacts of irrigation on 20th century temperature in the northern great plains", *Global and Planetary Change*, vol. 54, no. 1, pp. 1–18, 2006.

[49] J.-Y. Juang, G. Katul, M. Siqueira, P. Stoy, and K. Novick, "Separating the effects of albedo from eco-physiological changes on surface temperature along a successional chronosequence in the southeastern united states", *Geophysical Research Letters*, vol. 34, no. 21, 2007.

[50] P. J. Lawrence and T. N. Chase, "Investigating the climate impacts of global land cover change in the community climate system model", *International Journal of Climatology*, vol. 30, no. 13, pp. 2066–2087, 2010.

[51] M Trail, A. Tsimpidi, P Liu, K. Tsigaridis, Y Hu, A Nenes, B Stone, and A. Russell, "Potential impact of land use change on future regional climate in the southeastern us: Reforestation and crop land conversion", *Journal of Geophysical Research: Atmospheres*, vol. 118, no. 20, 2013.

[52] D. N. Wear and J. G. Greis, "Southern forest resource assessment-technical report", *Gen. Tech. Rep. SRS-53. Asheville, NC: US Department of Agriculture, Forest Service, Southern Research Station. 635 p.*, vol. 53, 2002.

[53] A. J. Arnfield, "Two decades of urban climate research: A review of turbulence, exchanges of energy and water, and the urban heat island", *International journal of climatology*, vol. 23, no. 1, pp. 1–26, 2003.

[54] H. Taha, "Urban climates and heat islands: Albedo, evapotranspiration, and anthropogenic heat", *Energy and buildings*, vol. 25, no. 2, pp. 99–103, 1997.

[55] B. Stone, "Urban and rural temperature trends in proximity to large us cities: 1951–2000", *International Journal of Climatology*, vol. 27, no. 13, pp. 1801–1807, 2007.

[56] L. Zhou, R. E. Dickinson, Y. Tian, J. Fang, Q. Li, R. K. Kaufmann, C. J. Tucker, and R. B. Myneni, "Evidence for a significant urbanization effect on climate in china", *Proceedings of the National Academy of Sciences of the United States of America*, vol. 101, no. 26, pp. 9540–9544, 2004.

[57] B. Stone, "Urban sprawl and air quality in large us cities", *Journal of Environmental Management*, vol. 86, no. 4, pp. 688–698, 2008.

[58] S. Conti, P. Meli, G. Minelli, R. Solimini, V. Toccaceli, M. Vichi, C. Beltrano, and L. Perini, "Epidemiologic study of mortality during the summer 2003 heat wave in italy", *Environmental research*, vol. 98, no. 3, pp. 390–399, 2005.

[59] J. Tan, Y. Zheng, X. Tang, C. Guo, L. Li, G. Song, X. Zhen, D. Yuan, A. J. Kalkstein, F. Li, *et al.*, "The urban heat island and its impact on heat waves and human health in shanghai", *International journal of biometeorology*, vol. 54, no. 1, pp. 75–84, 2010.

[60] T. Shen, H. L. Howe, C. Alo, and R. L. Moolenaar, "Toward a broader definition of heat-related death: Comparison of mortality estimates from medical examiners' classification with those from total death differentials during the july 1995 heat wave in chicago, illinois", *The American journal of forensic medicine and pathology*, vol. 19, no. 2, pp. 113–118, 1998.

[61] T. R. Karl, G. A. Meehl, C. D. Miller, S. J. Hassol, A. M. Waple, and W. L. Murray, "Weather and climate extremes in a changing climate", US Climate Change Science Program, Tech. Rep., 2008.

[62] E. J. Cooter and S. K. Leduc, "Recent frost date trends in the north-eastern usa", *International Journal of Climatology*, vol. 15, no. 1, pp. 65–75, 1995.

[63] A. T. DeGaetano, "Recent trends in maximum and minimum temperature threshold exceedences in the northeastern united states", *Journal of Climate*, vol. 9, no. 7, pp. 1646–1660, 1996.

[64] D. R. Easterling, "Recent changes in frost days and the frost-free season in the united states", *Bulletin of the American Meteorological Society*, vol. 83, no. 9, pp. 1327–1332, 2002.

[65] D. J. Gaffen and R. J. Ross, "Increased summertime heat stress in the us", *Nature*, vol. 396, no. 6711, pp. 529–530, 1998.

[66] IPCC, *Managing the risks of extreme events and disasters to advance climate change adaptation: Special report of the intergovernmental panel on climate change*. Cambridge University Press, 2012.

[67] B. Stone, J. J. Hess, H. Frumkin, *et al.*, "Urban form and extreme heat events: Are sprawling cities more vulnerable to climate change than compact cities", *Environmental health perspectives*, vol. 118, no. 10, pp. 1425–1428, 2010.

[68] G. A. Meehl and C. Tebaldi, "More intense, more frequent, and longer lasting heat waves in the 21st century", *Science*, vol. 305, no. 5686, pp. 994–997, 2004.

[69] C. Tebaldi, K. Hayhoe, J. M. Arblaster, and G. A. Meehl, "Going to the extremes: An intercomparison of model-simulated historical and future changes in extreme events", *Climatic change*, vol. 79, no. 3, pp. 185–211, 2006.

[70] S. Greene, L. S. Kalkstein, D. M. Mills, and J. Samenow, "An examination of climate change on extreme heat events and climate–mortality relationships in large us cities", *Weather, Climate, and Society*, vol. 3, no. 4, pp. 281–292, 2011.

[71] R. D. Peng, J. F. Bobb, C. Tebaldi, L. McDaniel, M. L. Bell, and F. Dominici, "Toward a quantitative estimate of future heat wave mortality under global climate change", *Environmental Health Perspectives*, vol. 119, no. 5, p. 701, 2011.

[72] A. Matzarakis, M. De Rocco, and G. Najjar, "Thermal bioclimate in strasbourg-the 2003 heat wave", *Theoretical and Applied Climatology*, vol. 98, no. 3-4, pp. 209–220, 2009.

[73] M. P. McCarthy, M. J. Best, and R. A. Betts, "Climate change in cities due to global warming and urban effects", *Geophysical Research Letters*, vol. 37, no. 9, 2010.

[74] P. L. Kinney, "Climate change, air quality, and human health", *American journal of preventive medicine*, vol. 35, no. 5, pp. 459–467, 2008.

[75] E. Tagaris, K.-J. Liao, A. J. DeLucia, L. Deck, P. Amar, and A. G. Russell, "Potential impact of climate change on air pollution-related human health effects", *Environmental science & technology*, vol. 43, no. 13, pp. 4979–4988, 2009.

[76] C. Rosenzweig, W. Solecki, and R. Slosberg, "Mitigating new york city's heat island with urban forestry, living roofs, and light surfaces", *A report to the New York State Energy Research and Development Authority*, 2006.

[77] M. A. Hart and D. J. Sailor, "Quantifying the influence of land-use and surface characteristics on spatial variability in the urban heat island", *Theoretical and applied climatology*, vol. 95, no. 3, pp. 397–406, 2009.

[78] L. S. Kalkstein and R. E. Davis, "Weather and human mortality: An evaluation of demographic and interregional responses in the united states", *Annals of the Association of American Geographers*, vol. 79, no. 1, pp. 44–64, 1989.

[79] L. S. Kalkstein, "A new approach to evaluate the impact of climate on human mortality.", *Environmental health perspectives*, vol. 96, p. 145, 1991.

[80] K. Laaidi, A. Zeghnoun, B. Dousset, P. Bretin, S. Vandentorren, E. Giraudet, and P. Beaudeau, "The impact of heat islands on mortality in paris during the august 2003 heat wave", *Environmental health perspectives*, vol. 120, no. 2, p. 254, 2012.

[81] T. Oke, "Advectively-assisted evapotranspiration from irrigated urban vegetation", *Boundary-Layer Meteorology*, vol. 17, no. 2, pp. 167–173, 1979.

[82] B. Kneen, "Restructuring food for corporate profit: The corporate genetics of cargill and monsanto", *Agriculture and human values*, vol. 16, no. 2, pp. 161–167, 1999.

[83] V. Shiva, *Stolen harvest: The hijacking of the global food supply*. Zed Books, 2000.

[84] B. Halweil, *Home grown: The case for local food in a global market*. Worldwatch Institute, 2002, vol. 163.

[85] K. Pothukuchi and J. L. Kaufman, "Placing the food system on the urban agenda: The role of municipal institutions in food systems planning", *Agriculture and Human Values*, vol. 16, no. 2, pp. 213–224, 1999.

[86] E. P. Agency, *How does your garden grow? brownfields redevelopment and local agriculture*, 2009.

[87] K. Pothukuchi and J. L. Kaufman, "The food system: A stranger to the planning field", *Journal of the American planning association*, vol. 66, no. 2, pp. 113–124, 2000.

[88] J. Smit and J. Nasr, "Urban agriculture for sustainable cities: Using wastes and idle land and water bodies as resources", *Environment and urbanization*, vol. 4, no. 2, pp. 141–152, 1992.

[89] J. Brock, *The structure of american industry*. Waveland Press, 2004.

[90] J. L. Kaufman and M. Bailkey, *Farming inside cities: Entrepreneurial urban agriculture in the united states*. Lincoln Institute of Land Policy Cambridge, MA, 2000.

[91] N. Goldstein *et al.*, "Vacant lots sprout urban farms", *BioCycle*, vol. 50, no. 10, pp. 24–26, 2009.

[92] B. Dousset, F. Gourmelon, K. Laaidi, A. Zeghnoun, E. Giraudet, P. Bretin, E. Mauri, and S. Vandentorren, "Satellite monitoring of summer heat waves in the paris metropolitan area", *International Journal of Climatology*, vol. 31, no. 2, pp. 313–323, 2011.

[93] J. Gornall, R. Betts, E. Burke, R. Clark, J. Camp, K. Willett, and A. Wiltshire, "Implications of climate change for agricultural productivity in the early twenty-first century", *Philosophical Transactions of the Royal Society of London B: Biological Sciences*, vol. 365, no. 1554, pp. 2973–2989, 2010.

[94] J. A. Patz, D. Campbell-Lendrum, T. Holloway, and J. A. Foley, "Impact of regional climate change on human health", *Nature*, vol. 438, no. 7066, pp. 310–317, 2005.

[95] B. Stone Jr, J. Vargo, P. Liu, D. Habeeb, A. DeLucia, M. Trail, Y. Hu, and A. Russell, "Avoided heat-related mortality through climate adaptation strategies in three us cities", *PLoS One*, vol. 9, no. 6, e100852, 2014.

[96] A. C. Bellows, K. Brown, J. Smit, *et al.*, "Health benefits of urban agriculture", *Community Food*, 2003.

[97] K. H. Brown and A. L. Jameton, "Public health implications of urban agriculture", *Journal of public health policy*, pp. 20–39, 2000.

[98] L. Bounoua, P. Zhang, G. Mostovoy, K. Thome, J. Masek, M. Imhoff, M. Shepherd, D. Quattrochi, J. Santanello, J. Silva, *et al.*, "Impact of urbanization on us surface climate", *Environmental Research Letters*, vol. 10, no. 8, p. 084 010, 2015.

[99] D. Kurn, S. Bretz, B. Huang, and H. Akbari, "The potential for reducing urban air temperatures and energy consumption through vegetative cooling", *Lawrence Berkeley Lab., CA (United States)*, 1994.

[100] L. Shashua-Bar and M. E. Hoffman, "Vegetation as a climatic component in the design of an urban street: An empirical model for predicting the cooling effect of urban green areas with trees", *Energy and Buildings*, vol. 31, no. 3, pp. 221–235, 2000.

[101] A Middel, K Häb, A. Brazel, C Martin, and B. Ruddell, "Linking shading patterns of trees in phoenix, az, to thermal comfort. presentation at the 11th symposium on the urban environment", in *American Meteorological Society 94th Annual Meeting*, 2014.

[102] A. Crimmins, J Balbus, J. Gamble, C. Beard, J. Bell, D Dodgen, R. Eisen, N Fann, M. Hawkins, S. Herring, *et al.*, "The impacts of climate change on human health in the united states: A scientific assessment", *Global Change Research Program: Washington, DC, USA*, 2016.

[103] R. Kaiser, A. Le Tertre, J. Schwartz, C. A. Gotway, W. R. Daley, and C. H. Rubin, "The effect of the 1995 heat wave in chicago on all-cause and cause-specific mortality", *American journal of public health*, vol. 97, no. Supplement_1, S158–S162, 2007.

[104] J. C. Semenza, C. H. Rubin, K. H. Falter, J. D. Selanikio, W. D. Flanders, H. L. Howe, and J. L. Wilhelm, "Heat-related deaths during the july 1995 heat wave in chicago", *New England journal of medicine*, vol. 335, no. 2, pp. 84–90, 1996.

[105] A. De Bono, P. Peduzzi, S. Kluser, and G. Giuliani, "Impacts of summer 2003 heat wave in europe", 2004.

[106]   A. Dorozynski, "Heat wave triggers political conflict as french death rates rise", *BMJ: British Medical Journal*, vol. 327, no. 7412, p. 411, 2003.

[107]   B. Arkell and G. Darch, "Impacts of climate change on london's transport systems", *Proceedings of the ICE–Municipal Engineer*, vol. 159, no. 4, pp. 231–7, 2006.

[108]   R. C. Hale, K. P. Gallo, T. W. Owen, and T. R. Loveland, "Land use/land cover change effects on temperature trends at us climate normals stations", *Geophysical Research Letters*, vol. 33, no. 11, 2006.

[109]   M. Rebetez, O. Dupont, and M Giroud, "An analysis of the july 2006 heatwave extent in europe compared to the record year of 2003", *Theoretical and Applied Climatology*, vol. 95, no. 1, pp. 1–7, 2009.

[110]   J. K. Rosenthal, P. L. Kinney, and K. B. Metzger, "Intra-urban vulnerability to heat-related mortality in new york city, 1997–2006", *Health & place*, vol. 30, pp. 45–60, 2014.

[111]   M. P. Naughton, A. Henderson, M. C. Mirabelli, R. Kaiser, J. L. Wilhelm, S. M. Kieszak, C. H. Rubin, and M. A. McGeehin, "Heat-related mortality during a 1999 heat wave in chicago", *American journal of preventive medicine*, vol. 22, no. 4, pp. 221–227, 2002.

[112]   N. L. Miller, K. Hayhoe, J. Jin, and M. Auffhammer, "Climate, extreme heat, and electricity demand in california", *Journal of Applied Meteorology and Climatology*, vol. 47, no. 6, pp. 1834–1844, 2008.

[113]   G. B. Anderson and M. L. Bell, "Lights out: Impact of the august 2003 power outage on mortality in new york, ny", *Epidemiology (Cambridge, Mass.)*, vol. 23, no. 2, p. 189, 2012.

[114]   NASA. (2017). Nasa, noaa data show 2016 warmest year on record globally. K. Northon, Ed.

[115]   P. Ciais, M Reichstein, N. Viovy, A Granier, J. Ogée, V Allard, M. Aubinet, N Buchmann, C. Bernhofer, A Carrara, *et al.*, "Europe-wide reduction in primary productivity caused by the heat and drought in 2003", *Nature*, vol. 437, no. 7058, pp. 529–533, 2005.

[116]   G. Churkina, F. Kuik, B. Bonn, A. Lauer, R. Grote, K. Tomiak, and T. M. Butler, "Effect of voc emissions from vegetation on air quality in berlin during a heatwave", *Environmental Science & Technology*, 2017.

[117] A Granier, N Bréda, P. Biron, and S Villette, "A lumped water balance model to evaluate duration and intensity of drought constraints in forest stands", *Ecological Modelling*, vol. 116, no. 2, pp. 269–283, 1999.

[118] C. Koppe, R Sari Kovats, B. Menne, G. Jendritzky, D. Wetterdienst, W. H. Organization, *et al.*, "Heat-waves: Risks and responses", 2004.

[119] P. J. Robinson, "On the definition of a heat wave", *Journal of applied Meteorology*, vol. 40, no. 4, pp. 762–775, 2001.

[120] F. C. Curriero, K. S. Heiner, J. M. Samet, S. L. Zeger, L. Strug, and J. A. Patz, "Temperature and mortality in 11 cities of the eastern united states", *American journal of epidemiology*, vol. 155, no. 1, pp. 80–87, 2002.

[121] J. Tan, Y. Zheng, G. Song, L. S. Kalkstein, A. J. Kalkstein, and X. Tang, "Heat wave impacts on mortality in shanghai, 1998 and 2003", *International journal of biometeorology*, vol. 51, no. 3, pp. 193–200, 2007.

[122] A. J. Teuling, S. I. Seneviratne, R. Stöckli, M. Reichstein, E. Moors, P. Ciais, S. Luyssaert, B. Van Den Hurk, C. Ammann, C. Bernhofer, *et al.*, "Contrasting response of european forest and grassland energy exchange to heatwaves", *Nature Geoscience*, vol. 3, no. 10, pp. 722–727, 2010.

[123] M. Siebers, "Impacts of heat waves on food quantity and quality of soy bean/corn in the midwest at ambient and elevated [co2]", PhD thesis, University of Illinois at Urbana-Champaign, 2014.

[124] A. Links, D. E. Beans, and G. Storage, "Impacts of extreme heat stress and increased soil temperature on plant growth and development impacts of extreme heat stress and increased soil temperature on plant growth and development june 21, 2016",

[125] P. H. Gleick, G. H. Wolff, and K. K. Cushing, *Waste not, want not: The potential for urban water conservation in california*. Pacific Institute for Studies in Development, Environment, and Security Oakland, CA, 2003.

[126] R. Attwater and C. Derry, "Achieving resilience through water recycling in peri-urban agriculture", *Water*, vol. 9, no. 3, p. 223, 2017.

[127] J. Nolasco, "Sustainable water management for urban agriculture: Planting justice, oakland", CA: Working Paper Pacific Institute, Tech. Rep., 2011.

[128] T. E. Parece, M. Lumpkin, and J. B. Campbell, "Irrigating urban agriculture with harvested rainwater: Case study in roanoke, virginia, usa", in *Sustainable Water Management in Urban Environments*, Springer, 2016, pp. 235–263.

[129] B. Gido, E. Friedler, and D. M. Broday, "Assessment of atmospheric moisture harvesting by direct cooling", *Atmospheric Research*, vol. 182, pp. 156–162, 2016.

[130] M. S. Pervez and J. F. Brown, "Mapping irrigated lands at 250-m scale by merging modis data and national agricultural statistics", *Remote Sensing*, vol. 2, no. 10, pp. 2388–2412, 2010.

[131] P. Dappen, "Using satellite imagery to estimate irrigated land: A case study in scotts bluff and kearney counties, summer 2002",

[132] M. Ozdogan, Y. Yang, G. Allez, and C. Cervantes, "Remote sensing of irrigated agriculture: Opportunities and challenges", *Remote sensing*, vol. 2, no. 9, pp. 2274–2304, 2010.

[133] S Irmak and D Mutiibwa, "On the dynamics of stomatal resistance: Relationships between stomatal behavior and micrometeorological variables and performance of jarvis-type parameterization", *Transactions of the ASABE*, vol. 52, no. 6, pp. 1923–1939, 2009.

[134] M. González-Sanpedro, T. Le Toan, J Moreno, L Kergoat, and E Rubio, "Seasonal variations of leaf area index of agricultural fields retrieved from landsat data", *Remote Sensing of Environment*, vol. 112, no. 3, pp. 810–824, 2008.

[135] L. Ji and A. J. Peters, "Assessing vegetation response to drought in the northern great plains using vegetation and drought indices", *Remote Sensing of Environment*, vol. 87, no. 1, pp. 85–98, 2003.

[136] J Wang, P. Rich, and K. Price, "Temporal responses of ndvi to precipitation and temperature in the central great plains, usa", *International journal of remote sensing*, vol. 24, no. 11, pp. 2345–2364, 2003.

[137] V. Brovkin, A. Ganopolski, and Y. Svirezhev, "A continuous climate-vegetation classification for use in climate-biosphere studies", *Ecological Modelling*, vol. 101, no. 2-3, pp. 251–261, 1997.

[138] J Schumacher, E Luedeling, J Gebauer, A Saied, K El-Siddig, and A Buerkert, "Spatial expansion and water requirements of urban agriculture in khartoum, sudan", *Journal of arid environments*, vol. 73, no. 4, pp. 399–406, 2009.

[139] M. Ozdogan, M. Rodell, H. K. Beaudoing, and D. L. Toll, "Simulating the effects of irrigation over the united states in a land surface model based on satellite-derived agricultural data", *Journal of Hydrometeorology*, vol. 11, no. 1, pp. 171–184, 2010.

[140] J. Kerr, L. Frank, J. F. Sallis, and J. Chapman, "Urban form correlates of pedestrian travel in youth: Differences by gender, race-ethnicity and household attributes",

Transportation Research Part D: Transport and Environment, vol. 12, no. 3, pp. 177–182, 2007.

[141] L. D. Frank, M. A. Andresen, and T. L. Schmid, "Obesity relationships with community design, physical activity, and time spent in cars", *American journal of preventive medicine*, vol. 27, no. 2, pp. 87–96, 2004.

[142] L. D. Frank, T. L. Schmid, J. F. Sallis, J. Chapman, and B. E. Saelens, "Linking objectively measured physical activity with objectively measured urban form: Findings from smartraq", *American journal of preventive medicine*, vol. 28, no. 2, pp. 117–125, 2005.

[143] P. Hess, A. Moudon, M. Snyder, and K. Stanilov, "Site design and pedestrian travel", *Transportation Research Record: Journal of the Transportation Research Board*, no. 1674, pp. 9–19, 1999.

[144] P. W. Newman and J. R. Kenworthy, "Transport and urban form in thirty-two of the world's principal cities", *Transport Reviews*, vol. 11, no. 3, pp. 249–272, 1991.

[145] R. Cervero and K. Kockelman, "Travel demand and the 3ds: Density, diversity, and design", *Transportation Research Part D: Transport and Environment*, vol. 2, no. 3, pp. 199–219, 1997.

[146] P. W. Newman and J. R. Kenworthy, "Gasoline consumption and cities: A comparison of us cities with a global survey", *Journal of the american planning association*, vol. 55, no. 1, pp. 24–37, 1989.

[147] K. Steemers, "Energy and the city: Density, buildings and transport", *Energy and buildings*, vol. 35, no. 1, pp. 3–14, 2003.

[148] C. Ratti, N. Baker, and K. Steemers, "Energy consumption and urban texture", *Energy and buildings*, vol. 37, no. 7, pp. 762–776, 2005.

[149] J. H. Kämpf and D. Robinson, "Optimisation of building form for solar energy utilisation using constrained evolutionary algorithms", *Energy and Buildings*, vol. 42, no. 6, pp. 807–814, 2010.

[150] R. Ewing and F. Rong, "The impact of urban form on us residential energy use", *Housing policy debate*, vol. 19, no. 1, pp. 1–30, 2008.

[151] I. D. Stewart and T. R. Oke, "Local climate zones for urban temperature studies", *Bulletin of the American Meteorological Society*, vol. 93, no. 12, pp. 1879–1900, 2012.

[152] T. R. Oke, "The energetic basis of the urban heat island", *Quarterly Journal of the Royal Meteorological Society*, vol. 108, no. 455, pp. 1–24, 1982.

[153] T. R. Oke *et al.*, "Initial guidance to obtain representative meteorological observations at urban sites", 2004.

[154] A. G. Davenport, C. S. B. Grimmond, T. R. Oke, and J. Wieringa, "Estimating the roughness of cities and sheltered country", in *Proceedings 12th Conference on Applied Climatology, Asheville, NC, American Meteorological Society, Boston*, 2000, pp. 96–99.

[155] J. Unger, S. Savić, and T. Gál, "Modelling of the annual mean urban heat island pattern for planning of representative urban climate station network", *Advances in Meteorology*, vol. 2011, 2011.

[156] L. See, C. Perger, M. Duerauer, S. Fritz, B. Bechtel, J. Ching, P. Alexander, G. Mills, M. Foley, M. O'Connor, *et al.*, "Developing a community-based worldwide urban morphology and materials database (wudapt) using remote sensing and crowdsourcing for improved urban climate modelling", in *Urban Remote Sensing Event (JURSE), 2015 Joint*, IEEE, 2015, pp. 1–4.

[157] P. P.-J. Yang, S. Y. Putra, and W. Li, "Viewsphere: A gis-based 3d visibility analysis for urban design evaluation", *Environment and Planning B: Planning and Design*, vol. 34, no. 6, pp. 971–992, 2007.

[158] J. Geletič, M. Lehnert, and P. Dobrovolnỳ, "Land surface temperature differences within local climate zones, based on two central european cities", *Remote Sensing*, vol. 8, no. 10, p. 788, 2016.

[159] B. Goldstein, M. Hauschild, J. Fernández, and M. Birkved, "Urban versus conventional agriculture, taxonomy of resource profiles: A review", *Agronomy for sustainable development*, vol. 36, no. 1, p. 9, 2016.

[160] L. J. Pearson, L. Pearson, and C. J. Pearson, "Sustainable urban agriculture: Stocktake and opportunities", *International journal of agricultural sustainability*, vol. 8, no. 1-2, pp. 7–19, 2010.

[161] G.-y. Qiu, H.-y. LI, Q.-t. Zhang, C. Wan, X.-j. Liang, and X.-z. Li, "Effects of evapotranspiration on mitigation of urban temperature by vegetation and urban agriculture", *Journal of Integrative Agriculture*, vol. 12, no. 8, pp. 1307–1315, 2013.

[162] R. Ewing, T. Schmid, R. Killingsworth, A. Zlot, and S. Raudenbush, "Relationship between urban sprawl and physical activity, obesity, and morbidity", *American journal of health promotion*, vol. 18, no. 1, pp. 47–57, 2003.

[163] C. Royo and D. Villegas, "Field measurements of canopy spectra for biomass assessment of small-grain cereals", in *Biomass-Detection, Production and Usage*, InTech, 2011.

[164] S. Goswami, J. Gamon, S. Vargas, and C. Tweedie, "Relationships of ndvi, biomass, and leaf area index (lai) for six key plant species in barrow, alaska", PeerJ PrePrints, Tech. Rep., 2015.

[165] SimWright, "Normalized difference vegetation index (ndvi) analysis for forestry and crop management", SimWright, Tech. Rep.

[166] H. Nouri, S. Beecham, S. Anderson, and P. Nagler, "High spatial resolution worldview-2 imagery for mapping ndvi and its relationship to temporal urban landscape evapotranspiration factors", *Remote sensing*, vol. 6, no. 1, pp. 580–602, 2014.

[167] J. Randolph, *Environmental land use planning and management*. Island Press, 2004.

[168] K. J. Oven, S. E. Curtis, S. Reaney, M. Riva, M. G. Stewart, R. Ohlemüller, C. E. Dunn, S. Nodwell, L. Dominelli, and R. Holden, "Climate change and health and social care: Defining future hazard, vulnerability and risk for infrastructure systems supporting older people's health care in england", *Applied Geography*, vol. 33, pp. 16–24, 2012.

[169] S. Irmak, "Impacts of extreme heat stress and increased soil temperature on plant growth and development", UNL CropWatch, Tech. Rep., 2016.

[170] K. M. Meehan and A. W. Moore, "Downspout politics, upstream conflict: Formalizing rainwater harvesting in the united states", *Water international*, vol. 39, no. 4, pp. 417–430, 2014.

[171] NCSL. (2017). State rainwater harvesting laws and legislation.

[172] M. Liebman, O. Jonasson, and R. Wiese, "The urban stormwater farm", *Water Science and Technology*, vol. 64, no. 1, pp. 239–246, 2011.